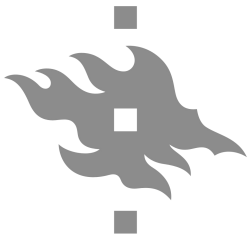

Master's thesis
Master's Programme in Geology and Geophysics
Solid Earth Geophysics

Forward and inverse modelling of terrestrial cosmogenic nuclides to detect past glaciations

Lotta Ylä-Mella

6/2020

Supervisors: Ilmo Kukkonen
David Whipp

University of Helsinki
Faculty of Science
Department of Geoscience and Geography

Box 64 (Gustaf Hällströmin katu 2)
00014 University of Helsinki

HELSINGIN YLIOPISTO
HELSINGFORS UNIVERSITET
UNIVERSITY OF HELSINKI
MATEMAATTIS-LUONNONTIETEELLINEN TIEDEKUNTA
MATEMATISK-NATURVETENSKAPLIGA FAKULTETEN
FACULTY OF SCIENCE

Tiedekunta – Fakultet – Faculty	Koulutusohjelma – Utbildningsprogram – Degree programme
Faculty of Science	Master's programme in Geology and Geophysics

Opintosuunta – Studieinrikting – Study track
Solid Earth Geophysics

Tekijä – Författare – Author
Lotta Kristiina Ylä-Mella

Työn nimi – Arbetets titel – Title
Forward and inverse modelling of terrestrial cosmogenic nuclides to detect past glaciations

Työn laji – Arbetets art – Level	Aika – Datum – Month and year	Sivumäärä – Sidoantal – Number of pages
Master's thesis	6/2020	74 + 18

Tiivistelmä – Referat – Abstract
Terrestrial cosmogenic nuclides can be used to date glacial events. The nuclides are formed when cosmic rays interact with atoms in rocks. When the surface is exposed to the rays, the number of produced nuclides increases. Shielding, like glaciation, can prevent production. Nuclide concentration decreases with depth because the bedrock attenuates the rays. The northern hemisphere has experienced several glaciations, but typically only the latest one can be directly observed. The aim of the study was to determine if these nuclides, produced by cosmic rays, can be used to detect glaciations before the previous one by using a forward and an inverse model.

The forward model predicted the nuclide concentration with depth based on a glacial history. The longer the exposure duration was, the higher was the number of nuclides in the rock. In the model, it was possible to use three isotopes. ^{10}Be, ^{14}C and ^{26}Al. The forward model was used to produce synthetic samples, which were then used in the inverse model. The purpose of the inverse model was to test which kind of glacial histories produce similar nuclide concentrations than what the sample had. The inverse model produced a concentration curve which was compared with the concentration of the samples. The misfit of the inverse solution was defined with an "acceptance box". The box was formed from the thickness of the sample and the corresponding concentrations. If the curve intersected with the box, the solution was accepted. Small misfit values were gained if the curve was close to the sample. The idea was to find concentration curves which have as similar values as the samples.

The inverse model was used in several situations, where the number of limitations was varied. If the timing of the last deglaciation and amount of erosion were known, the second last deglaciation was found relatively well. With looser constraints, it was nearly impossible to detect the past glaciations unless a depth profile was used in the sampling. The depth profile provided a tool to estimate the amount of erosion and the total exposure duration using only one isotope.

Avainsanat – Nyckelord – Keywords
modelling, cosmogenic nuclides, forward, inverse, depth profile

Säilytyspaikka – Förvaringställe – Where deposited
HELDA

Muita tietoja – Övriga uppgifter – Additional information

HELSINGIN YLIOPISTO
HELSINGFORS UNIVERSITET
UNIVERSITY OF HELSINKI
MATEMAATTIS-LUONNONTIETEELLINEN TIEDEKUNTA
MATEMATISK-NATURVETENSKAPLIGA FAKULTETEN
FACULTY OF SCIENCE

Tiedekunta – Fakultet – Faculty	Koulutusohjelma – Utbildningsprogram – Degree programme
Matemaattis-luonnontieteellinen tiedekunta	Geologian ja geofysiikan maisteriohjelma

Opintosuunta – Studieinrikting – Study track
Kiinteän maan geofysiikka

Tekijä – Författare – Author
Lotta Kristiina Ylä-Mella

Työn nimi – Arbetets titel – Title
Forward and inverse modelling of terrestrial cosmogenic nuclides to detect past glaciations

Työn laji – Arbetets art – Level	Aika – Datum – Month and year	Sivumäärä – Sidoantal – Number of pages
Pro gradu	6/2020	74 + 18

Tiivistelmä – Referat – Abstract
Kosmogeenisia isotooppeja voidaan käyttää jääkausien ajoittamiseen. Isotoopit syntyvät, kun kosmiset säteet vuorovaikuttavat kivissä olevien atomien kanssa. Kun maanpinta on paljastuneena säteille, syntyneiden isotooppien pitoisuus kallioperässä kasvaa. Isotooppeja ei synny, jos säteiden kulku on estynyt esimerkiksi jäätikön takia. Isotooppien määrä vähenee, kun syvyys kasvaa, sillä kallioperä vaimentaa säteitä. Pohjoinen pallonpuolisko on kokenut monia jääkausia, mutta tyypillisesti vain viimeisimmästä voidaan saada suoria todisteita. Tämän pro gradun tarkoituksena on määrittää voiko näitä isotooppeja käyttää edellisten jääkausien ajoittamiseen käyttämällä inversiomallinnusta.

Jäätiköitymishistorian perusteella mallinnettiin isotooppien konsentraatioita kallioperässä. Mitä kauemmin säteille on altistuttu, sitä enemmän isotooppeja syntyi. Mallissa oli mahdollista käyttää kolmea eri isotooppia ^{10}Be, ^{14}C ja ^{26}Al. Mallia käytettiin synteettisten näytteiden luomiseen, joita puolestaan käytettiin inversiomallissa. Inversiomallin tarkoitus oli testata, millaisilla jäätiköitymishistorioilla saadaan tuotettua samanlaiset isotooppipitoisuudet kuin synteettisissä näytteissä. Mallien paremmuutta arvioitiin sillä, kuinka lähellä pitoisuuskäyrä oli näytteen pitoisuutta. Syvyyden vaihteluvälinä käytettiin näytteen paksuutta, jonka avulla määritettiin vaihteluväli myös pitoisuudelle. Jos mallin pitoisuuskäyrä osui vaihteluvälien muodostamaan laatikkoon, malli hyväksyttiin.

Inversiomallia käytettiin useissa erilaisissa tapauksissa, joissa mallia rajoitettiin eri tavoin. Jos viimeisimmän jääkauden lopetusaika sekä jäätikön aiheuttama eroosio tiedettiin, oli mahdollista saada tietoa myös tätä edeltäneestä jääkaudesta. Jos rajoitteita mallille ei ollut niin montaa, edellisten jääkausien havaitseminen oli liki mahdotonta, ellei näytteenotossa käytetty syvyysprofiilia. Syvyysprofiili tarjosi mahdollisuuden eroosion ja kokonaispaljastumisen keston arviointiin käyttämällä vain yhtä isotooppia.

Avainsanat – Nyckelord – Keywords
mallinnus, kosmogeeniset isotoopit, inversiomalli, syvyysprofiili

Säilytyspaikka – Förvaringställe – Where deposited
HELDA

Muita tietoja – Övriga uppgifter – Additional information

Contents

1 Introduction

Glaciations have shaped landscapes through the history of Earth. Even during the past 2.6 Ma, the planet has experienced at least 20 glacial periods. The most extensive ones have occurred in the last 900 ka (Ehlers and Gibbard, 2007). Europe has also witnessed more than 10 glacial periods in the past million years (Frakes et al., 1992). Glacial periods have occurred frequently, however, from a geological point of view, we often have information only from the latest glaciation. The reason is that the glaciers erode the bedrock and remove the traces left by the earlier glaciations (Benn and Evans, 2014). Terrestrial cosmogenic nuclide (TCN) dating can be a key to find out more about the past glacial history. The conditions of the past can be used to predict events in the future and therefore we need to know what has happened before.

The climate is and has been, constantly changing. The global temperatures were much higher 65 Ma ago than they are nowadays (Burke et al., 2018) but during Late Miocene, the temperatures began to decrease (Zachos et al., 2001) (Figure 1). After that, the Northern hemisphere has experienced numerous glacial periods (Pillans and Gibbard, 2012). One of the major reasons for the change was the Milankovitch Cycle (Shackleton and Hall, 1997). The cycle includes three different parts that are related to the position of Earth; eccentricity, obliquity and precession (Wong, 2016). The change of eccentricity is the change of the shape of Earth's orbit, and its periodicity is about 100 000 years (Berger, 2001). The obliquity tells how tilted is the axis of Earth. The angle varies from 21.5° to 24.5° in a period of 41 000 years. The precession is the direction of the rotation axis and its period is 21 000 years (Berger, 2001). These three parameters affect the amount of received energy from the sun and therefore they also affect to the climate. The Milankovitch cycle does not explain all the variation in the climate, but it has a remarkable part in it (Wong, 2016).

Besides the climate, also glaciers are constantly changing and so is the bedrock beneath. Subglacial erosion is shaping the bedrock by scoring and polishing it while the glacier is moving (Benn and Evans, 2014). The abrasion removes bedrock, and if the amount of removed rock is large enough, also the evidence of the past glaciations

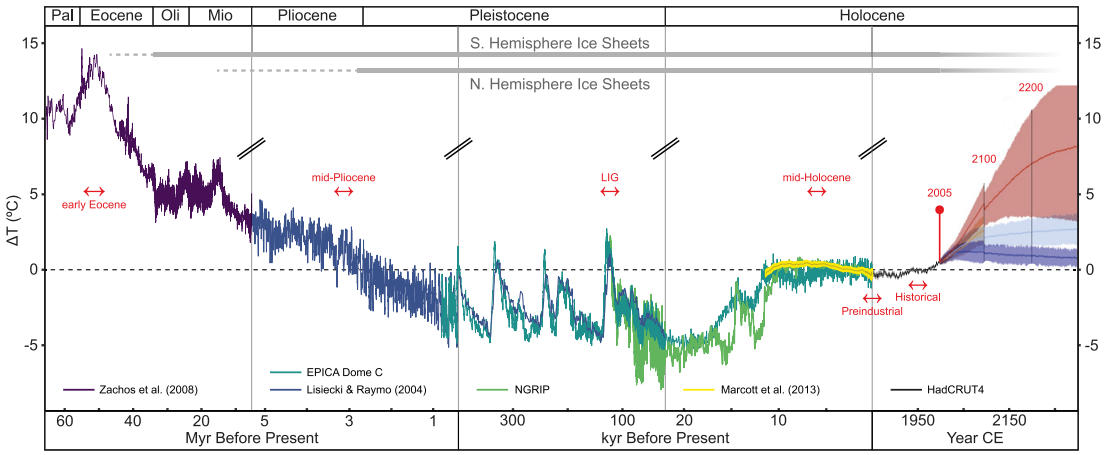

Figure 1. Historical temperature trends of Earth relative to 1961-1990 global means. Temperatures have been higher in the past, but 45 Ma ago the trend began to decrease. The coldest period was experienced about 20-100 ka ago. Adopted from Burke et al. (2018).

are removed (Li et al., 2005). There are still ways to study climate history and past glaciations. The history can be studied with marine sediments or ice cores, but they do not provide information on the local history (Ivy-Ochs and Briner, 2014). One way to detect past events is TCN dating. It is based on the interaction between cosmic rays from space and atoms in minerals, and it can be used to determine the time when the bedrock has been exposed to cosmic rays. The effect of exposure to the number of end products can be modelled and the model can be used to find out the possible glaciation histories that the rock has faced. It is also possible to study erosion caused by the glaciations because the glacier erosion affects also the number of nuclides in the rocks (Ivy-Ochs and Briner, 2014).

TCN has been used to study landscape evolution (e.g. Heimsath et al., 2001; Placzek et al., Placzek et al. (2010); Strobl et al., 2012). Due to the abrasive nature of glaciers, they create fresh surfaces that are exposed to the cosmic rays after the retreat of the glacier. If the nuclides inherited from the earlier exposures are removed, the surface can be used to date the time of the retreat (Balco, 2011). If the erosion has been small, there are inherited nuclides that can be used to study earlier exposures. A small amount of erosion and dating with two isotopes, can provide more information of the complicated exposure histories. The amount of erosion controls the information that can be found (Corbett et al., 2013).

1.1 Previous studies

The basic theory of terrestrial cosmogenic nuclide dating is relatively old. Grosse (1934) came up with an idea of "cosmic radio-elements", which would explain the unknown radioactivity of rocks. Davis and Schaeffer (1955) were the first ones to apply the method in a geological setting. The target mineral was ^{36}Cl since the properties, like half-life, were suitable, and it was geochemically significant in the target rocks. Davis and Schaeffer were interested in studying geological processes during glaciations in Pleistocene. They assumed that because the half-life of ^{36}Cl was 308 000 years, they could date events in the past million years. Davis and Schaeffer calculated the age of a sample with measured activity, the weight of chlorine, and the production rate. Still, erosion was not considered because the samples were selected from areas where erosion was not significant. They measured an age of 24 000 years for an igneous rock sample from New Hampshire. That was promising, but the method was not yet adopted by others. The main reason was that there were limitations to calculate the activity at that time (Gosse and Phillips, 2001).

Lal and Peters (1967) presented the theoretical background for cosmogenic nuclides. They focused mostly on nuclides in the atmosphere, but they also brought out some new aspects to TCN and pointed out that the production in the lithosphere was relatively small compared to the atmosphere. The authors suggested that TCN could be used to study geophysical processes, for example, erosion, and the nuclides might also be used to find out more about cosmic ray flux in the past and intensity of stellar neutrinos. Lal and Peters stated that there had already been studies with ^{14}C and that ^{10}Be, ^{26}Al and ^{36}Cl could also be used in a similar way. They clearly recognized the possibility of TCN, but the atmospheric and oceanic cosmogenic nuclides received more attention at that time.

The development of accelerator mass spectrometry (AMS) increased the precision of the measurements in the 1980s. The conventional mass spectrometry was functional if the mass difference between isobars was large enough, about 84 000. The AMS did not need as vast difference, and at that time, the difference of 200-400 was enough to be detected. As a result, the sample size was reduced, and the sensitivity of the measurement was increased (Elmore and Phillips, 1987). The possibilities of ^{10}Be in geosciences were utilized already back then. Klein et al. (1982) were able to detect only 100 atoms g^{-1} in basalts. One of the first applications of in situ ^{10}Be and the ratio of ^{26}Al/^{10}Be was a study of the history of Libyan Desert glass together with fission-track data. The main conclusions were that the exposure history was not the same in different samples, which may have been caused by redistribution of the glass during 100 ka period. (Klein et al., 1986).

Kohl and Nishiizumi (1992) managed to improve and standardize the sample processing so well that it is still in use in many places even today (for example Skov et al. (2020) and Ceperley et al. (2020). They managed to remove the atmospheric and meteoric component by dissolving at least 30% of a quartz sample, which was meaningful for the further use of quartz. The method has been fine-tuned during the years, but the basic principle is still the same.

The recent studies have used TCN in many ways, for example to date events like rockslides (Hilger et al., 2019), deglaciations (Briner et al. 2016; Wirsig et al. 2016; Ceperley et al. 2020) and floods (Balbas et al., 2017), to study erosion rates (Dühnforth et al. 2010; Margreth et al. 2016; Lehmann et al. 2020; Skov et al. 2020) and denudation (Strunk et al., 2017). In Fennoscandia, TCN has been mainly used in dating deglaciation and history of Fennoscandian Ice Sheet (Rinterknecht et al. 2004; Goehring et al. 2008; Cuzzone et al. 2016; Stroeven et al. 2016).

1.2 The aim of the study

This study aims to design forward and inverse modelling methods and software to study the exposure and erosion histories of past glaciations. In forward modelling, the nuclide concentrations are predicted with depth based on a glaciation history. In inverse modelling, synthetic samples are used to produce plausible glaciation histories that the samples may have experienced. Together these modelling methods give information on how the sampling should be done, and how much does the erosion affect to the TCN concentrations.

This thesis has three main chapters. Chapter 2 provides a theoretical background to TCN. Chapter 3 describes the forward and the inverse model created for this thesis. It also covers the details that are needed to understand how the models are run. Chapter 4 presents the results for different types of models. There I will show that it is possible to find out the timing of the Late Weichselian glaciation, but the Middle and Early Weichselian are more challenging if there are no proper limitations set for the models. I will also present that sampling with depth profiles will improve the results compared to suing only surface samples. After that chapter, there is discussion and conclusions.

2 Background

2.1 TCN

2.1.1 Principle of TCN

TCN dating is based on the number of reaction products in minerals caused by the bombardment of cosmic rays. Minerals have elements that interact with cosmic rays, creating a reaction that produces new elements, which can be analysed. The number of products is proportional to the time that the rock has been exposed to the rays (Dunai, 2010). Cosmic rays are not actual rays, i.e. electromagnetic radiation, but neutrons that interact with elements in the Earth. Most of the sources of these neutrons originate inside the Milky Way galaxy, but a small part of the sources are from outside of our galaxy. Primary radiation produces stable and radioactive elements in the rock, while the secondary radiation produces particles before they interact with the rock (Gosse and Phillips, 2001).

There are over 20 different cosmogenic nuclides that are used in the measurements. They can be separated into two groups; stable and radioactive isotopes. The stable isotopes are noble gases like ^{3}He or ^{36}Ar. The radioactive isotopes include, for example, ^{10}Be and ^{14}C. The most important nuclides in terrestrial applications are ^{3}He, ^{21}Ne, ^{22}Ne, ^{10}Be, ^{26}Al and ^{36}Cl because of their low geological background and their abundance in accessible minerals and rocks (Dunai, 2010).In the case of ^{10}Be, the basic primary reaction is caused by ^{16}O and neutrons, producing ^{10}Be, ^{3}He and α particle. It is also possible to produce protons and neutrons instead of ^{3}He and α. Dunai (2010) also presents other possible elements that interact with cosmic rays, most frequently ^{14}C, ^{26}Al and ^{36}Cl. ^{26}Al is often used in the measurements, and it is the end result of a reaction between a neutron and ^{28}Si (Gosse and Phillips, 2001).

Dunai (2010) defines six conditions that should be fulfilled if TCN dating is going to be applied successfully. (1) The target element is uncommon in geological materials. This is important because if the element has many sources, it is hard to detect which of the atoms have been formed because of cosmic rays and which have formed in

some other way. (2) The element is stable or has a long half-life. If the half-life is short, a significant amount of element is decayed before the measurements. The time scale studied with cosmogenic nuclides is thousands of years, so also the half-life should be longer than that. (3) Natural disturbances, like geological background, can be determined analytically. (4) The production mechanism is well-known. (5) The analysis of the nuclide is possible. (6) The element is contained in common minerals, which are easily accessed.

2.1.2 Production of cosmogenic nuclides

There are several ways to produce cosmogenic nuclides. Neutron spallation is the most important one of them (Dunai, 2010). There high-energy neutrons interact with target nuclei (like ^{16}O or ^{28}Si) and produce neutrons, protons and a lighter nucleus (like ^{10}Be or ^{26}Al). The most common reactions are presented in Table 1. Another significant reaction is negative muon capture. There the nucleus catches electrons, which have fallen into a lower electron shell because the electrons have captured the negative muon (Dunai, 2010). This reaction is not as frequent as spallation but is significant in deeper depths (Gosse and Phillips, 2001) (Figure 2). Muogenic reactions produce 2% of ^{10}Be and 2.1% of ^{26}Al in total. At a depth of 3 m, muogenic reactions and spallation produce an equal amount of ^{10}Be; thus, the muogenic part cannot be ignored (Dunai, 2010).

One of the conditions to be filled was the presence of the isotope in the minerals. To be a useful element in TCN dating, the element must occur in common minerals of Earth. ^{14}C and ^{26}Al can be extracted from quartz and ^{10}Be also from olivine, magnetite and possibly from plagioclase (Gosse and Phillips, 2001). ^{36}Cl is commonly found from feldspars or carbonates (Dunai, 2010).

There are also other ways to produce TCN, but they are not as significant in the production of ^{10}Be and ^{26}Al as neutron spallation and negative muon capture. Fast muons produce secondary neutrons with high energy, and this process is significant at deep depths (Dunai, 2010). Thermal neutron capture produces TCNs when the velocity of neutrons is decreased. This reaction does not typically produce either ^{10}Be or ^{26}Al (Dunai, 2010).

The number of produced atoms also depends on other things than the production path. The flux of cosmic rays is not constant; it varies both spatially and temporally (Beer et al., 2002). The geomagnetic field acts as a shield that prevents approaching particles, and its strength depends on the latitude and time. The efficiency of the shield also depends on the properties of the particles like an electric charge,

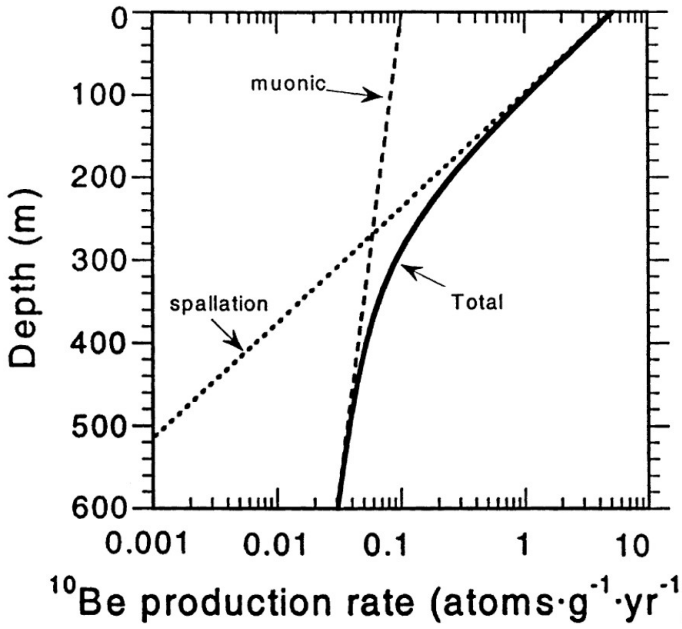

Figure 2. Spallation and muogenic production of ^{10}Be with depth. The spallation reactions are more important near the surface, but the muogenic production becomes more important after 2.8 m. Adopted from Gosse and Phillips (2001).

energy and the angle of inclination. (Masarik and Beer, 1999). The production rate increases with latitude. The highest value is reached after 60°. The magnetic field is inversely proportional to latitude; therefore, when the intensity of the field is decreased, the production rate is increased (Masarik and Beer, 1999). The magnetic field has varied in the past, but its effect on the production rate also depends on the latitude. The variance has a larger impact at low latitudes than it has in mid or high latitudes (Gosse and Phillips, 2001).

The production rate depends on altitude. The increase in the production rate is approximately exponential in the first 4 km above sea level. After that, the increase is not as steep (Masarik and Reedy, 1995). The solar-cycle changes the production

Table 1: Production reactions. Adapted from Dunai (2010).

Isotope	Spallation reaction	Negative muon capture
^{10}Be	^{16}O(n,^{3}He α)^{10}Be ^{16}O(n,4p3n)^{10}Be ^{28}Si(n,x)^{10}Be	^{16}O(μ^-,α pn)^{10}Be ^{28}Si(μ^-,x)^{10}Be
^{14}C	^{16}O (n,2pn)^{14}C ^{28}Si (n,x) ^{14}C	^{16}O (μ^-,pn)^{14}C
^{26}Al	^{28}Si(n,2np)^{26}Al	^{28}Si(μ^-,2n)^{26}Al

rate too. For solar minimum, the production rate increases by a factor of 1.49 while with solar maximum, it decreases by factor 0.63 (Masarik and Reedy, 1995).

Locally the production rate can be disturbed by shielding, which may prevent some of the cosmic radiation. If the sampling site is on a sloping surface, the angle and the direction of the slope affect the arriving ray flux. That is called topographic shielding (Gosse and Phillips, 2001). In mass shielding, there is a solid mass that prevents radiation. It can be vegetation, soil, snow or anything that blocks the rays temporarily or permanently (Dunai, 2010). The effect of shielding in spallogenic reactions is:

$$f_{cover} = e^{-z\rho/\Lambda}, \tag{2.1}$$

where z is the thickness of the cover, ρ is the density of the cover and Λ is the attenuation coefficient (Dunai, 2010). The snow coverage is a special case of mass shielding, and its effect can be determined:

$$f_{snow} = \frac{1}{12}\sum_{i}^{12} e^{\frac{-\left(z_{snow}-z_{sample}\right)\rho_{snow}}{\Lambda}}, \tag{2.2}$$

where z_{snow} is the average monthly snow depth, z_{sample} is the height of the sampling point above the land surface (e.g., in case of a boulder) and ρ_{snow} is the average monthly snow density (Gosse and Phillips, 2001).

2.1.3 Age determination

The age determination with cosmogenic nuclides usually refers to the dating of either exposure or burial age, but it can also involve the determination of erosion or uplift rates. The exposure dating is determining the time when a surface was exposed to the cosmic rays. This surface can be formed by deposition, erosion or endogenic forces (Dunai, 2010). The exposure dating has been successfully applied in many different settings such as alluvial fan deposits (Dühnforth et al., 2007), moraine boulders (Putkonen and Swanson, 2003), deltaic deposits (Ciampalini et al., 2015) and mass movement events (Soldati et al., 2018). The erosion rate can be detected as a part of exposure age dating if the measured age is treated as a minimum exposure age. To find both the exact exposure age and the erosion rate, the measurements must be done at least with two nuclides (Dunai, 2010). In burial dating, there is a sample that has been exposed previously, but is now shielded from rays. It can be applied in dating cave sediments (Häuselmann and Granger, 2016), in archaeological studies (Granger et al., 2015) or in debris covered glaciers (Mackay and Marchant, 2016) for example.

The dating is a complicated process, but the main structure of the method and techniques have remained relatively similar to the process presented by Kohl and Nishiizumi (1992). The first step of the dating process is sampling, which is the most critical step because if it is done incorrectly or the sampling site is not ideal, the results may not be reliable or accurate (Ivy Ochs, 1996). The sampling site should have experienced the event, which is tried to be dated, while still being stable and exposed. Typically the samples are from a surface of the bedrock or from a boulder. The amount of rock needed depends on the rock type and the mineral used in the dating. For example, 0.5-1 kg of granitic rock can have 50 g of quartz, which may be enough in ^{10}Be or ^{26}Al dating (Ivy Ochs, 1996).

After the collection, the samples are prepared for the measurements where the amount of cosmogenic nuclide is determined. To succeed with that, the nuclide must be extracted from the mineral, and the mineral must be separated from the rock sample (Dunai, 2010). Typically mineral processing includes crushing, sieving and separation. Crushing can be started with a sledge hammer and continued with a jaw crusher (Ivy Ochs, 1996). The target grain size is under 2 mm, but the exact size varies from 250-350 µm (Gosse and Phillips, 2001) to 1-2 mm (Ivy Ochs, 1996) and depends on the isotope that is going to be used and the grain size of the mineral. The separation of minerals can be done with magnetic separation (e.g., Franz magnetic separator), density-based separation (e.g., heavy liquid separation), hand picking of the wanted grains or with chemical dissolution (Gosse and Phillips, 2001). The final step of the sample processing is to extract the nuclide from the mineral. The procedure of nuclide extraction depends on the chosen mineral and isotope, but commonly the sample is treated several times with different acids (like HF, HNO_3 and HCl). Eventually, the sample is dried in the heat, mixed with copper and pressed into target holders (Ivy Ochs, 1996).

Accelerator mass spectrometry (AMS) is used to measure the abundance of nuclides in the sample. AMS does not measure the exact number of the isotope but a ratio between two isotopes. The main principle is to extract ions from the sample, accelerate them and then separate them based on the atomic mass. The separation is done with a uniform magnetic field which is perpendicular to the plane of motion. The field affects the ion, and its path will curve. The lighter ions curve more than heavier ones, which can be detected.

2.1.4 Cosmogenic nuclide age calculators

The exposure age can be used to determine when the surface has been exposed to the cosmic rays. It can be calculated analytically from:

$$N_m(z,t,\epsilon) = S\sum_i \frac{J_i}{\frac{\epsilon}{\Lambda_i}+\lambda_m}\left[e^{\left(\frac{-z}{\Lambda_i}\right)} - e^{\left(-\lambda_m t - \frac{z+\epsilon t}{\Lambda_i}\right)}\right], \tag{2.3}$$

where N is the number of nuclides, S is a shielding parameter, J_i is a production coefficient of production path i, ϵ is the erosion rate, Λ is attenuation length, λ_m is the decay constant of isotope m, z is depth and t is the exposure time (Gosse and Phillips, 2001). Equation 2.3 can be simplified in special cases like if the sample is taken from the surface ($z = 0$) or there is no erosion ($\epsilon = 0$). The shielding parameter depends on elevation, latitude, topography and coverage, and the production coefficient considers the production rate and the path constants. The number of nuclides increases with time and decreases with depth. The decrease is caused by the production rate, which also decreases with depth (Gosse and Phillips, 2001). The production rate of ^{26}Alis over six times larger than the production rate of ^{10}Be(Balco et al., 2008). The larger production rate leads to a higher number of produced nuclides, even if the exposure time would be the same.

Equation 2.3 is not the only form used in calculations, and thus another way is presented in section 3.1. To make the calculations easier, the researchers have published age calculators. The original CRONUS calculator is an exposure age calculator invented by Balco et al. (2008). The calculator was built because there was not a way to compare age results from different studies. The goals of the calculator were to create accurate and precise results and standardize the scaling models. The calculator has a free web interface provided by the University of Washington. Version 3 provides exposure ages, erosion rates and calibration of production rates for nuclides ^{3}He (pyroxene, olivine), ^{10}Be (quartz) and ^{26}Al (quartz). It is currently under development for ^{3}He, ^{14}C and ^{21}Ne in quartz. To calculate the exposure age, the user must give some information related to the sample, sampling site and nuclide concentrations. The needed data is a sample name, a latitude, a longitude and elevation (m) or pressure (hPa) of a sample site, elevation/pressure handling flag, a sample thickness and a density, a shielding correction, an erosion rate (independent evidence, $\mathrm{cm\,a^{-1}}$), and a date of a sample collection. The calculator also needs the type of the used mineral, measured nuclide concentration and uncertainty ($\mathrm{atoms\,g^{-1}}$), and the name of standardization. The output provided includes different exposure ages with uncertainties for three different scaling schemes.

There are also newer versions of the age calculator. Marrero et al. (2016) extended the calculator of Balco et al. (2008) to have also a multi-sample depth-profile cal-

culator and a single-sample surface exposure age calculator for multiple isotopes. The extended version can also calculate erosion rates, and in addition, it has several calibration options to choose from. The base of the program is the prediction of concentration at a certain depth and time.

2.1.5 Paired nuclides

The limitation of a single nuclide is that both the age and the erosion rate can not be determined at the same time. If the surface has been eroding, the minimum age estimate can be discovered, but not the exact age. Since the nuclide concentration depends at least two independent variables (Equation 2.3), there must be measurements at least with two isotopes to find values for both variables. This method is called paired nuclides.

Paired nuclides can be used to calculate exposure and burial histories and to find out erosion rates(Bierman et al., 1999). The most typical pair is ^{10}Be and ^{26}Al because they have different half-lives, which is an advantage when the complete glaciation history is estimated. During the burial, the isotope ratio depends only on the half-lives, but during the exposure, it is also controlled by the production rate (Strunk et al., 2017). The nuclide data, collected during the past decades, is mostly from bedrock surfaces (Knudsen and Egholm, 2018), but a similar idea can also be used with samples from different depths. ^{10}Be and ^{26}Al can be measured from the same sample, and the single-nuclide calculations of exposure ages and erosion rates can be done based on the measurements. Even if the results are consistent, the exact exposure history can not be determined. If the results are differing and ^{10}Be age is older than ^{26}Al, the sample has experienced a shielding during the exposure, which could have occurred during the initial exposure or after it (Bierman et al., 1999).

The possible exposure and burial times can be found from Equation 2.4 if it is applied to two different nuclides:

$$N_{nuclide} = \frac{P_{nuclide}}{\lambda}[1 - e^{-\lambda t_e}]e^{-\lambda t_b}, \tag{2.4}$$

where N is the amount of nuclide, P is the production rate, λ is the decay constant, t_e is exposure time and t_b is burial time (Bierman et al., 1999). The minimum total time of exposure is the sum of the exposure time and the burial time.

The production rate ratio of ^{10}Be and ^{26}Al is known to be 6.75 (Balco 2008, Knudesen 2018). Lately, there has been discussion if the ratio is not known as well as it was thought before. Corbett et al. (2017) presented several reasons why the ratio is still uncertain. (1) There are not as many measurements of ^{26}Al than there is

with ^{10}Be, and therefore the production rate of ^{26}Al is not known as well. (2) The standards of the measurements have changed during the years, but the used values are not always presented, which causes uncertainty. (3) Muon interaction may cause a higher ratio than just a spallation reaction. (4) Estimating production ratios have uncertainties. Corbett et al. (2017) measured 24 samples from high latitudes (61–77 °N) in Greenland. The measured ratio for summed spallogenic/muogenic reactions was 7.3 ± 0.3, and the ratio for spallation-only was 7.25. They both are significantly higher than previously used 6.75. Corbett et al. (2017) discussed that might be explained by high latitudes, but it needs to be studied further before any conclusions.

There are also other pairs or groups of nuclides that are used in the measurements. The pilot study of Wirsig et al. (2016) presented a new combination of ^{10}Be, ^{14}C and ^{36}Cl. In the article, they discuss whether the burial and erosion history of Grueben glacier in the Swiss Alps can be studied with those three isotopes. They present a theoretical model that predicts what kind of ages are measured in three different situations. If the exposure has been continuous, apparent ages are the same for all isotopes. If there has been a short burial, ^{14}C should show younger apparent ages, and if there has been both burial and erosion, ^{14}C ages should be the youngest and ^{36}Cl should be the oldest. The authors found out that the study with these three isotopes was proved to be useful. They pointed out that using three isotopes reduces the number of assumptions made of the history of the area and that the assumptions can also be tested with this kind of study. Multiple nuclides provide more reliable results of temporary burial and depth of erosion than one nuclide study.

2.1.6 Scaling schemes

Scaling schemes are used to normalize measurements, and they are needed to neutralize the differences, such as elevation, latitude and the slope of the surface, in the sampling sites (Gosse and Phillips, 2001). Typically the schemes are scaling the reference production rate at the sample sites because there are different types of production and time-dependent changes in the rates (Balco et al., 2008) and the production rates also depend significantly on the location of the sampling site (Gosse and Phillips, 2001). Scaling models are based on the measured data from the sample sites. There are two different ways to do the scaling: (1) the model is based mostly on the neutron monitor data or (2) the model is based both on the data from neutron monitors and from nuclear decay in photographic emulsions. Assumed conditions of all scaling models are at the sea level and high latitude (SLHL) (Lifton et al., 2014).

There are several different schemes, and Balco et al. (2008) present five of them

that can be selected in the CRONUS calculator (presented in section 2.1.4). The simplest one, called "St" model, is based on Stone (2000) and Lal (1991). It takes into account variation in the spallogenic production rates caused by latitude and atmospheric pressure, but the production rate is assumed not to be depending on time. The problem with the model is that it does not work well in high geomagnetic latitudes, and it underestimates altitude dependence (Lifton et al., 2014). Three other scaling models, Dunai (2001) ("Du"), Lifton et al. (2005) ("Li") and Desilets et al. (2006) ("De") are also mostly based on the model of Lal (1991), but there are some major differences when compared to the St model. They consider elevation dependence and changes in the magnetic field or solar activity. The fifth model ("Lm") is also based on the model of Lal, but it also contains a paleomagnetic correction from Nishiizumi et al. (1989). The problem with these four models is that they overestimate the altitude dependence.

The newest model, LSD (Lifton et al., 2014), differs significantly from the previous models. It is analytical, and therefore it is not based on measurements. The model is time-dependent and considers both the magnetic field and solar activity (Marrero et al., 2016). It was created to predict scaling better, and it provides scaling for each nuclide separately (Lifton et al., 2014).

2.2 Glaciations in the northern hemisphere

There have been several glaciations in the northern hemisphere since the Late Pleistocene (Figure 3). In Europe, there have been three major glaciation periods; Early, Middle and Late Weichselian, while in North America, the same periods are known as Early, Middle and Late Wisconsinan glaciations (Ehlers and Gibbard, 2007). In Europe, the Weichselian glaciations were less extensive than the glaciations during the Pleistocene, but in North America, the difference was not large (Ehlers and Gibbard, 2007). The last glacial maximum (LGM)is typically determined from sea-level records. The problem with the records is that the sea-level can be the same when the global ice sheet has grown to its maxima and when the local ice sheet is temporally varying. However, the TCN has been used to date the global ice sheet extent. LGM was reached about 26.5 ka ago, and the ice began to retreat about 19 ka ago (Clark et al., 2009).

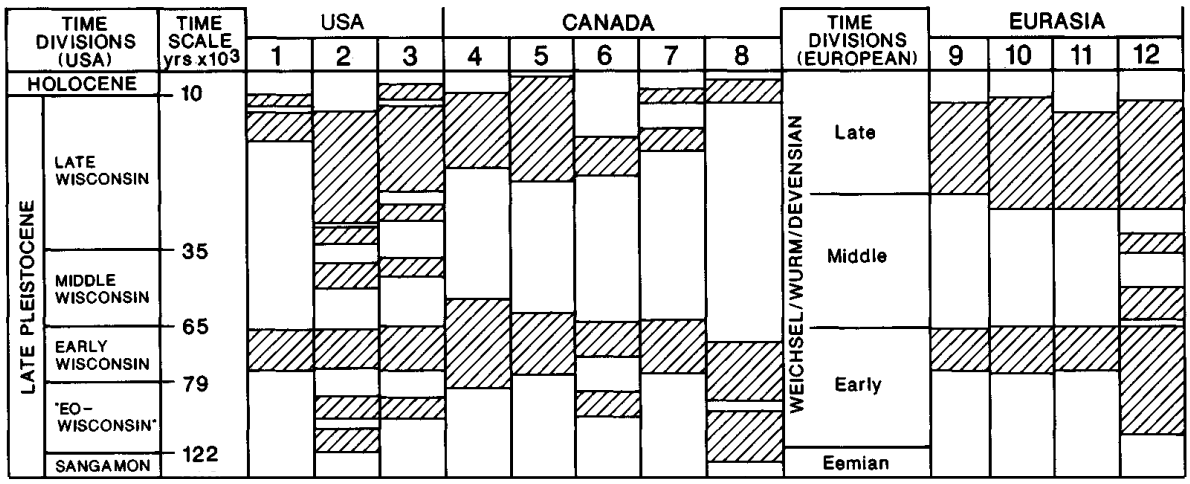

Figure 3. Glaciation history of northern hemisphere during the last 130 ka. Adapted from Frakes et al. (1992).

2.2.1 Glaciation history of Finland

During Pleistocene, Finland experienced many glaciation cycles. Johansson et al. (2011) have gone through the most important ones. During Saalian stage glaciation in Middle Pleistocene (ca. 130 ka) whole Finland had was covered with ice. Later during the several Weichselian glaciations in Late Pleistocene, the glaciation coverage was not as extensive (Figure 4). Lapland has experienced more glaciations than southern Finland. The most important ones in southern Finland are First Mid-Weichselian (ca. 75-60 ka), Second Mid-Weichselian (ca. 50-35 ka) and Late Weichselian (ca. 25-10 ka). Southernmost Finland did not experience the Second Mid-Weichselian. Although Finland has experienced several glaciations, the landscape is shaped particularly by Late Weichselian glaciation (Ehlers and Gibbard, 1996).

The timing of the deglaciation is dated with several different methods. One of the most popular has been varved dating (Saarnisto and Saarinen, 2001). The deglaciation is also dated by thermoluminescence, optically stimulated luminescence and ^{14}C dating (Mäkinen, 2005) and by using cosmogenic nuclides (Tschudi et al., 2000; Rinterknecht et al., 2004).

After the Late Weichselian, the sea level was higher than nowadays due to the glacioisostatic compensation. Even though the margin of the retreating glacier was at the location of the present First Salpausselkä esker in southern Finland at 11 ka ago, there were not many exposed rock surfaces between the glacier and the south coast (Björck, 1995). In addition to postglacial land uplift effects, the sea level began to rise after the connection to the ocean was closed about 10.8 ka ago (Tikkanen and

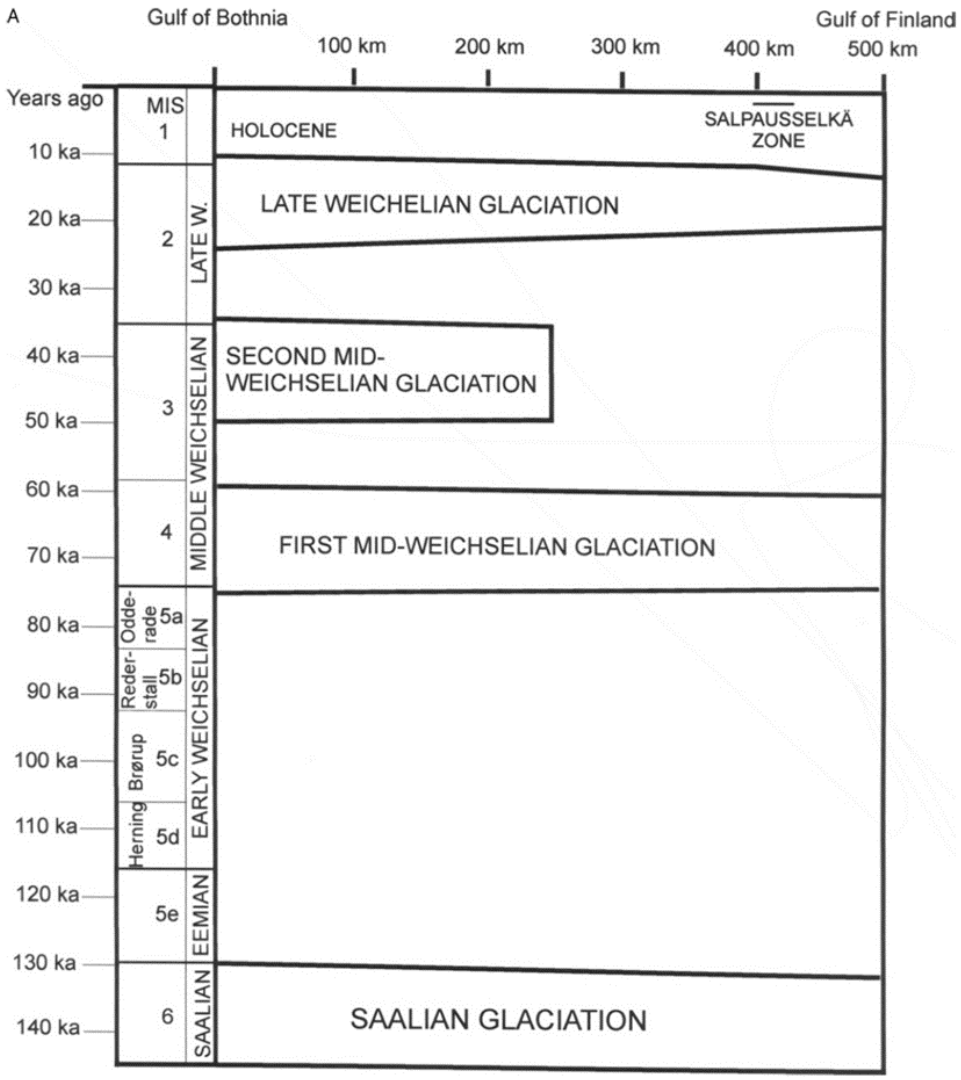

Figure 4. Glaciation history of Finland. Adopted from Johansson et al. (2011).

Oksanen, 2002). For example, Helsinki was covered with 115 m of water (Tikkanen and Oksanen, 2002), which would mean that the surface was not exposed to the cosmic rays, even though it was no longer covered with ice. The exposure history can be estimated from the sea level history, the geodetic and geological land uplift history and the present day topographic altitude (Tikkanen and Oksanen, 2002; Poutanen and Steffen, 2015). The typical attenuation coefficient is 160 g cm^{-2}, and thus the attenuation length in granite (2.7 g cm−3) would be 59 cm and in water 160 cm (Gosse and Phillips, 2001).

3 Methods

The purpose of the modelling is to re-create real life phenomena in a smaller, and usually in a simpler, scale. With models, we can study how different factors affect the phenomenon and understand relations between those factors. In this thesis, I am modelling the concentrations of cosmogenic nuclides with depth while trying to find out if this model can be used to predict the possible glaciation histories based on the concentrations. I am also going to study if we could use this model to determine erosion caused by the glaciers during glaciations. The Python scripts are available at https://github.com/lylamell/master-thesis.

According to Aster and Thurber (2013) if we have an equation

$$G(m) = d, \tag{3.1}$$

the forward model uses a known model or parameters, m, to find some kind of data, d. The inverse model is the opposite of that. There d is known, and it is used to solve m. In this thesis, the forward model predicts concentrations based on a given glaciation history, while the inverse model predicts glaciation histories based on the nuclide concentrations. To get variation to the solutions, noise (ϵ) can be added to the true solution

$$d = G(m_{true}) + \epsilon \tag{3.2}$$

Noise can be, for example, an estimated error of depth or sample thickness.

3.1 Theory

The base of the model is the idea of decreasing nuclide concentration with depth. The cosmic rays are attenuated by the bedrock because the rays interact with atoms in rocks and lose their energy (Dunai, 2010). The basic equation for surface concentrations is defined by Vermeesch (2007)

$$N(t,\epsilon,\tau) = Pe^{-\lambda_m \tau} \sum_{i=0}^{3} \frac{S_i F_i}{\lambda_m + \epsilon\rho/\Lambda_i} \left(1 - e^{-t(\lambda_m + \epsilon\rho/\Lambda_i)}\right), \tag{3.3}$$

where t is exposure time (a), ϵ is constant erosion rate ($\mathrm{m\,a^{-1}}$), τ is burial time (a), P is production rate ($\mathrm{atoms\,kg^{-1}\,a^{-1}}$), λ_i is the decay constant of isotope m ($\mathrm{a^{-1}}$), S_i is scaling factor, F_i is relative production and ρ is density ($\mathrm{kg\,m^{-2}}$). The subscript i refers to the production path. Scaling factor is defined as

$$S_i = e^{-x/\Lambda_i} = e^{-z\rho/\Lambda_i}, \tag{3.4}$$

where x is the thickness ($\mathrm{g\,cm^{-2}}$), but it can be handled as a product of depth (m) and density ($\mathrm{kg\,m^{-3}}$). The density of the bedrock is assumed to be 2650 $\mathrm{kg\,m^{-3}}$.

If there is no burial, τ can be set to zero. The number of nuclides of one isotope as a function with depth is a combination of Equations 3.3 and 3.4

$$N(t,\epsilon,z) = P \sum_{i=0}^{3} \frac{F_i}{\lambda + \epsilon\rho/\Lambda_i} e^{-z\rho/\Lambda_i} \left(1 - e^{-t(\lambda + \epsilon\rho/\Lambda_i)}\right), \tag{3.5}$$

Equation 3.5 is used to model nuclide concentrations with depth, and it also takes into account muons, which have a large effect in deeper depths.

After radioactive decay, the number of nuclides left is determined with basic decay equation

$$N = N_0 e^{-\lambda_{isotope} t}, \tag{3.6}$$

where the N_0 is the initial number of the isotope, $\lambda_{isotope}$ is the decay constant of the isotope and t is the duration of the decay (Braun et al., 2006).

3.2 Forward model

The effect of a glaciation history on the nuclide concentrations is modelled with a forward model. The concentration depends on the periods of exposure and shielding. During the exposure, the concentration increases because the cosmic rays are interacting with the atoms in rocks and producing new elements. During the shielding, these new elements are not produced, because the ice coverage is attenuating the rays and preventing the interaction. The produced elements are decaying during

the shielding, but the effect is not large if the half-lives of the produced elements are much larger compared to the duration of shielding.

The periodicity of exposure and shielding is used in the forward model. The model is based on the equations 3.5 and 3.6 and considers four possible production paths; neutron, fast muon and two different slow muons paths. It is possible to use the model with three isotopes, ^{10}Be, ^{14}C and ^{26}Al. The flowchart of the model is presented in Figure 5, which covers all the steps to produce a forward solution.

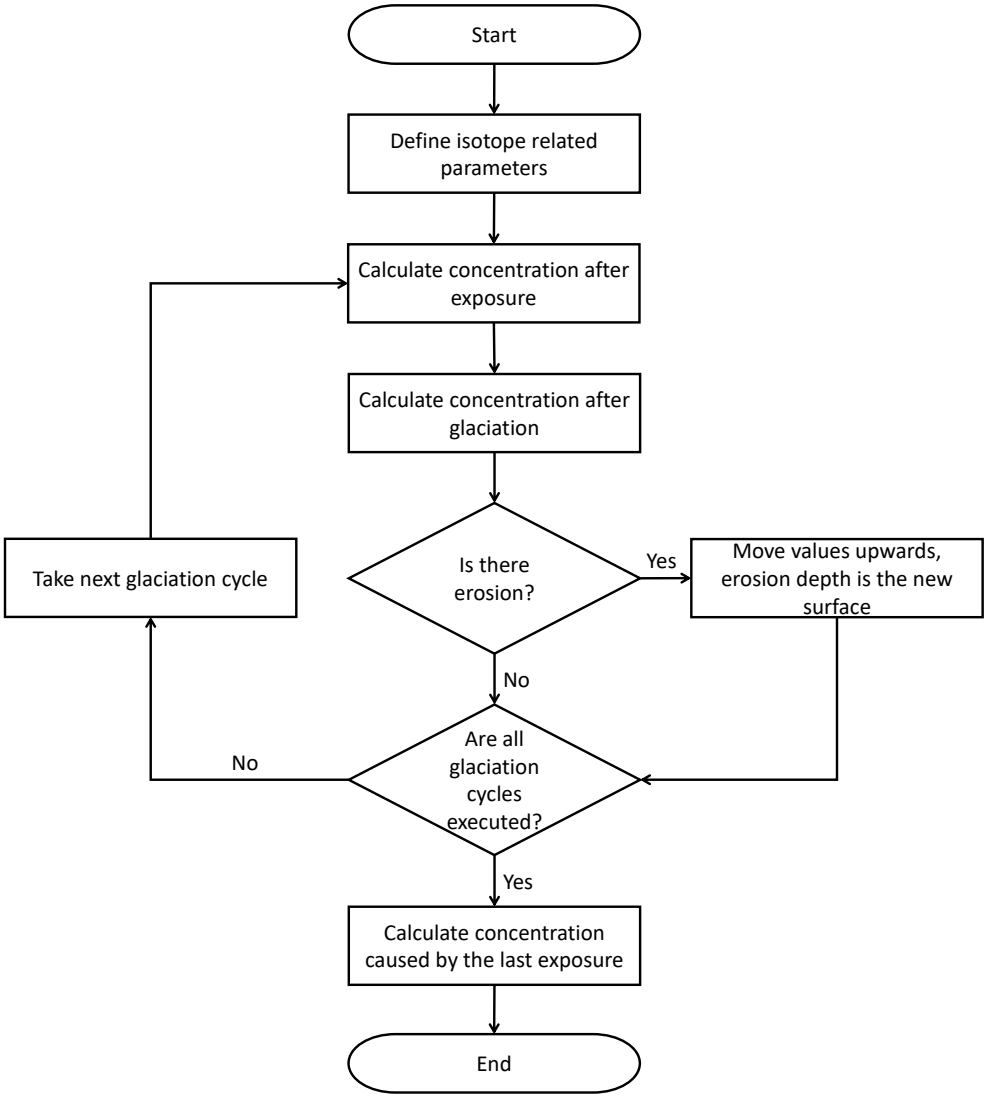

Figure 5. Flowchart of the forward model

There are three major steps in the model. The first one is the calculation of the number of nuclides after the first exposure. The first exposure is the exposure occurred the longest time ago. In the case of glaciation history presented in the

inset figure of Figure 6, the first exposure is between 25 and 35 ka. The second step is the calculation of the number of decayed nuclides during the glaciation, in Figure 6, between 10 and 25 ka. Finally, in the third step, the model takes into account possible block erosion caused by the glaciation. The assumption is that the glacier breaks off the top part of the bedrock during the glaciation. All the remained nuclides are moved upwards as the amount of erosion. This three-step loop can be repeated as many times as needed. The very last step is the calculation of the number of nuclides after the most recent exposure. To complete the series of steps successfully, the required input parameters are the isotope, time arrays for starting time of deglaciations and glaciations and the amount of erosion. Other values like the density of the bedrock, the vertical attenuation length of different production paths or half-lives of different isotopes are treated as constants, and their values are already included in the code. Input and output values are described in Table 2. The example of the concentration curves of ^{10}Be and ^{26}Al is showed in Figure 6.

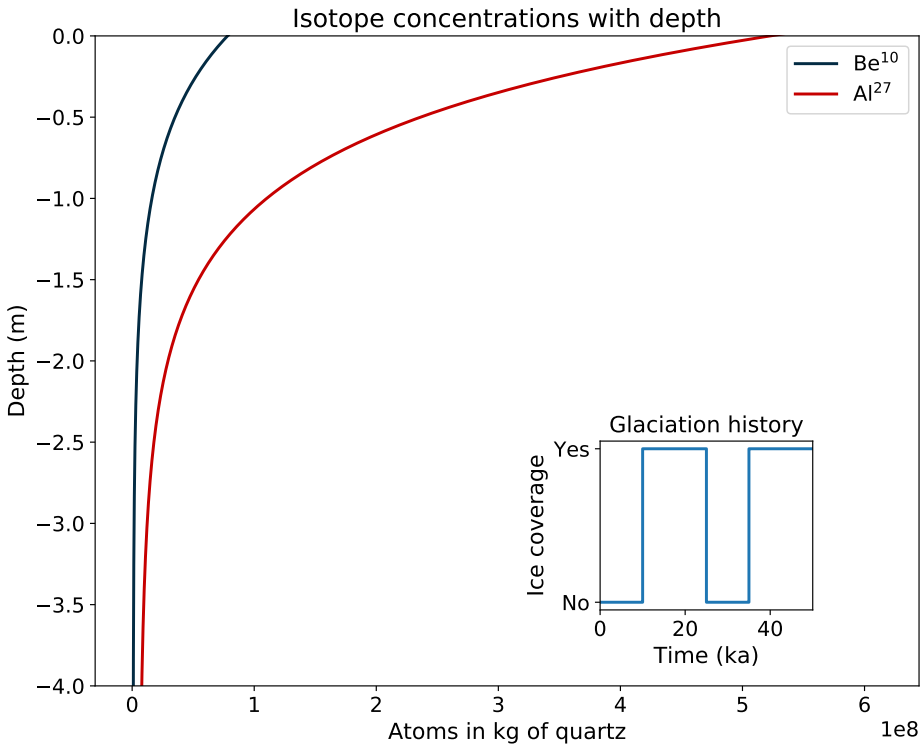

Figure 6. ^{10}Be and ^{26}Al concentrations as a function of depth with the glaciation history (inset figure) of two exposure periods. The total exposure time is 20 ka. The concentration of ^{26}Al is higher than ^{10}Be concentrations, and they both decrease rapidly with depth.

Nuclide concentrations depend on the modelled isotope and depth (Figure 6). Even though the glaciation history is the same for all isotopes, the relative production

Table 2: Input and output variables in the forward model

Input					
Variable name	**Description**	**Unit**	**Example**	**Type**	**Note**
`isotope`	Used isotope. 1 ^{10}Be, 2 ^{26}Al, 3 ^{14}C		1	Integer	
`time_ice`	Ice coverage starting time	ka	[25,0]	NumPy array	
`time_degla`	Deglaciation starting time	ka	[35,10]	NumPy array	
`block_erosion`	Erosion at the deglaciation	m	[2]	NumPy array	Length 1 value shorter than `time_degla`
`const_erosion`	Constant erosion	$\mathrm{cm\,a^{-1}}$	0.3	Float	
Output					
`N_final`	Nuclide concentration	atoms in kg of quartz	[6e7,...,1e4]	NumPy array	
`z`	Depth	m	[0.0,...,10.0]	NumPy array	

(Table 3) and the production rate is not (Table 4). ^{10}Be is produced more by neutrons, while the ^{26}Al has higher production in muonic paths. The production rate of ^{26}Al is 6.76 times higher than the production rate of ^{10}Be. ^{26}Al is produced more near the surface of Earth than ^{10}Be.

Table 3: Values of path parameters used in the forward model. Adapted from Vermeesch (2007).

	Neutrons	**Slow muons**	**Slow muons**	**Fast muons**
Attenuation length Λ_i ($\mathbf{g\,cm^{-2}}$)	160	738	2688	4360
Relative production F_i (^{10}Be)	0.9724	0.0186	0.004	0.005
Relative production F_i (^{26}Al)	0.9655	0.0233	0.005	0.0062
Relative production F_i (^{14}C)	0.83	0.0691	0.0809	0.02

Table 4: Values of constants used in the forward model.

	Production rate (atoms g^{-1} a^{-1})	**Reference**	**Half life (a)**	**Reference**
^{10}Be	3.95	Stroeven et al. (2015)	1 387 000	Korschinek et al. (2010)
^{26}Al	26.71	Stroeven et al. (2016)	705 000	Nishiizumi (2004)
^{14}C	15.5	Miller et al. (2006)	5730	Dunai (2010)

3.3 Inverse model

The inverse model is based on the forward model. It calculates the possible ice coverage histories when the concentration and the depth of a sample are known. It can handle samples from several depths. In this thesis, the inverse model is used in a synthetic case, where the samples are taken from the forward model.

The steps in the inverse model begin with the calculation of an acceptance box (Figure 7). The box is defined based on the nuclide concentration and thickness of the sample. In a synthetic case, the samples are created from the forward model, and each sample forms its own box. After that, a new forward model is calculated by using random times for glaciations. These times are possible inverse solutions. If the concentration curve, based on the glaciation times, goes through the acceptance box (Figure 7) for all of the samples, the times are accepted as a possible inverse solution, and the misfit value is calculated. The inverse model returns arrays that contain information on the tested times and their misfit values. If the model is not accepted, the misfit value is not calculated at all because the calculation of the misfit value is based on the similarity of the curves inside the acceptance box. All of the steps are also presented in Figure 8.

The needed information to calculate the inverse model is provided in Table 5. At this point, the inverse model uses synthetic samples from the forward model. Therefore the deglaciation and glaciation times are needed as input values even though the forward model is used as a real sample.

It is possible to choose the times for the inverse model randomly. It requires that the maximum number of deglaciations is defined as the complexity of the model. The random times generator produces time combinations that are tested for the solution. As input values, generator needs the complexity of the times that are looked for, the maximum and minimum times for the solution and if there is some other conditions for the duration of one glaciation or the duration between glaciations. Here it is assumed that the duration for both glaciation and interglacial period can be the same, and its default value is set to be 0.5 ka. Also, the lower limit for the time has

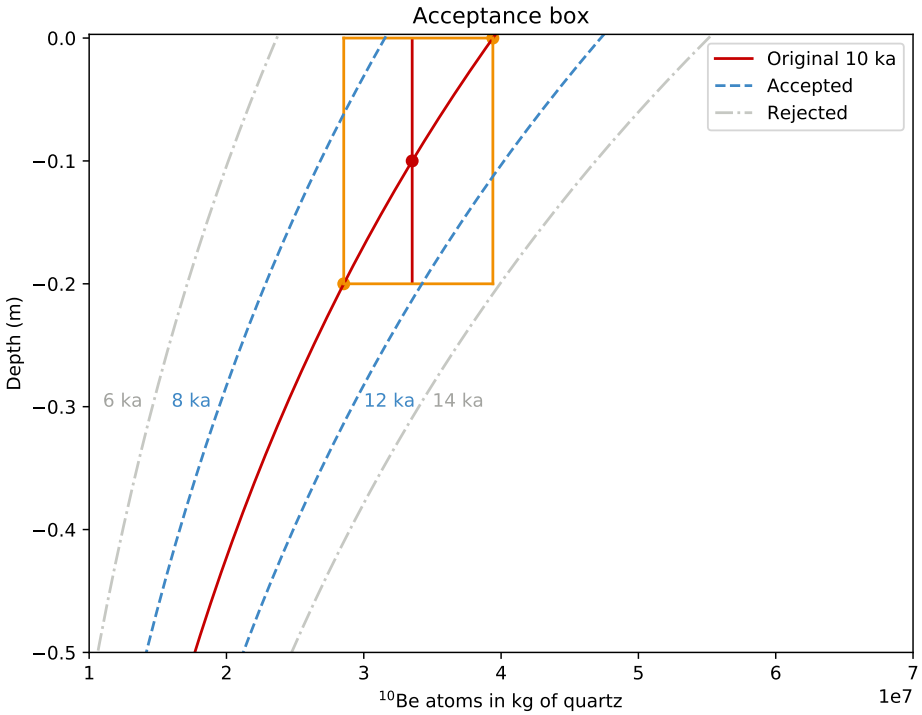

Figure 7. Acceptance box is formed from the thickness of the sample and corresponding nuclide concentration values. Models are accepted if they cross the orange box. Grey dash-dotted curves are not accepted, but the blue dashed curves are. The red solid curve is the reference curve.

a default value of 0. The random times generator then finds times that fulfill the conditions. The generator sets the exposure times first, and after that, it will set the glaciation times between the known exposure times. If the complexity is set to be 3, it will find time ranges with three deglaciation events. Finally, the generator tests that the chosen times pass the conditions for the durations. If it does not pass it, the times are generated again. When the chosen times are good enough, the output is two arrays of deglaciation and glaciation starting times that are then used in the inverse model.

Models are accepted if their concentration curve goes through a box which size depends on the error of depth (Figure 7). The error can be chosen manually, and it is one of the parameters needed to run the inverse model. Each sample has its own box, and to be accepted, the curve must pass through all of them, which means that it must be accepted at every sample depth. The model is rejected if the curve does not pass all of the boxes. For example, Figure 7 has a sample from a depth of 0.1 m with an error of ±0.1 m. The error is the same thing as the sample thickness. The box is formed based on the depth error by finding the corresponding concentration values from the same depth of the original 10 ka exposure curve. These concentration values

Table 5: Variables used in the inverse model.

Input					
Variable name	**Description**	**Unit**	**Example**	**Type**	**Note**
`z_chosen`	Sample depths	m	[0,2]	NumPy array	
`z_error`	Error in sample depth	m	0.05	Float	
`isotope`	Used isotope. 1 ^{10}Be, 2 ^{26}Al, 3 ^{14}C		1	Integer	
`time_ice_fwd`	Ice coverage starting time in forward solution	ka	[25,0]	NumPy array	
`time_degla_fwd`	Deglaciation starting time in forward solution	ka	[35,10]	NumPy array	
`erosion_fwd`	Erosion at the deglaciation in forward solution	m	[2]		Length 1 value shorter than `time_degla`
`time_ice_inv`	Ice coverage starting time in forward solution	ka	[25,0]	NumPy array	Default value: None
`time_degla_inv`	Deglaciation starting time in forward solution	ka	[35,10]	NumPy array	Default value: None
`erosion_inv`	Erosion at the deglaciation in forward solution	m	[2]		Length 1 value shorter than `time_degla`. Default value: None
`complexity`	Number of deglaciations in the inverse solutions		1	Integer	Default value: 1
`tied`	Last deglaciation time tied	ka	10	Float	Default value: None
Output					
`free_para`	Free parameters: isotope		[1]	NumPy array	
`all_info`	Deglaciation and ice coverage times, erosion	ka, m	[12.8,5.1,10.8,0,2.0]	NumPy array	
`misfit`	Total misfit value for all samples		1200	Float	
`misfit_arr`	Misfit values for each sample and their sum		[700, 500, 1200]	NumPy array	

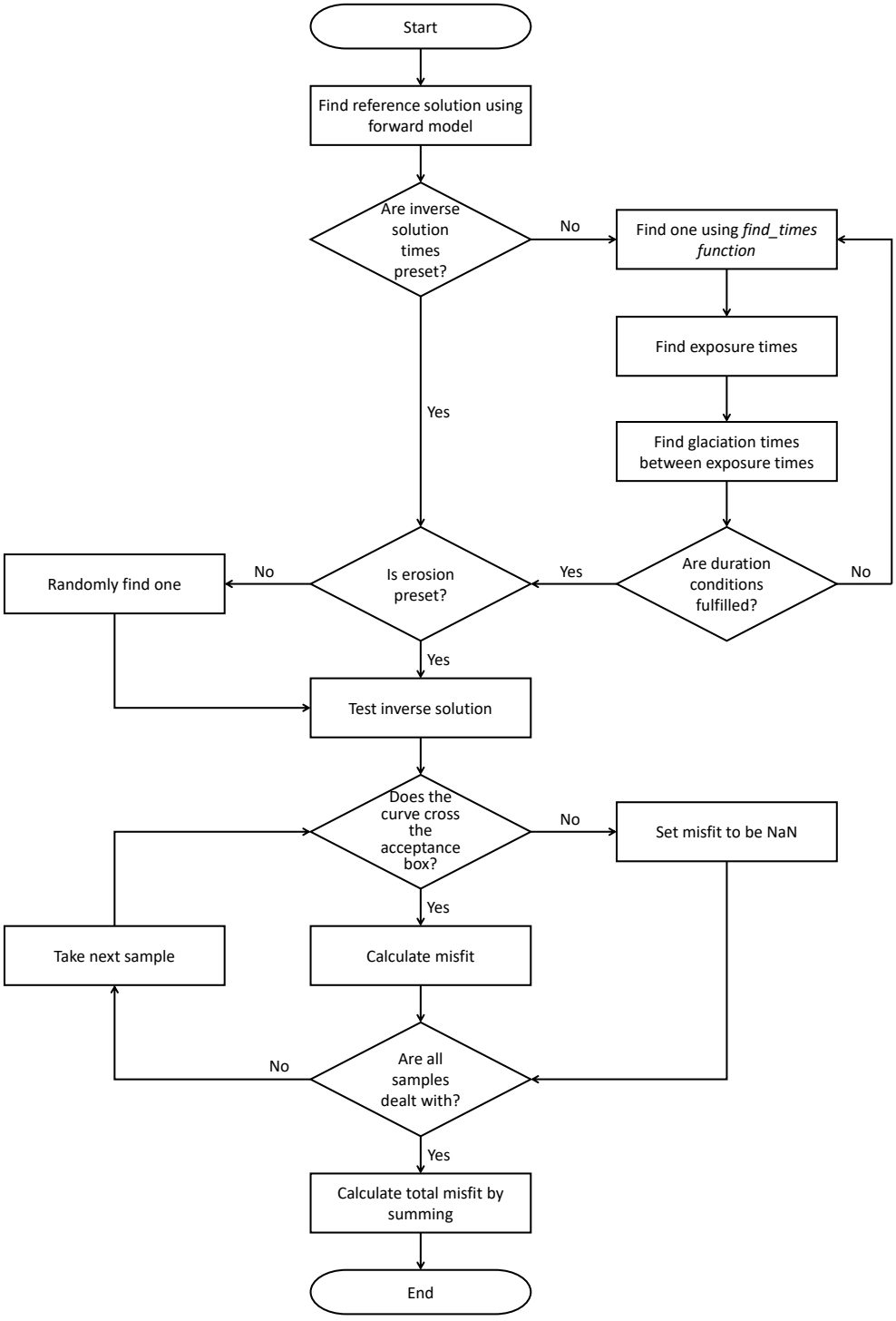

Figure 8. Flowchart of the inverse model

form the corners of the acceptance box. The other two corners are formed based on the now known maximum and minimum concentration values and the maximum and minimum depths. If the first two corners are maximum depth and maximum concentration, and minimum depth and minimum concentration, then logically, the

other two are minimum depth and maximum concentration, and maximum depth and minimum concentration.

The models that are fitted to the reference model can have one to four exposure periods. The model with one exposure contains only one deglaciation after infinite glaciation, and therefore it has only one exposure period. That model can not have erosion since it would not matter because there are no inherited nuclides. It also does not have any additional glaciation periods. Similarly, two exposure model has two deglaciations and two exposure periods between glaciations. It can have erosion only once at the last deglaciation. Between the two deglaciations, it has one glaciation. The number of erosions and glaciations are then always one smaller than the number of deglaciations. With the same patter, three exposure models have three deglaciations, three exposure periods, two glaciations and two erosions. Four exposure models have four deglaciations and exposure periods and three glaciations and erosions.

3.4 Misfit

There are several ways to define how well a curve fits another curve or discrete data points. One way is the Chi-Squared test, which tests how well expected values represent observed values. Taylor (1997) presents the base for the Chi-Squared test by focusing on the difference between expected and observed values.

$$O_i - E_i \tag{3.7}$$

where O_i is the observed value in bin i, and E_i is the expected value in bin i. If the difference is small, the fit should be better than if it would be large. The difference must be normalized so that the fit would be more exact and more easily to be compared to other fit values. It is assumed that the observed values will fluctuate around the expected value with a standard deviation of $\sqrt{E_i}$, which is the expected size of the fluctuations.

$$\frac{O_i - E_i}{\sqrt{E_i}} \tag{3.8}$$

Probably some of the observed values will be smaller than the expected value, while some of them will be larger. To cancel the effect of positive and negative numbers, Equation 3.8 should be squared for each bin i (Taylor, 1997). That will produce the number called chi-squared.

$$\chi^2 = \sum_{i=1}^{n} \left(\frac{O_i - E_i}{\sqrt{E_i}} \right)^2 = \sum_{i=1}^{n} \frac{(O_i - E_i)^2}{E_i} \tag{3.9}$$

where the n is the total number of bins. If the observed and expected values are the same, the value of chi-squared will be zero.

A modified version of chi-squared can also be used. There instead of eliminating the effect of positive and negative values by squaring, they are eliminated with taking an absolute value of the difference.

$$\text{gof} = \sum_{i=1}^{n} \frac{|O_i - E_i|}{E_i} \tag{3.10}$$

I have used another modified version of Equation 3.9 in this thesis.

$$\text{misfit} = \sum_{i=1}^{n} \frac{\sum_{i=1}^{N} |O_i - E_i|}{N} \tag{3.11}$$

The n, in this case, is the number of samples taken, and N is the number of points compared. This method compares two curves, forward and inverse solution, to each other and normalizes it with the number of points. Its benefits are that (1) it takes into account the average distance of the curve and the sample, and (2) it also works in a situation where the depth of the sample and the curve is not exactly the same. The first benefit is important because then the misfit value is truly based on the distance between the sample point and the curve. The second benefit is significant since the number of points compared from the curve is not constant. The curve may pass the acceptance box briefly, and then the number of data points inside the box is small. Then if that is compared to another solution that has more data points inside the box, the misfit value will be poorer even if the fit would actually be better.

An example of the misfit is presented in Figure 9. The forward model contains one exposure 10 ka years ago. The inverse model uses one 20 cm thick sample at a depth of 0.1 m, the same situation as in Figure 7. The best misfit value is gained at the correct exposure time 10 ka. The age range of accepted models varies from 7.3 ka to 13.7 ka, which means that the error of the acceptance is asymmetric. There are more accepted models with higher ages than the best fitting age. The asymmetry is due to the curvature of the concentration curves and the shape of the acceptance box (Figure 7).

3.5 Realistic glaciation history

Realistic glaciation history contains two exposure periods, one between 25 and 35 ka ago and the second from 10 ka to the present day. The total exposure duration is the sum of interstadials and time since deglaciation, and its value is 20 ka in this history. It is assumed that before 35 ka, there has been only ice coverage, Second Mid-Weichselian, and the concentration of the cosmogenic nuclides is zero before that (Figure 10). This assumption is a simplified version of the history presented in Section 2.2.1. This is the reference model used in most of the results. If the simplified history has erosion, it will occur between the points C and B in Figure 10, where at the onset of the Late Weichselian deglaciation. Theoretically, erosion could also occur at point D, deglaciation of Second Mid-Weichselian. Because there are no inherited nuclides due to the assumption of the infinite duration of glaciation, the erosion would not have any effect to the concentrations. Notice that the ordinal number used are referring to chronological order. If the event is "first", it has occurred first in the glaciation history and before the second event. The first deglaciation has occurred before the second deglaciation. It is also assumed that

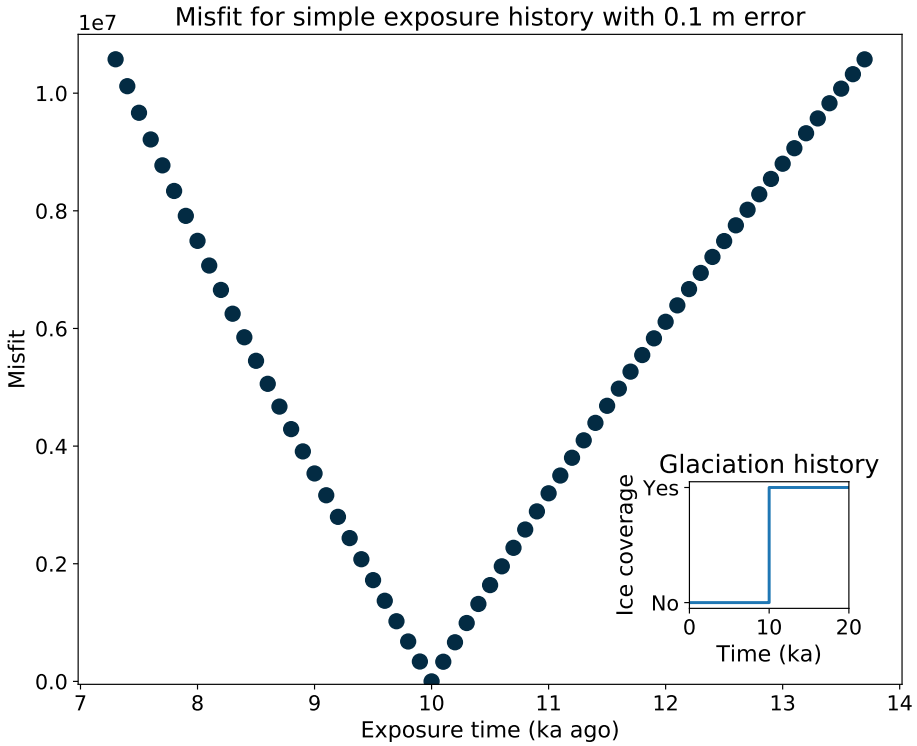

Figure 9. Misfit as a function of exposure age. Accepted inverse models when the forward model has exposure 10 ka ago and infinite ice cover before that. The error of the sample is 0.1 m. The best fit is 10 ka. The range of accepted models varies from 7.3 ka to 13.8 ka.

the deglaciation happens before the corresponding glaciation, and therefore the first deglaciation is an earlier event than the first glaciation.

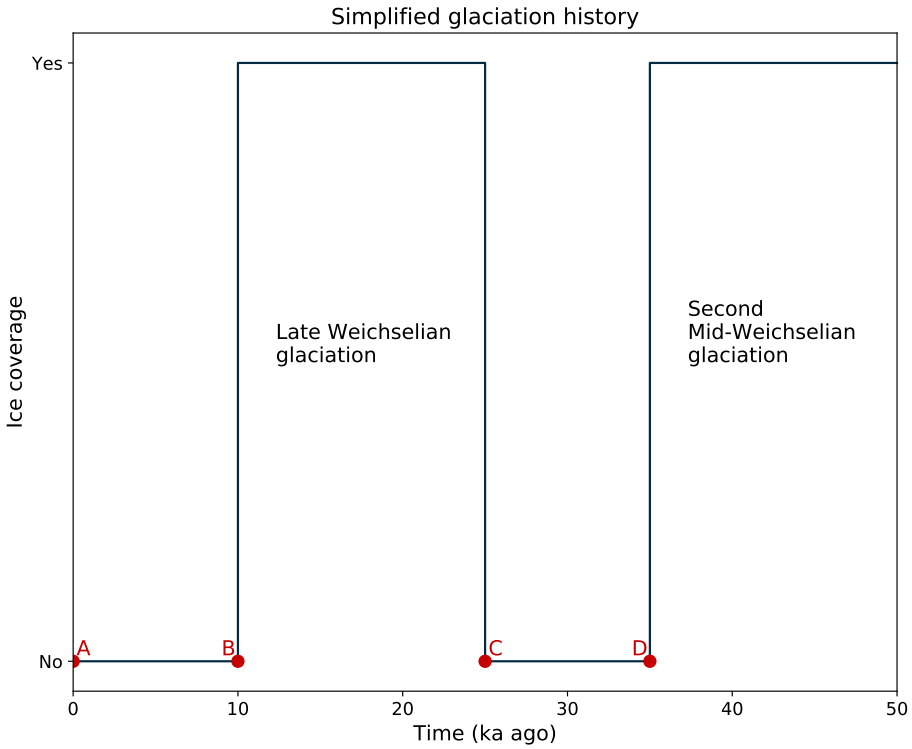

Figure 10. Simplified glaciation history based on Johansson et al. (2011). Point A is the present day and the ending time of the last exposure period. Point B is the ending time of the last glaciation, Late Weichselian deglaciation, and point C is the starting time of the Late Weichselian. Point D is the starting time of the second last exposure period, interglacial between Second Mid-Weichselian and Late Weichselian glaciations. It can also be called the Second Mid-Weichselian deglaciation. Point C could also be called the first glaciation and point D, the first deglaciation.

4 Results

In this section, I am going to present what can be done with the forward and the inverse model. At first, I am going to show how the sampling thickness and depth affect the accepted solutions when there is not erosion present. Then I am demonstrating different cases for how the erosion and other parameter limitations influence the solutions. Finally, I show which kind of models are accepted when the samples are taken from different depths, and there has been erosion present. Parameter values used in each section can be found from Appendix 6 Table A1. I have used only one isotope, ^{10}Be, in every section.

4.1 Simple exposure history and error in depth

Simple exposure history contains just one deglaciation. The assumption was that the latest exposure was the only exposure that the rock experienced. At all other times, it had been buried beneath a thick ice sheet without any interaction with cosmic rays. To understand the working principle of the inverse model, the model was tested with this simple exposure history. The test sample experienced one exposure period, which began 10.0 ka ago. Before that, there had not been any exposures, which meant that there were no inherited nuclides at all. It was assumed that during the exposure, there had not been any shielding or coverage. Thus, all cosmic rays coming from the space had interacted with the bedrock. The question now was which kind of simple models were accepted with these assumptions. If the model works correctly, the time of deglaciation should have the best fit.

Figure 11 presents the misfit of the accepted models as a function of time with different errors in depth. If there was no error in sampling depth, the sample could be thought to be point-sized. Then the only accepted inverse solution was the exact time of deglaciation at 10.0 ka ago, and the absolute misfit value was zero. When the error in depth was increased, the sample size was increasing as well. The error of ± 2.5 cm corresponds to the thickness of 5.0 cm. The number of accepted models and the misfit value were increased with thickness. The variation of exposure time

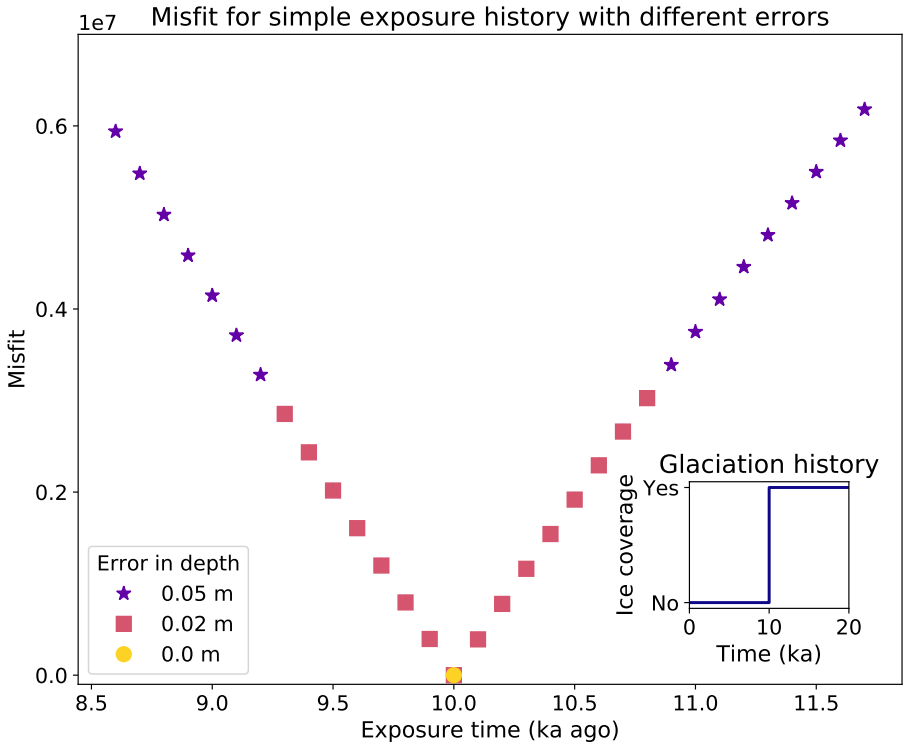

Figure 11. Misfit as a function of exposure time with different errors in the sample depth. The glaciation history is presented in a smaller figure. The deglaciation was at 10.0 ka ago, and before that, there had not been any exposure. The only accepted model is the same as the real history if there is no error in the sample depth. If the error in depth is 2.5 cm, then the variation of accepted ages is larger. The 5 cm error causes the largest variance in the acceptance.

was $10^{+0.8}_{-0.7}$ ka when the error in depth was ±2.5 cm. When the error was increased to ±5 cm, also the range of accepted ages was increased to $10^{+1.7}_{-1.4}$ ka. The error of accepted solutions is asymmetrical (Figure 11). More solutions were accepted with higher than lower age. This was caused by the acceptance method presented in Section 3.4.

The absolute misfit value depends on the depth of the sample. If the sample is near the surface, its isotope concentration is higher, and thus also the misfit value is higher since it depends on the concentrations (Equation 3.11). Sample in Figure 11 was taken at 10 cm depth, so its misfit values are rather large, magnitude of 10^6. The models with the highest misfit values have the poorest fit to the original model. When the error is doubled, also the misfit value is doubled. The value of misfit also depends on the error used for the sample depth (see section 4.2). Based on these results, the inverse model is working correctly and can be used with more complicated situations.

4.2 Sample depth and number of samples

Simple glaciation history was also used to study the effect of sampling depth. Figure 12 displays accepted models with different sampling depths when the original model had one exposure 10 ka ago. The sample thickness was assumed to be ±5 cm. Samples were taken at the surface and depths of 1.0 m, 2.0 m and 3.0 m. All the samples had the best fitting age at 10 ka, which was the time of exposure in the original model. The age range of accepted models was largest when the sample was taken at the surface, $10^{+1.7}_{-1.4}$ ka. Then the youngest accepted model was 8.6 ka, and the oldest was 11.7 ka. When the depth was increased, the range diminished. At 1.0 m depth, only the upper boundary was decreased with 100 years to $10^{+1.6}_{-1.4}$ ka. At 2.0 m depth, the decrease was more significant, and the accepted solutions were $10^{+1.2}_{-1.1}$ ka. At 3.0 m, the range of accepted models was decreased to more than half of the accepted surface age range, $10^{+0.7}_{-0.6}$ ka. This indicates that the depth of the sample controls the solutions that are accepted. Near the surface, there are more possible solutions than in deeper depths, although there was no difference between a surface sample and a sample from 1.0 m depth.

The absolute value of misfit depended greatly on sampling depth. The best misfit value in all of the samples was zero at the age of 10.0 ka. In other ages, the misfit was poorer. At the surface, the highest misfit value was $3.0 \cdot 10^6$. The value decreased rapidly with sampling depth. Already at 1.0 m, the misfit was decreased to $0.6 \cdot 10^6$ and at 3.0 m, the largest misfit was $0.2 \cdot 10^6$.

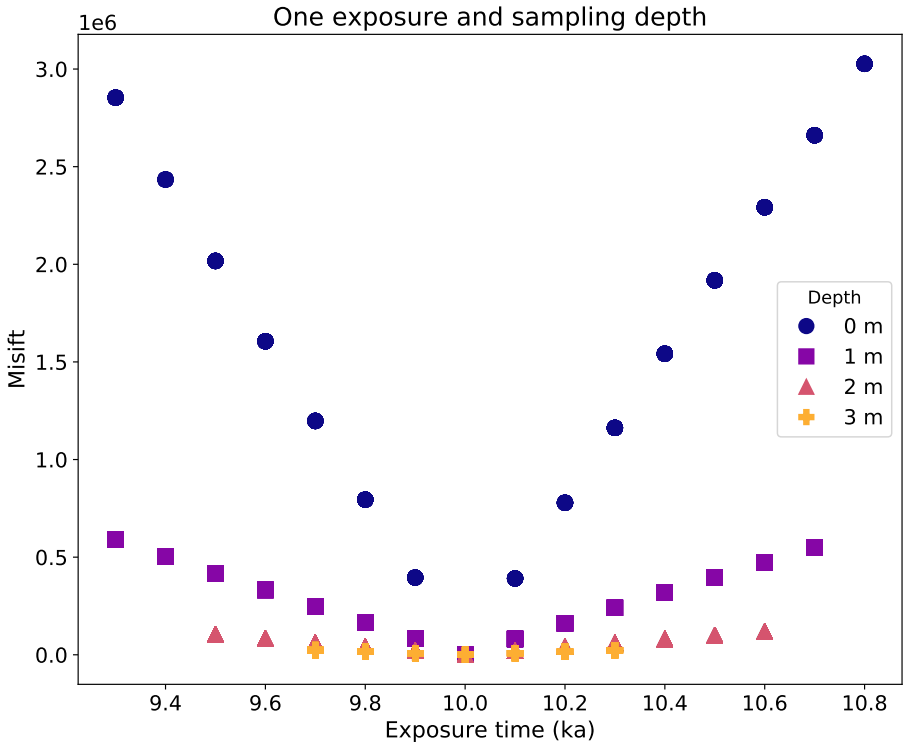

Figure 12. Exposure time as a function of the misfit. Each marker presents one sample taken at different depths and shows the accepted solutions for a simple 10.0 ka exposure model. The sample at the surface has the broadest range of accepted models, whereas the deepest sample at 3.0 m has the least number of accepted models. Misfit has a minimum at the 10.0 ka in each case. The error in depth is ±0.25 m.

4.3 Realistic exposure history without erosion

The effects of possible glaciation histories were studied by comparing different models to the realistic glaciation history (Figure 10). The realistic history had a total exposure time of 20.0 ka and the last deglaciation at 10.0 ka. The first deglaciation was at 35 ka, so in total, there were two exposure periods. When the realistic model did not have erosion at the end of the last glaciation, the best fit of the one exposure model was $19.9^{+1.6}_{-1.5}$ ka (Figure 13). One exposure models have the same duration for both last exposure and total exposure. The best fitting time was close to the total exposure time of the reference model and it differed from the actual timing of the last exposure. If the reference model did not have erosion, the one exposure model revealed the total exposure time.

Two exposure models (Figure 13) showed somewhat different behaviour when the last deglaciation time was presented as a function of total exposure time. The best

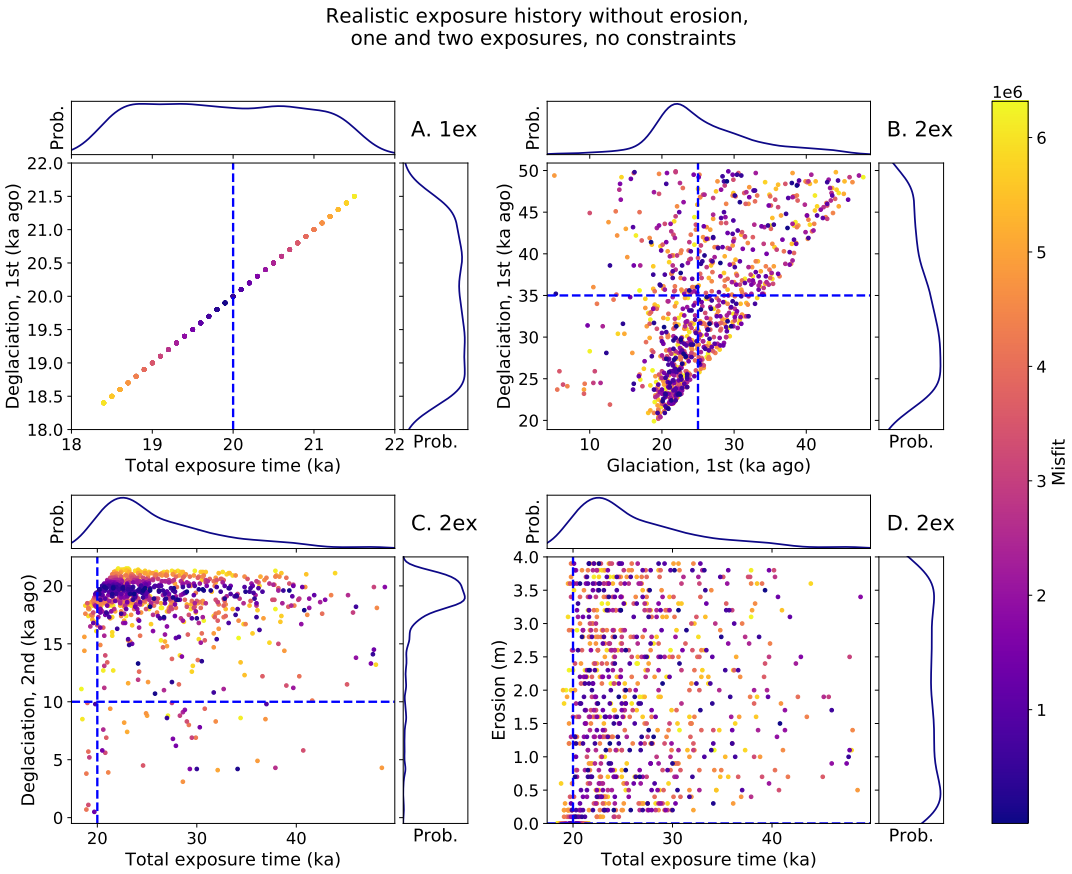

Figure 13. Realistic history without erosion compared to the one and two exposure models. The limitation for the maximum duration of the model was 50 ka, and the maximum erosion was 4.0 m in one glaciation. The models can have erosion, even if the reference model did not have. Each dot presents one model, and its color presents the misfit value so that darker corresponds to a smaller and better misfit value. The blue dashed line presents the parameter values used in the reference model. Density functions are shown adjacent to the axes for each parameter. A. One exposure model. The total exposure time is the same as the last deglaciation time. The best fit is at 19.9 ka, which differs from the expected value. B. Two exposure model. The first glaciation and deglaciation. There are several very different combinations that have a good fit. The glaciation values are concentrated below 30 ka, while the deglaciation has a wider range of values. C. Two exposure model. The last deglaciation has the best fit around 20 ka, while the total exposure time varies from 18 to 50 ka. D. Two exposure model. Erosion varies from 0 to 4 m, and the best solutions are widely spread.

fitting last deglaciation time was the same than in one exposure models, but the range of total exposure time was different. The last deglaciation had a minimum misfit around 20 ka, but the small misfit values were also reached between 5 and 15 ka. The total exposure time had a huge variation from 18 to 50 ka. It also seemed that there was not an area of best fit for the total exposure time. Most of the values were concentrated below 30 ka. In other words, it seems that the model is more sensitive to the total exposure duration than the deglaciation time when there is no erosion present in the reference model. The same trend can also be observed from the three and four exposure models (Figures B1 and B2).

Figure 14 presents what kind of models are accepted. The two exposure models could have an identical solution with the reference model, but in reality, the models differed from the reference quite much. The last deglaciation began between 18 and 20 ka, while in the reference, it began at 10 ka. Also, the deglaciation before that or the glaciation starting time did not fit the reference model. The accepted models had erosion, while the reference did not. It seems that when there is no erosion in the reference, the accepted models are sensitive to the total exposure duration rather than the timing of deglaciation.

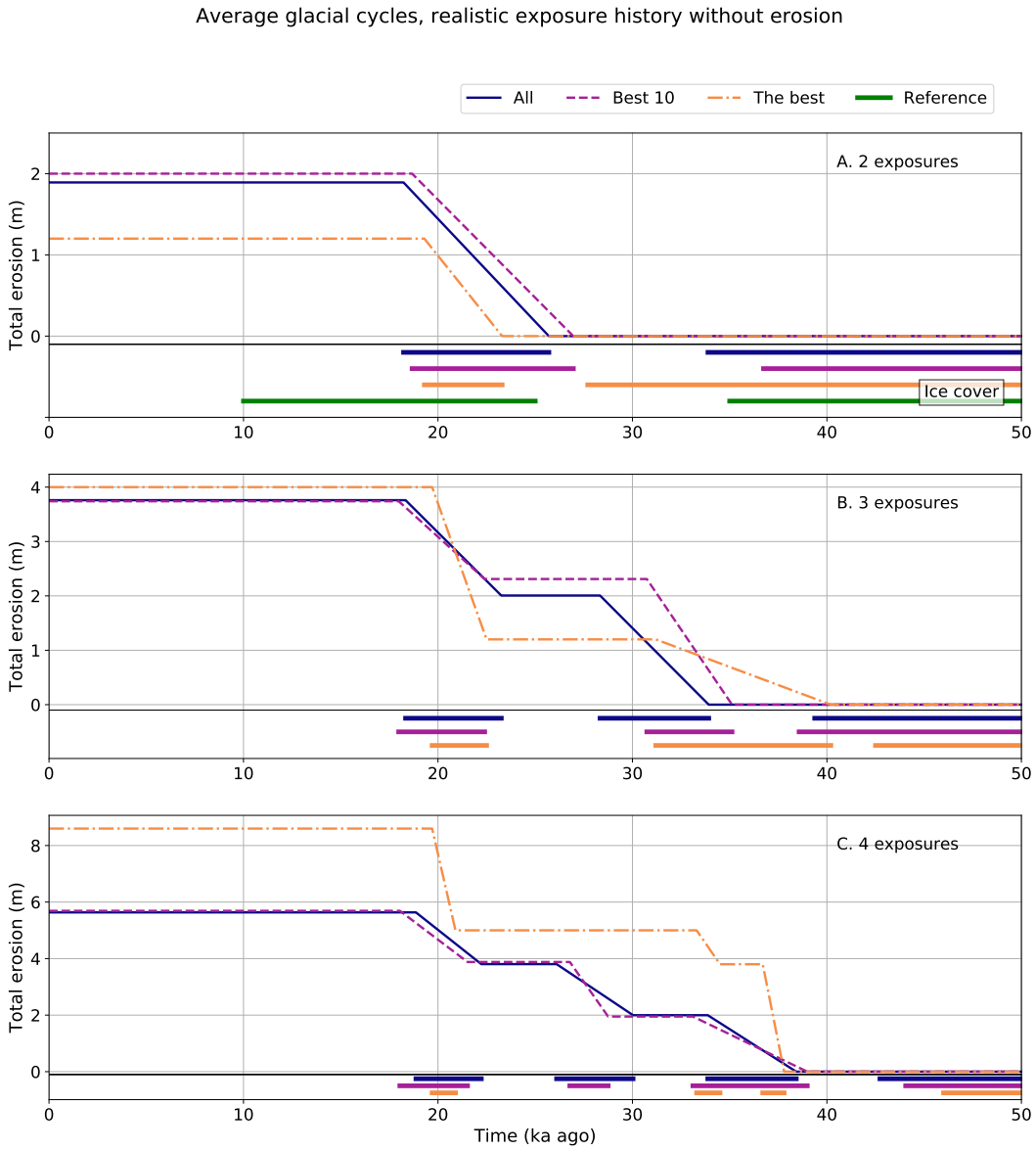

Figure 14. The glacial cycles of all the model types. The curve "All" (solid, dark blue) refers to an average of all accepted models. "Best 10" (dashed, violet) presents ten solutions that had the the smallest misfit value. "The best" (dot-dashed, orange) displays the solution with the smallest misfit and the "reference" (dotted, green) is the realistic glaciation history. The y-axis is the total amount of erosion experienced during the glaciations. The erosion rate can be observed from the slope. During an interglacial, there is no erosion, and the rate is then 0. The x-axis is time, and 0 refers to the present day. Thick lines in the bottom of each figure are presenting the glaciation history. The solid line is the glaciation, and the white area is an interglacial. A. Two exposures. The amount of erosion and the last deglaciation time fit relatively well to the reference model when all of the models or the best ten models are averaged. The best model has a very different solution than the reference model. B. Three exposures. The total erosion is much larger in each case than in the reference model, but the amount of erosion during the last glaciation is rather good in "All" and "Best 10" averages. The last deglaciation is relatively precise in the average of all of the models. The duration of the last glaciation is short in the best model. C. Four exposures. All of the cycles have rather good fit the last deglaciation of the reference model, but the total erosion is too large. The amount of erosion during the last glaciation is almost the same in the "All" than it is in the reference. The best solution has a relatively small amount of erosion in the end.

4.4 Realistic history with erosion

The other, and more likely, option for realistic history is to include erosion during the glaciation. The realistic history has two exposure periods from 0-10 ka and 25-35 ka with 2.0 m erosion during glaciation 10-25 ka. In these models, I have chosen to use the erosion value of 2.0 m because that could have been the real amount that has been eroded (Li et al., 2005). It may have been higher or lower than that, but it is a rough estimate and suitable for the testing of the models. The erosion occurs during the glaciations except for the infinite one. If the erosion is constant, the amount of rock eroded is the same in every glaciation. If the erosion has a random value, it can be anything between 0 and 4 m unless stated otherwise. In this section, I have tested different kinds of parameter combinations to find out which of them produce acceptable solutions. I am going to start with the most strict limitations and loosen them gradually.

4.4.1 Tied last deglaciation and constant erosion

The first step with the limitations was to preset a value for erosion and last deglaciation. Erosion was set to be 2.0 m, which is the same as in the reference model. The last deglaciation was fixed to 10.0 ka. The fixed deglaciation limits the one exposure models and they do not have any variation. Therefore they are not presented in here.

Two exposure models showed sensitivity to the total exposure time around 20 ka (Figure 15), which is the same value as in the reference model. Still the results did not confirm anything sure of the past glaciations because the range of values for the last deglaciation was wide, between 20 and 50 ka. It could be said that the timing of the second last deglaciation must have occurred more than 20 ka ago, but the exact time can not be found. To find more precise information, there must be at least an educated guess of the duration of the latest glaciation.

Three exposure model results were also good with these strict constraints (Figure B3). Similarly than in two exposure case, the last glaciation and the second last deglaciation had a linear dependency. The best fit was reached with a combination where the total exposure duration and the second last deglaciation were both at least 20 ka. This indicates, that we can found the time when the second last deglaciation could have earliest occurred.

The results of the four exposure models were relatively similar to three exposure models. Nothing sure could be found, but it set some constraints to the possible

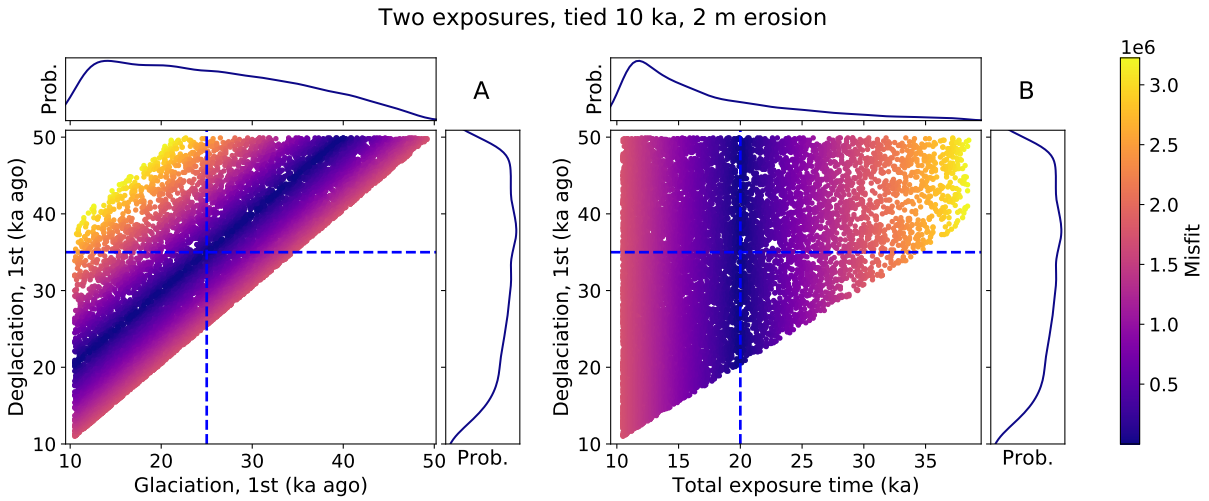

Figure 15. Two exposure models with tied last deglaciation and constant erosion. The maximum exposure time was limited to 50 ka. Each dot presents one model, and its color presents the misfit value so that darker corresponds to a smaller and better misfit value. The blue dashed line presents the parameter values used in the reference model. Density functions are shown adjacent to the axes for each parameter. A. The first glaciation and deglaciation are directly proportional to each other. B. The total exposure time remains constant at 20 ka when the timing of the last (and only) deglaciation time increases.

solutions. The duration of total exposure should be over 20 ka to have a small misfit value (Figure B4), and also, if the duration of the latest glaciation was known, the previous deglaciation can be detected.

While the scatter plots did not seem to reveal too much of the previous glaciations, the figure of average glacial cycles did. The glacial cycles had an excellent result when the limitations were extensive. The two exposure models had almost perfect timing in the starting time of the glaciation. The first deglaciation was also detected well (Figure 16). Only the average of ten best models had a bit longer duration of the glaciation than in the reference model. The best model with the smallest misfit value differed only by 200 years in the first deglaciation. That is the most precise result that was achieved. The average of all could also predict the second last deglaciation rather well.

Three and four exposure models did not provide as good results even though the starting time of the glaciation of the best solutions was rather close to the reference model (Figure 26). Surprisingly also, the best solution for the first deglaciation in these models seemed to be relatively close to the reference model. Four exposure models did not fit to the reference model at all.

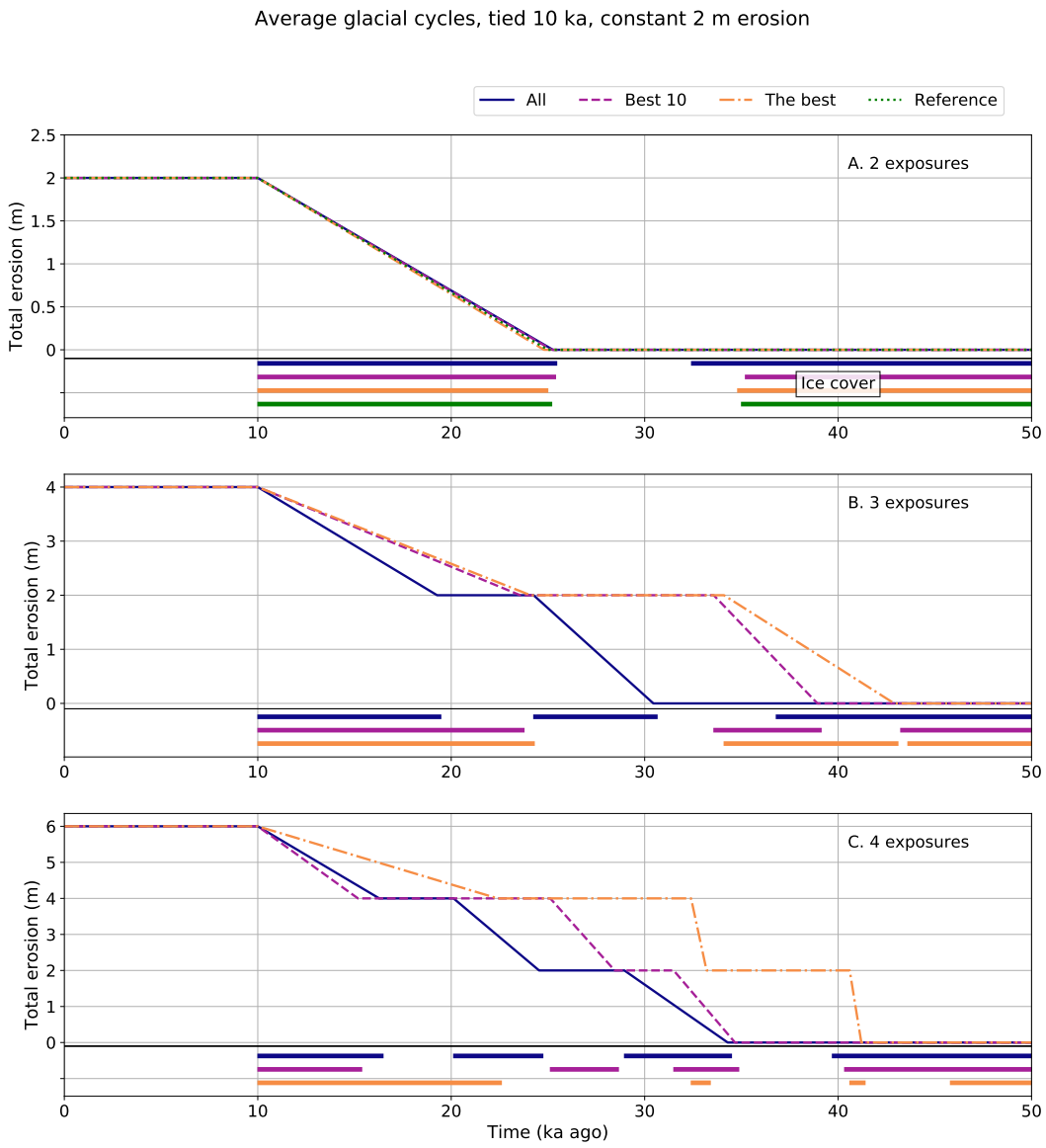

Figure 16. Average glacial cycles when the solutions have constant 2.0 m erosion, and the last deglaciation is tied to 10 ka. See the explanations from Figure 14. A. The glaciation period is fitting well with the reference model in all of the cases. The first deglaciation is also detected rather well since the difference to the reference model is only a couple hundred years. The second last deglaciation can not be dated as well as the glaciation starting time, but the values are close. B. Three exposure models also find the start of glaciation relatively well except the average of all. Other timings are not so good. C. Four exposure models have a large variation in the solutions, and they do not fit to the reference model except for the best solution.

Sample depth of 2.0 m

The special case of models with tied deglaciation and constant erosion was the increase of the sample depth to 2.0 m. Two exposure models with these limitations seemed to be sensitive to the total exposure time (Figure 17), which had the best fit at 20 ka. It seems that deglaciation is sensitive to the timing of glaciation. The patterns in both cases were similar to the surface sample except they were narrower and the absolute misfit value was smaller.

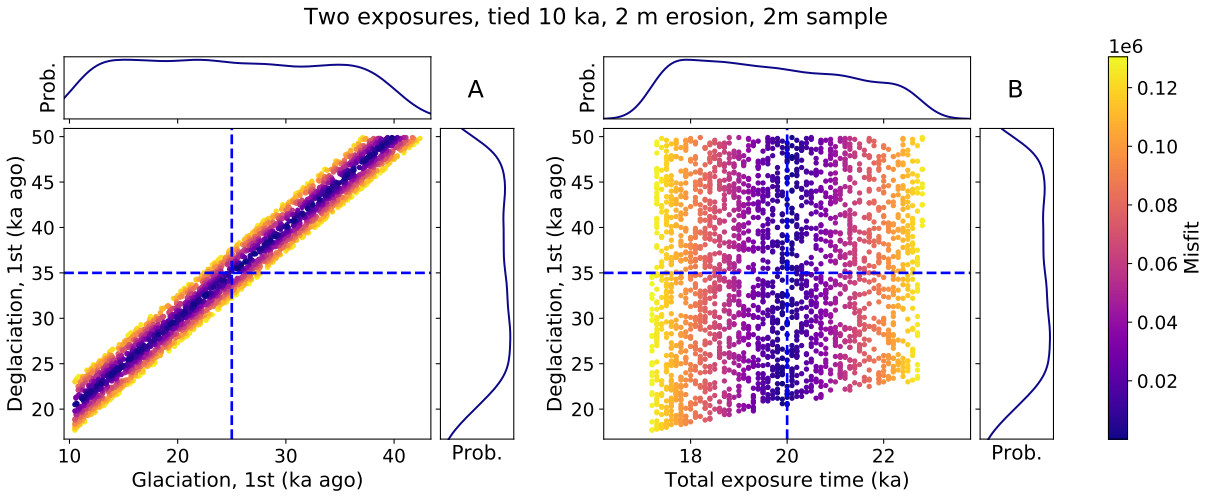

Figure 17. Two exposure models with tied last deglaciation, constant erosion and sampling depth of 2.0 m. The maximum exposure time was limited to 50 ka. Each dot presents one model, and its color presents the misfit value so that darker corresponds to a smaller and better misfit value. The blue dashed line presents the parameter values used in the reference model. Density functions are shown adjacent to the axes for each parameter. A. The first glaciation and deglaciation are proportional to each other. The best fit zone is in the middle, and it is relatively wide compared to the whole width of the zone of accepted solutions. B. Total exposure time and second last deglaciation. The total exposure time has the smallest misfit value around 20 ka, while the deglaciation varies from 15 to 50 ka.

Three and four exposure models have rather similar results than they had with the surface samples except the ranges are narrower, and there are less accepted models (Figures B5 and B6).

The average of two exposure models provided a great fit when compared to the reference model (Figure 18). The model could almost correctly predict the timings of the first glaciation and the beginning time of the second glaciation. The best solutions, which had the smallest misfit values, did not provide as good result even though that might have be the presumption. The three and four exposure models did not seem to have any useful information since their timings were rather far from the reference model.

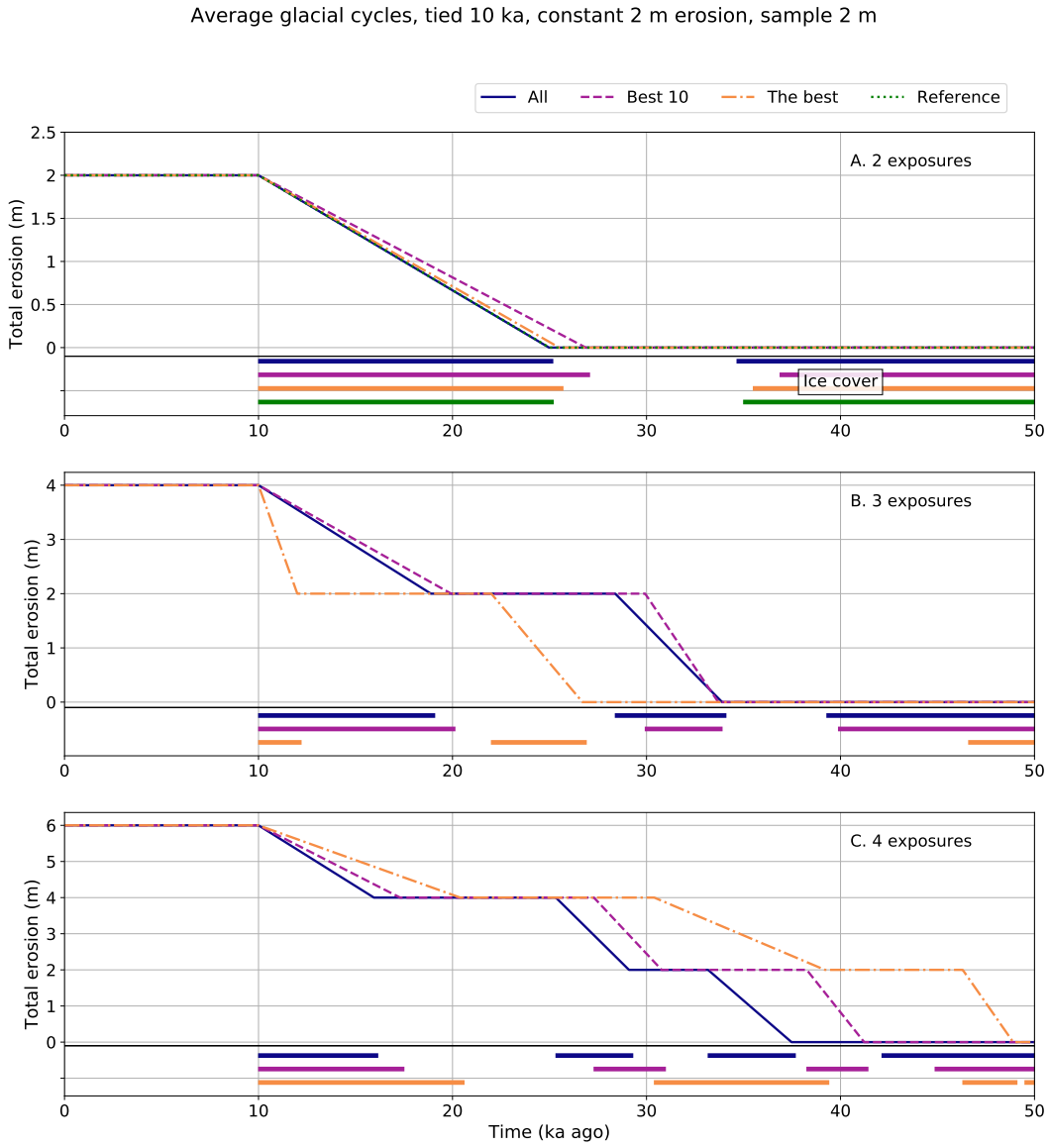

Figure 18. Average glacial cycles when the solutions have constant 2.0 m erosion, and the last deglaciation is tied to 10 ka. See the explanations from Figure 14. A. The average of all accepted two exposure models fits almost perfectly to the reference model. The solutions with the best misfit values do not fit to the reference model as well. B. Three exposure models are not sensitive to the beginning time of the glaciation or to other glaciations. C. Four exposure models also have a rather poor fit to the reference model.

4.4.2 Tied last deglaciation and random erosion

The last deglaciation was tied to 10.0 ka to observe how the erosion varies. This could occur also in reality if the deglaciation has been dated with other dating methods like using radiocarbon or varve dating. The amount of erosion was limited to 4.0 m maximum ,and the total exposure time was limited to 50.0 ka.

This approach meant that there was no variation in the one exposure solutions since the only deglaciation was tied. Two exposure models had a connection between the amount of erosion and the total exposure time (Figure 19). When the erosion increased, also the total exposure time increased. The best fit was increasing logarithmically, and the smallest misfit value was reached at total exposure time of 21.1 ka and erosion of 2.1 m. These values are close to the reference model values 20.0 ka and 2.0 m.

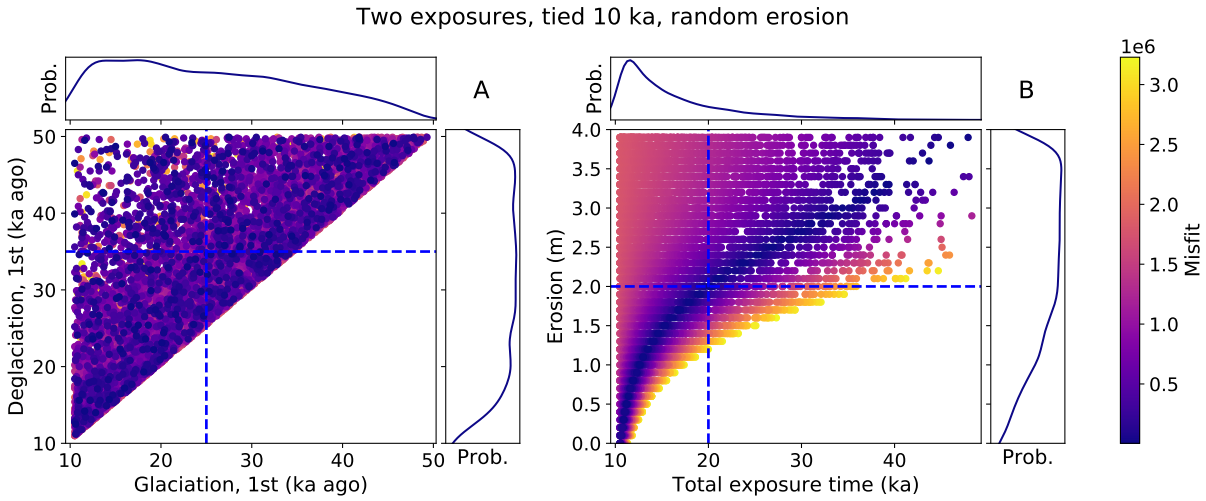

Figure 19. Two exposure models with tied timing of last deglaciation and randomly selected erosion fitted to realistic history with 2.0 m erosion. The maximum exposure time was limited to 50 ka. Each dot presents one model and its color presents the misfit value so that darker corresponds to a smaller and better misfit value. The blue dashed line presents the parameter values used in the reference model. Density functions are shown adjacent to the axes for each parameter. A. The timing of deglaciation and glaciation do not have a clear pattern of the smallest misfit. The values are rather uniformly distributed between 10 and 50 ka. B. Erosion and total exposure time form a distinct area of the smallest misfit. When erosion increases, also the total exposure time increases.

Three exposure models provided rather similar results than the two exposure models. Deglaciation and glaciation timings seemed not to have too much sensitivity, but the last erosion and total exposure time certainly did (Figure B7). The dependency was also logarithmic, although not as clear as in the two exposure cases. When the erosion increased, also the total exposure time increased.

The four exposure models did not provide too much new information. The most

significant results were that the erosions before the last one did not seem to be affecting the end result (Figure B8). There the values varied from the minimum to the maximum without any pattern. Another interesting result was the last erosion and the total exposure time. It looked rather like the three exposure model version except the best fitting points were concentrated on smaller values of erosion.

Even though the last deglaciation was tied to 10.0 ka, the glaciation cycles were not too sensitive to the reference model before the last glaciation (Figure 20). The amount of erosion was close to the reference model, but the timing of the last glaciation varied much, even in the two exposure models. The best two exposure solution was really far from the reference, although the amount of erosion was close. The average of all models was relatively close to the reference, and the starting time of the glaciation was almost the same as the reference, but the erosion was slightly higher. Other model types were considerably far from the reference. Only the amount of erosion seemed to be somewhat close.

Sample from 2.0 m depth

The special case of models with tied deglaciation and random erosion was tested. There the sampling depth was 2.0 m instead of the surface. As could be expected, the misfit values and the range of accepted models were smaller than with the surface sample (see Section 4.1). The most striking thing that differed from the results of surface samples is the relationship between erosion and total exposure time. While it was almost logarithmic before, now it is rather linear with a changing slope (Figure 21). This behaviour might be explained with the depth and the production rates since before the last exposure, the sample has been at depth 2 to 6 m, depending on the amount of erosion. The spallogenic production is not as strong below 3 m as muogenic production (Figure 2). It also attenuates with depth, so samples below the surface have nuclides produced with other ways than those on the surface, and this may cause the difference in behaviour.

Three and four exposure models (Figures B9 and B10) did not have similar good-fit zone as the two exposure models. There the solutions were more widely scattered and the linear trend was almost nonexistent. There seemed to be a weak linear trend in the three exposure models, which is missing in the four exposure models.

The most interesting result was the two exposure glacial cycle because there the average of all models was almost the exact copy of the reference model (Figure 22). The starting time of the glaciation was off only by a couple hundred years and the erosion was almost on the spot too. To top it all, the starting time of the first

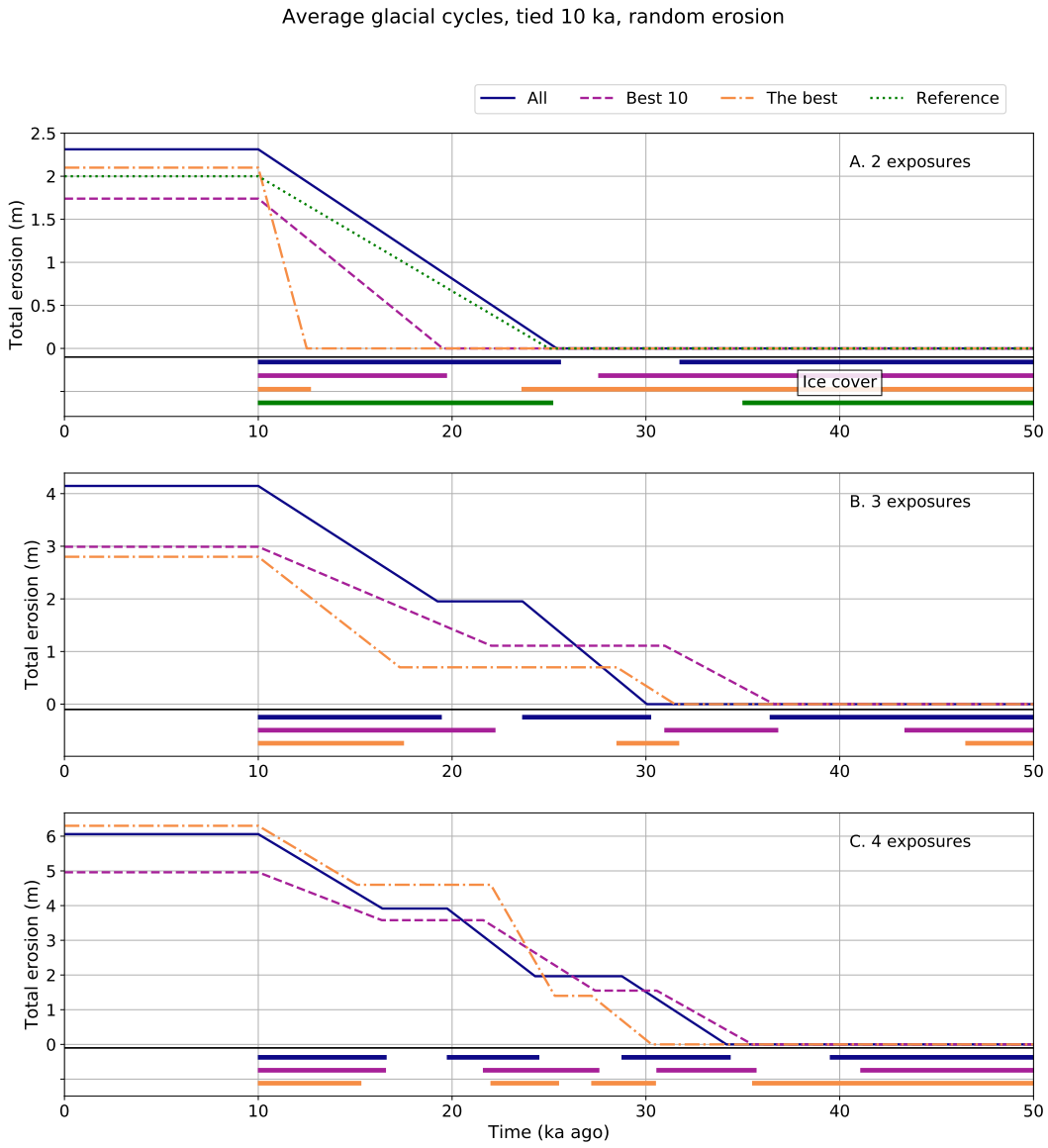

Figure 20. Average glacial cycles when the last deglaciation is tied 10.0 ka and erosion is random. See the explanations from Figure 14 A. Two exposure models have one glaciation after the infinite one. Its timing varied greatly between 12 and 25 ka. Erosion has less variation and in the best solution it is almost the same than in the reference model. B. Three exposure models do have large variation in the first glaciation after the infinite glaciation. Also the amount of erosion varies, but the average of all has about 2 m erosion during the last glaciation. C. Four exposure models. The first two glaciations vary quite much. The last glaciation do not, but it is still rather far from the reference model. The amount of erosion in the average of all is rather close to the reference.

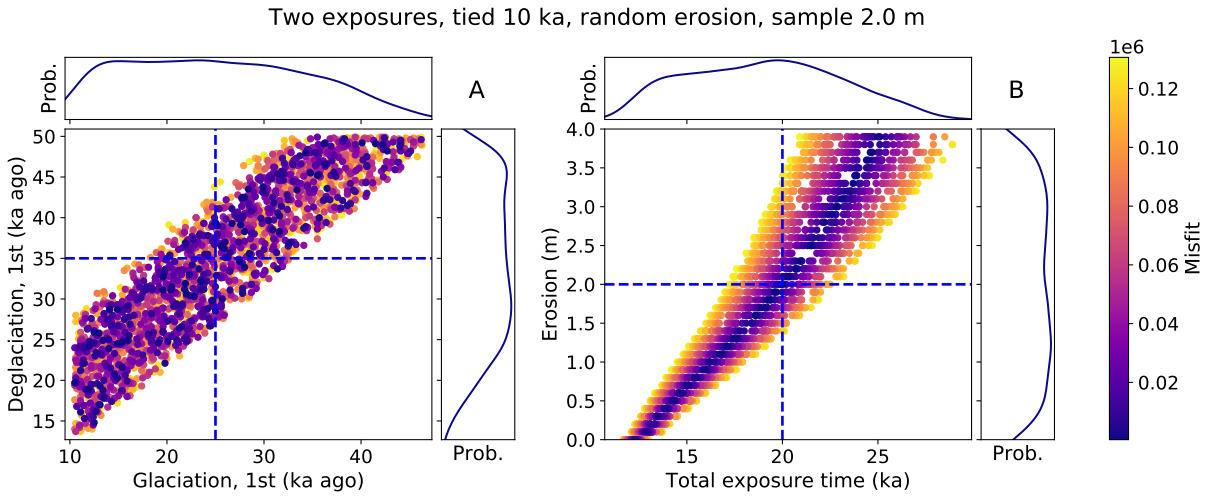

Figure 21. Two exposure models with tied timing of the last deglaciation and randomly selected erosion fitted to realistic history with 2.0 m erosion. The sampling depth is 2.0 m. The maximum exposure time is limited to 50 ka. Each dot presents one model and its color presents the misfit value so that darker corresponds to a smaller and better misfit value. The blue dashed line presents the parameter values used in the reference model. Density functions are shown adjacent to the axes for each parameter. A. Deglaciation and glaciation are scattered, and the minimum misfit is reached at several occasions. B. The relationship between erosion and the total exposure time is rather linear. The slope changes around 2 m of erosion.

glaciation differed only by 800 years. The average solution was fitting very well to the reference model. The models with the smallest misfit were not as good except when the first deglaciation time was considered since the difference there was only 100 years.

Three exposure models provided a rather good estimation of the erosion when the average solutions were plotted. The timing of the models was rather far from the reference. Similar behaviour can be observed from the four exposure models too. The amount of erosion was somewhat correct in the average of all solutions, but the timings had a very poor fit.

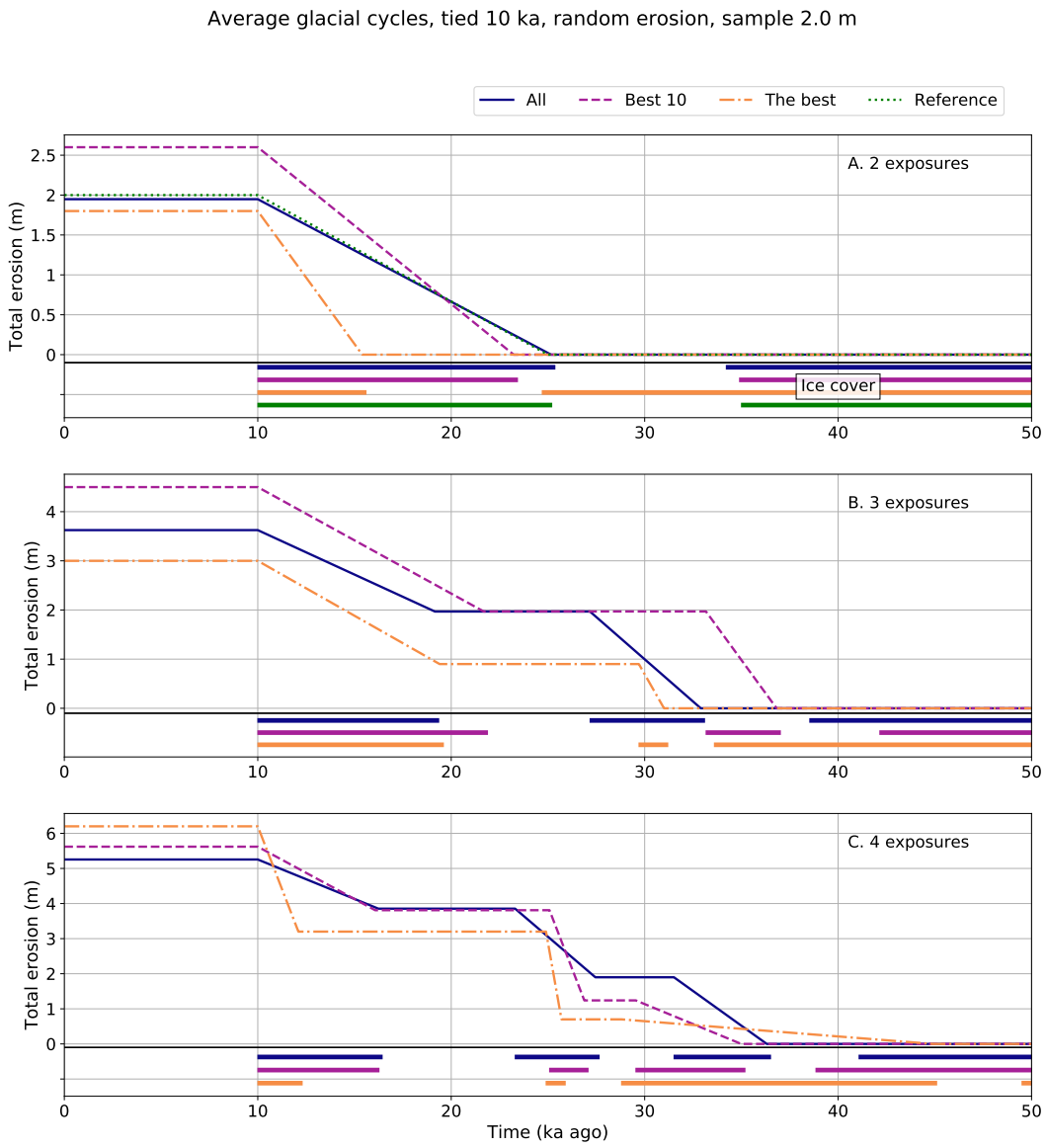

Figure 22. Average glacial cycles when the last deglaciation of the solutions is tied to 10.0 ka and erosion is random. The sampling depth is 2.0 m. See the explanations from Figure 14. A. Two exposure models provide an excellent similarity between the average of all accepted solutions and the reference model. The amount of erosion and the starting time of the glaciation are close to the reference model. The best ten solutions are the closest ones when the timing of the first deglaciation is determined. B. Three exposure models have good correspondence in the erosion, but the timings are rather far from the reference. C. The average of all accepted four exposure models provides rather good fit. The actual times of the cycles are not close to the reference model.

4.4.3 Solutions with constant erosion

To eliminate the effect of erosion, it was set to be constant, 2.0 m. That is the same value than in the reference model. This kind of approach could reveal if the correct timings can be found when the erosion does not alter the results. The one exposure solution can not have erosion because the only deglaciation it experiences is the deglaciation of the infinite glaciation. at that point, there is no inherited nuclides and therefore the amount of erosion does not matter.

In one exposure models, the timing of deglaciation (Figure 23) was varying between 9.5 ka and 11.5 ka. The distribution of accepted solutions is relatively even, and there is a clear minimum misfit at 10.5 ka. One exposure model has just one deglaciation which defines also the total exposure time therefore the accepted models forms a line with a positive slope. More models are accepted with higher misfit values than near the best fit.

Two exposure model reached the minimum misfit when the total exposure time and the last deglaciation were 10.5 ka (Figure 23). The minimum misfit was continuously reached when the total time increased and the last deglaciation decreased. The farthest accepted model had the total exposure duration of 44 ka and last deglaciation at 8.9 ka. One of the smallest misfit values was gained with total exposure time of 20.0 ka and the last deglaciation at 10.3 ka, which is nearly the reference model. Most of the accepted solutions had a total exposure time between 10 and 20 ka, which is in line with the 20.0 ka of the reference model. The highest probability of the last deglaciation was concentrated around 10 ka. This result could imply that if the erosion is known, the last deglaciation can be dated relatively well. It does not work as well with the total exposure time since its variation is much larger, and the largest values are over twice as large as the total exposure time of the reference model.

Three and four exposure models provided again rather similar kind of results (Figures B11 and B12). The only significant variable pair was the last deglaciation and the total exposure time. Both model types had quite constant timing of last deglaciation while the total exposure time increased. Three exposure models had a small decrease in the deglaciation when the total exposure time increased. It seems that the last deglaciation can be dated comparatively well, but the total exposure time does not have that kind of sensitivity.

The average glacial cycles had an excellent fit in the last deglaciation compared to the reference model since the values were only a bit over 10 ka (Figure 24). All the different scenarios had a higher erosion rate during the glaciation than the reference

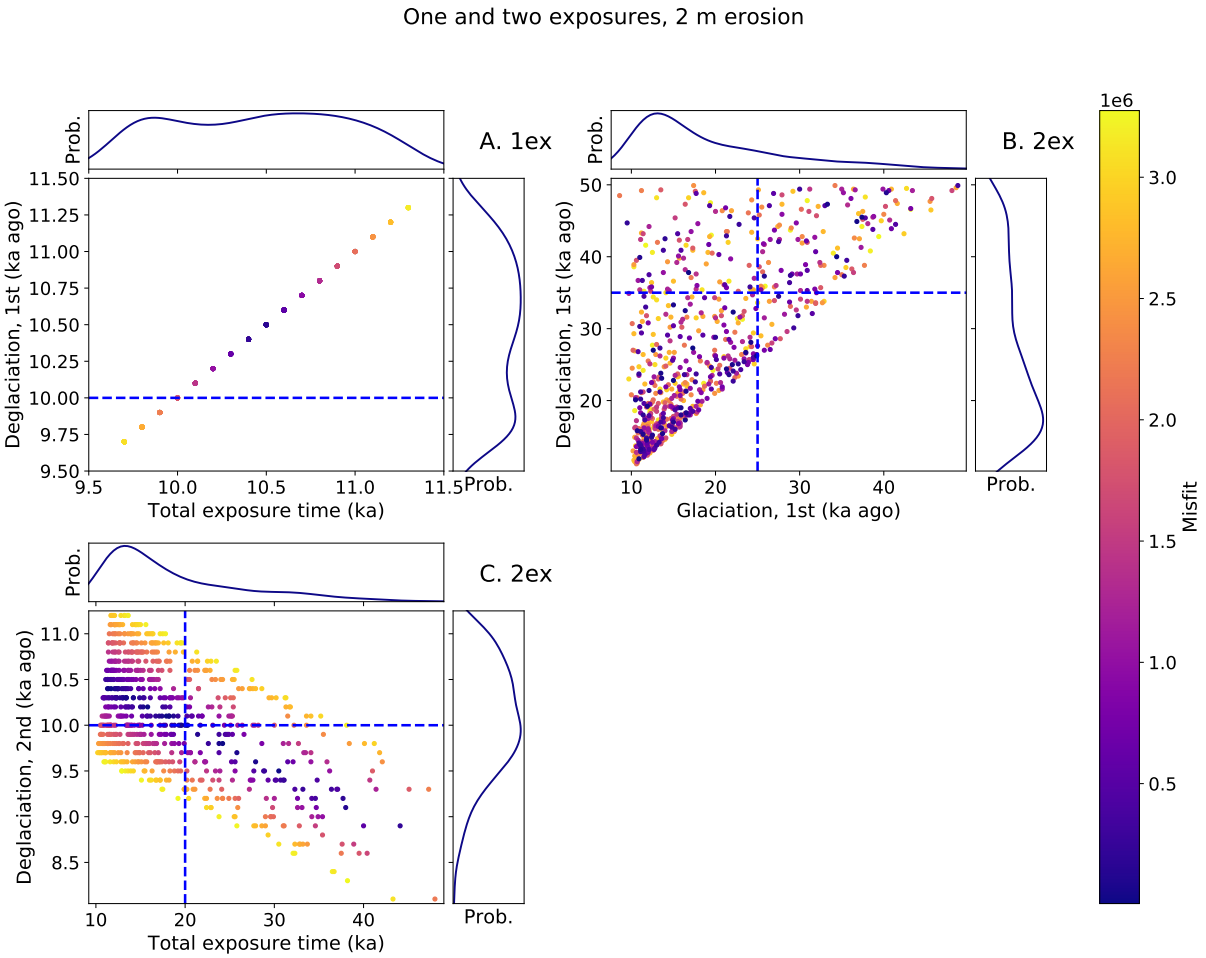

Figure 23. One and two exposure models with constant 2.0 m erosion during glaciations fitted to realistic history with 2.0 m erosion. The maximum exposure time was limited to 50 ka. Each dot presents one model and its color presents the misfit value so that darker corresponds to a smaller and better misfit value. The blue dashed line presents the parameter values used in the reference model. Density functions are shown adjacent to the axes for each parameter. A. One exposure model. Deglaciation and total exposure time have the same pattern as before. The values of accepted models vary from 9.7 to 11.3 ka, and the best fit is around 10.5 ka. B. Two exposure models and the first glaciation starting time and deglaciation. The best fit is gained with different combinations, but most of them have the glaciation starting time below 20 ka and deglaciation time below 30 ka. C. Total exposure time and the last deglaciation time of two exposure models. They are inversely proportional. The best fit is reached when the last deglaciation began 10.4 ka ago and the total exposure time was 11.0 ka. One of the best fit models is similar as the reference model, where the total exposure time was 20.0 ka and the last deglaciation at 10.0 ka ago.

model because the duration of the last glaciation was shorter than in the reference while the amount of erosion was the same. The model with the lowest misfit value was quite different than the reference model, but instead, the average of the best ten models were rather close to the reference. This clarifies the problem with the inverse model, a small misfit value may not present a model which is the most realistic one. The same behaviour can be observed from the three and four exposure models, although they had many other problems as well. More complicated solutions may have a small misfit, but the solution may not be paleoclimatically realistic. The best fitting four exposure model did have a glaciation between 31 and 32 ka, which seems a bit short time for a large scale glaciations, but may have occurred locally. Interestingly, two, three and four exposure models have the last deglaciation around 10 ka, so it seems that when the erosion is known it is possible to find the deglaciation time.

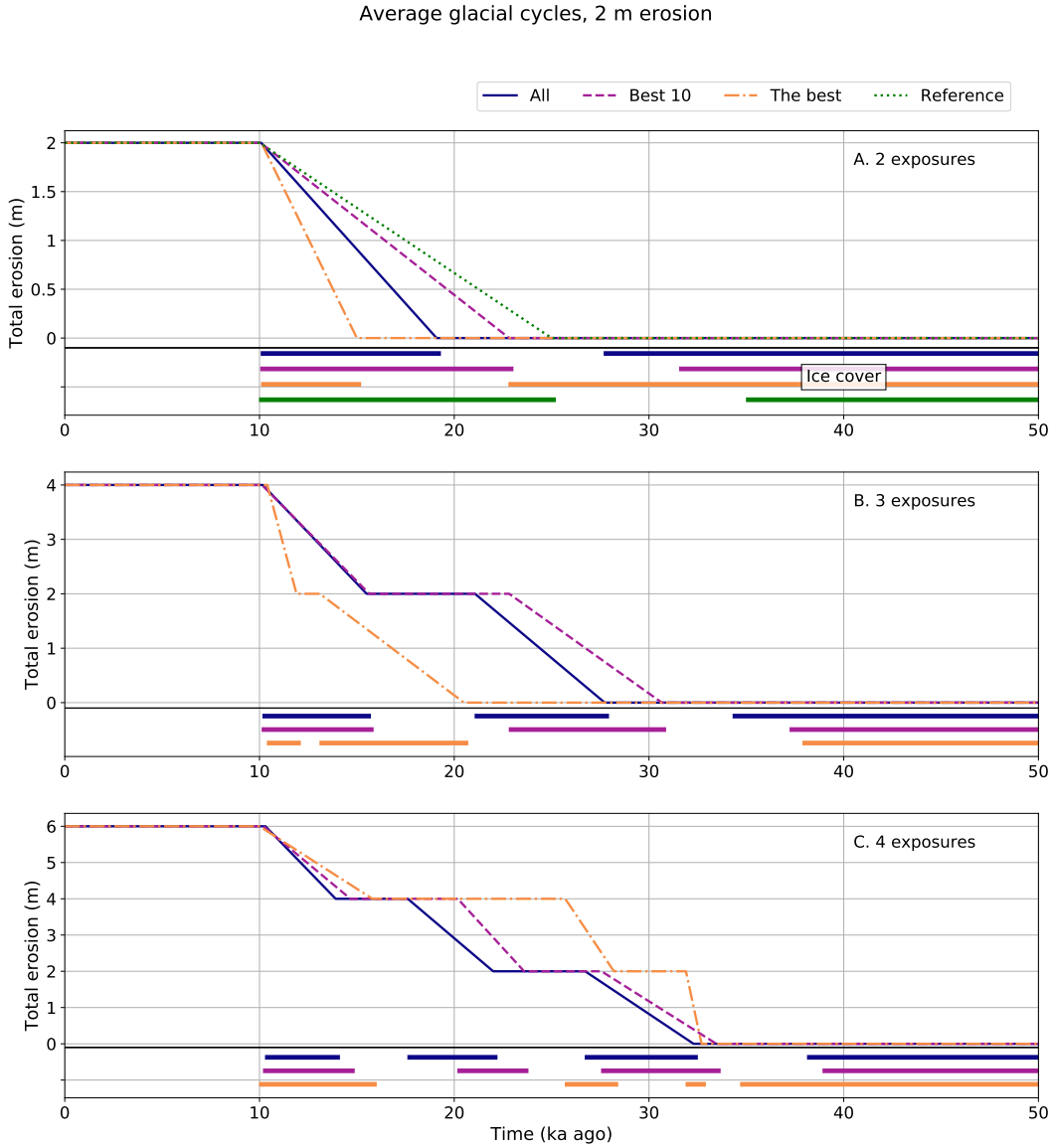

Figure 24. Average glacial cycles when the solutions have a constant 2.0 m erosion. See the explanations from Figure 14. A. Two exposure models have a very good fit in the timing of the last deglaciation. All of the models fit to the reference model. The duration of the last glaciation varies quite much, but the average of the best ten solutions is rather close. B. The timing of the last glaciation is almost the same than in the reference model. The model with the best misfit value is not fitting to the real cycle very well. C. Four exposure models also have a good fit in the last deglaciation, but the other timings are rather poor.

4.4.4 Fitted models without erosion

The next step was to study which kind of solutions are accepted if they do not have erosion at all even though the reference model has. That could reveal what happens if the erosion is underestimated. The total exposure time was limited to 50 ka. The one exposure model did not provide anything new since it was already underestimation of the reference model with fewer exposure periods. The best fit of the one exposure solutions was around 10.5 ka in total exposure time and the last and only deglaciation time (Figure 25). The solution was identical to the case presented in the Section 4.4.3 where the models did have any constant erosion. Basically, the one exposure solutions are identical in these cases since the erosion does not affect when there is no previous exposure periods.

Two exposure models, on the contrary, had different results than before. It seemed that the total exposure time had a clear minimum when the models did not have erosion at all (Figure 25C). The total exposure time had the best fit around 10.5 ka, and the last glaciation varied almost from 0 to 11 ka. Without erosion in the solutions, they are sensitive to the total exposure time. The total exposure duration is not the same as in the reference model. The value is closer to the last deglaciation time.

Three exposure models did not provide any clear indication which kind of solutions were better than others. In Figure B13 all the changing variables were presented, and it seemed like there is no obvious trend. Even the total exposure time is not concentrated around one value as it was in two exposure case. It is clustered between 10 and 20 ka, but there are well-fitting solutions up to 40 ka. The last deglaciation have also smaller values than before, but they are widely scattered between 0 and 11 ka.

Four exposure models (Figure B14) had the same problem as the three exposure models; they were too scattered to provide information from the past glaciations. There were dozens of solutions, which had a good fit to the reference model, but they were spread rather far from each other. There was a small good-fit cluster in the third glaciation-deglaciation plot (Figure B14C) between 0 and 20 ka in both axis. It means that the glaciation before the last one occurred only a short time before.

The behaviour of two exposure models was different from the other exposure models. Two exposure models had a minimum in misfit at total exposure time of 10.5 ka. The other more complicated models did not show any clear results for the timing of any deglaciation or glaciation. This could not be observed from the average glacial

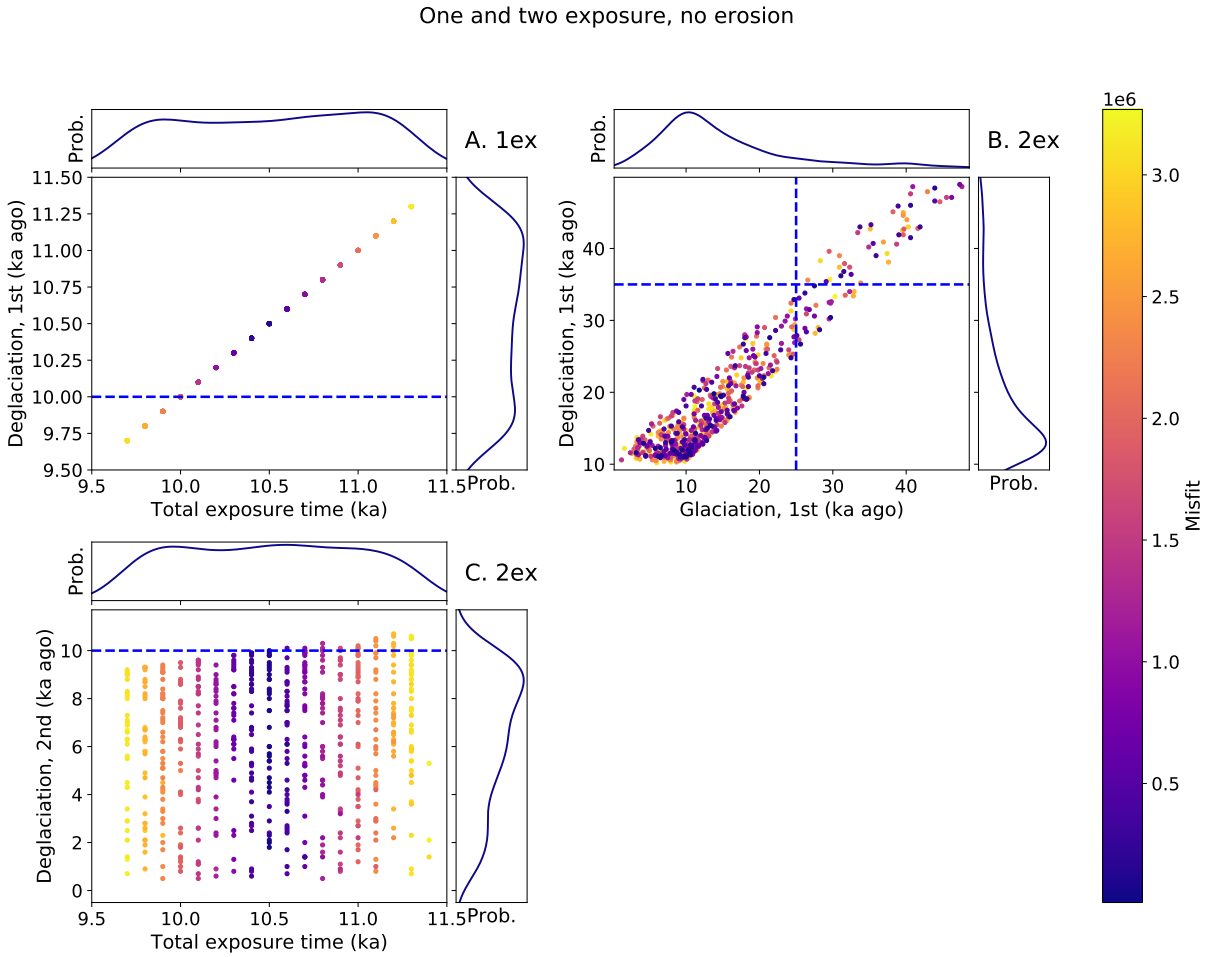

Figure 25. One and two exposure models without erosion fitted to realistic history with 2.0 m erosion. The maximum exposure time was limited to 50 ka. Each dot presents one model and its color presents the misfit value so that darker corresponds to a smaller and better misfit value. The blue dashed line presents the parameter values used in the reference model. Density functions are shown adjacent to the axes for each parameter. A. One exposure model. The total exposure time is the same than last deglaciation time. The best fit is at 10.5 ka. B. Two exposure model. The first glaciation starting time as a function of the first deglaciation time. Most of the values are concentrated between 0 and 20 ka in both axes. It seems that there is a small cluster of small misfit values at glaciation of 10 ka and deglaciation of 12 ka. C. Two exposure model. Total exposure time and the second deglaciation time, which is also the most recent deglaciation. The total exposure time is concentrated around 10.5 ka with the range similar to one exposure model. The deglaciation has values between 0 and 11 ka.

cycles (Figure 26), where the fit is rather poor for every exposure type.

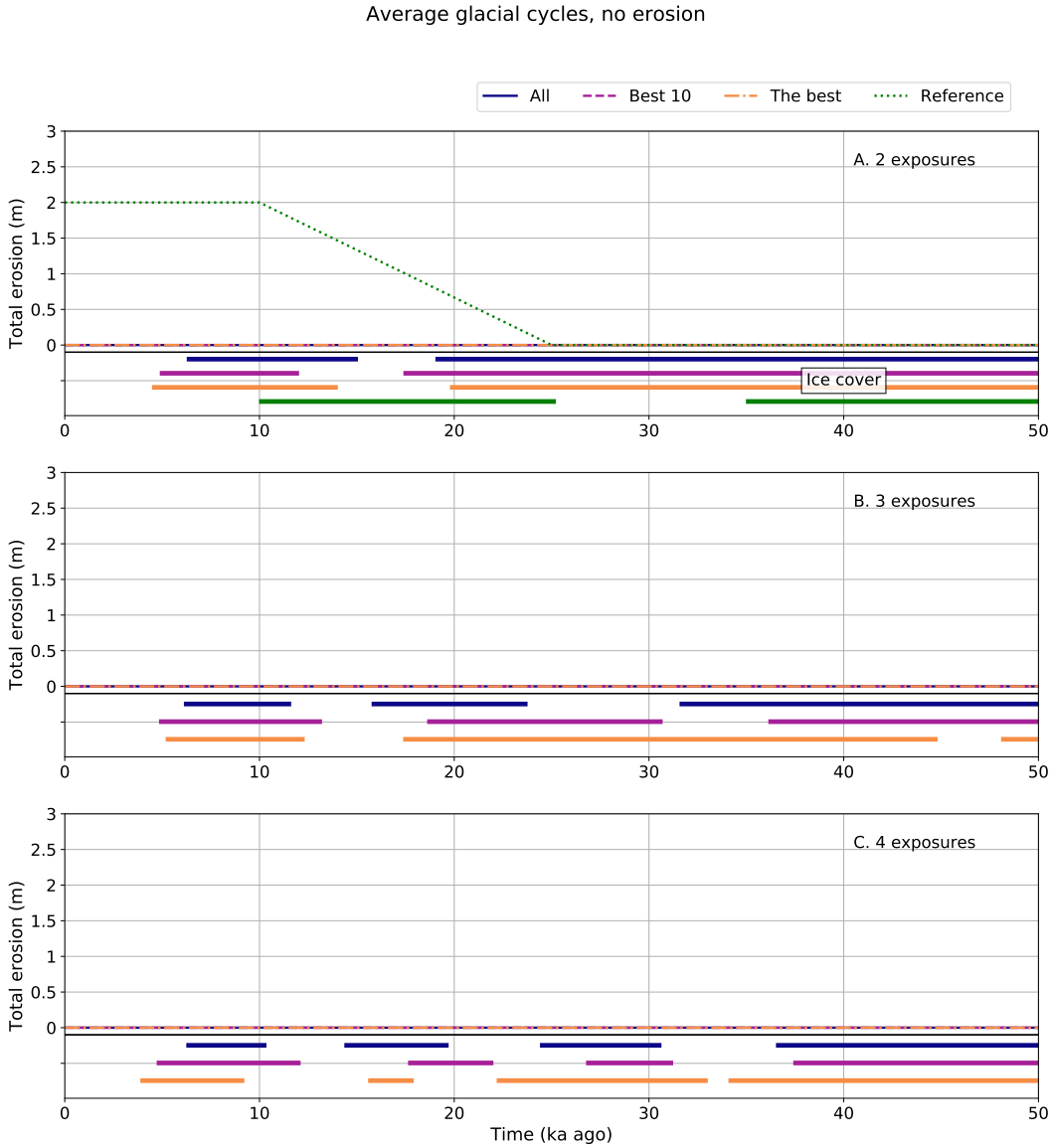

Figure 26. Average glacial cycles when the solutions do not have erosion, but the reference model does have. Therefore the total erosion is zero. See the explanations from Figure 14. A. Two exposures have rather small values for the last deglaciation. Also, the starting time of the glaciation is underestimated. The average of all accepted solutions fits the best, but it still is not good. B. Three exposure models. The last deglaciation occurs too late in each case in comparison to the reference model. The average of all is the closest one. C. Four exposure models have the most complicated result and they are quite poor fitting.

In other words, it seems that two exposure models had some sensitivity to the total exposure duration. When the reference model had erosion, it removed the uppest layer of rock and exposed a fresh surface with small amount of inherited nuclides. When model without erosion is fitted to that situation, it seems that the total exposure duration is

4.4.5 No constraints

Finally, the inverse model was run without any major constrains. The upper boundary of the time was raised to 100.0 ka and the maximum erosion to 10.0 m. The maximum number of deglaciations was limited to four, because too complicated solutions can produce a good fit, but they are paloclimatically impossible.

The one exposure model had similar results as in previous sections. The timing of deglaciation (Figure 27) was varying between 9.5 ka and 11.5 ka. The distribution of accepted solutions was relatively even, and there is a clear minimum misfit at 10.5 ka. One exposure model has just one deglaciation which also defines the total exposure time therefore, the accepted models formed a line with a positive slope. More models were accepted with higher misfit values than near the best fit.

Two exposure models have two deglaciations (Figure 27). The only variable, which seemed to have some kind of trend, was the timing of the last deglaciation. It was concentrated around 10.5 ka no matter how long the total exposure duration was. The other deglaciations, glaciations or erosion did not show a particular sensitivity to one way or another. More solutions were accepted when deglaciation and glaciation were below 20 ka but the best fitting solutions were spread. A similar thing occurred with erosion.

Three exposure models had similar behaviour than two exposure cases. The other parameters seemed not to have a minimum misfit at a specific place except the last deglaciation, which was concentrated around 10.5 ka (Figure B15). The total exposure time had a bit more variation than in the two exposure case, but it still was not cumulated to anywhere. One thing that can be observed is that the first glaciation and deglaciation occurred clearly before the second glaciation and deglaciation, like they should. The difference was significant. For example the second deglaciation has most of the values below 30 ka, while the first deglaciation has much wider distribution. It also seems that the amount of erosion do not matter in the case without constraints. The erosion varied from 0 to 10 m, even if it occurred during the last glaciation.

Four exposure models did not provide too much new information (Figure B16). The last deglaciation had the best fit around 10.5 ka, while all the other parameters varied considerably. Statistically it becomes clear that the later glaciations and deglaciations are concentrated to smaller values in time and thus also the best fitting combinations are also concentrated to there but otherwise any major conclusions can not be made.

The glacial cycles of all the model types are presented in the Figure 28. The last

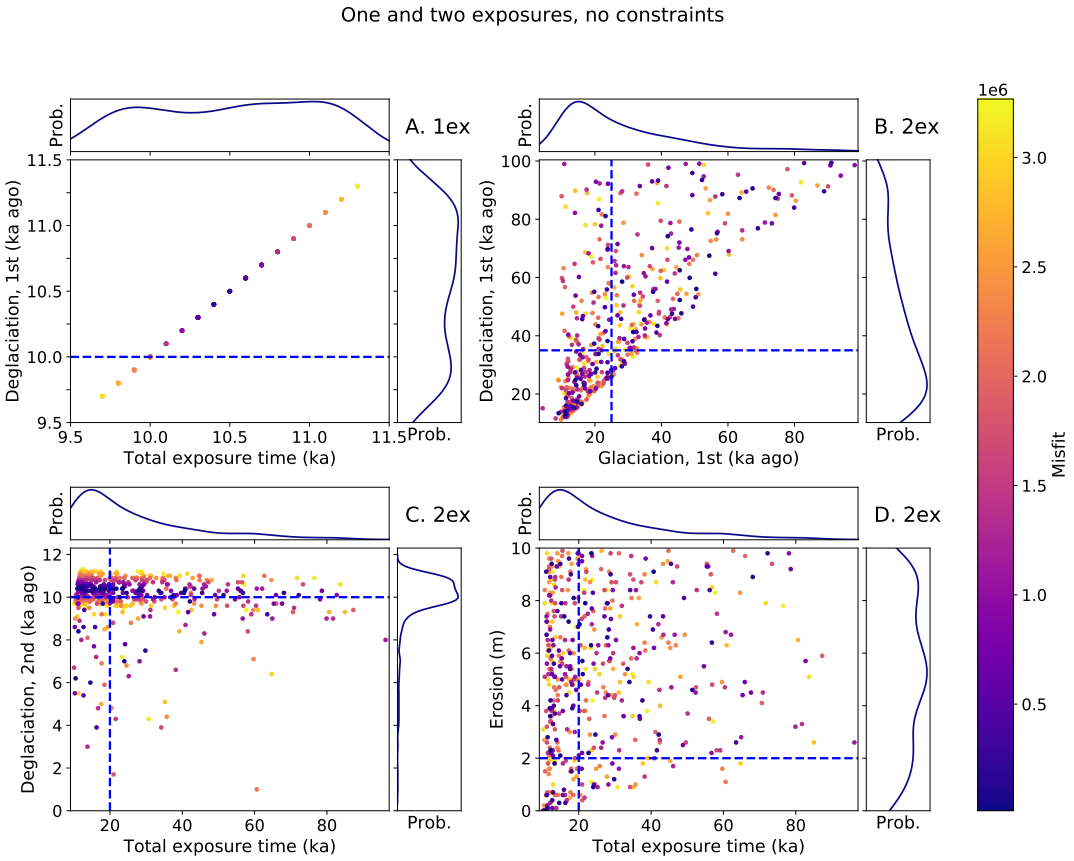

Figure 27. One and two exposure models without constraints fitted to realistic history with 2.0 m erosion. The only limitations were the maximum erosion of 10.0 m and the maximum duration of 100.0 ka. Each dot presents one model and its color presents the misfit value so that darker corresponds to a smaller and better misfit value. The blue dashed line presents the parameter values used in the reference model. Density functions are shown adjacent to the axes for each parameter. A. One exposure model. The total exposure time is the same than last deglaciation time. The best fit is at 10.5 ka. B. Two exposure model. The first glaciation and deglaciation. There are several very different combinations which produce a good fit. The values are concentrated below 30 ka. C. Two exposure model. The last deglaciation has the best fit around 10.5 ka while the total exposure time varies from 10 to 90 ka. D. Two exposure models. Erosion varies from 0 to 10 m and the best solutions are widely spread.

glaciation which has been timed rather well even though the erosion was much larger than in the reference model. Interestingly, the best solution, which had the smallest misfit value, was not always the best fit for the reference model. One thing that could be also pointed out, was the timing in the two exposure models. The reference model has two exposures and despite that, there was not a perfect match. The solution with the smallest misfit value had relatively correct timing for the last deglaciation, but everything else did not fitting to the reference model. Based on this, we can say that without constraints the past glaciations can not be detected.

All in all, it seems that the accepted solutions are rather far from the reference solutions, except for the last deglaciation. It can be predicted quite well. The amount of erosion can not be found easily without any constraints. This section can be summarized with a conclusion, that constraints are needed to produce solutions that have most likely occurred.

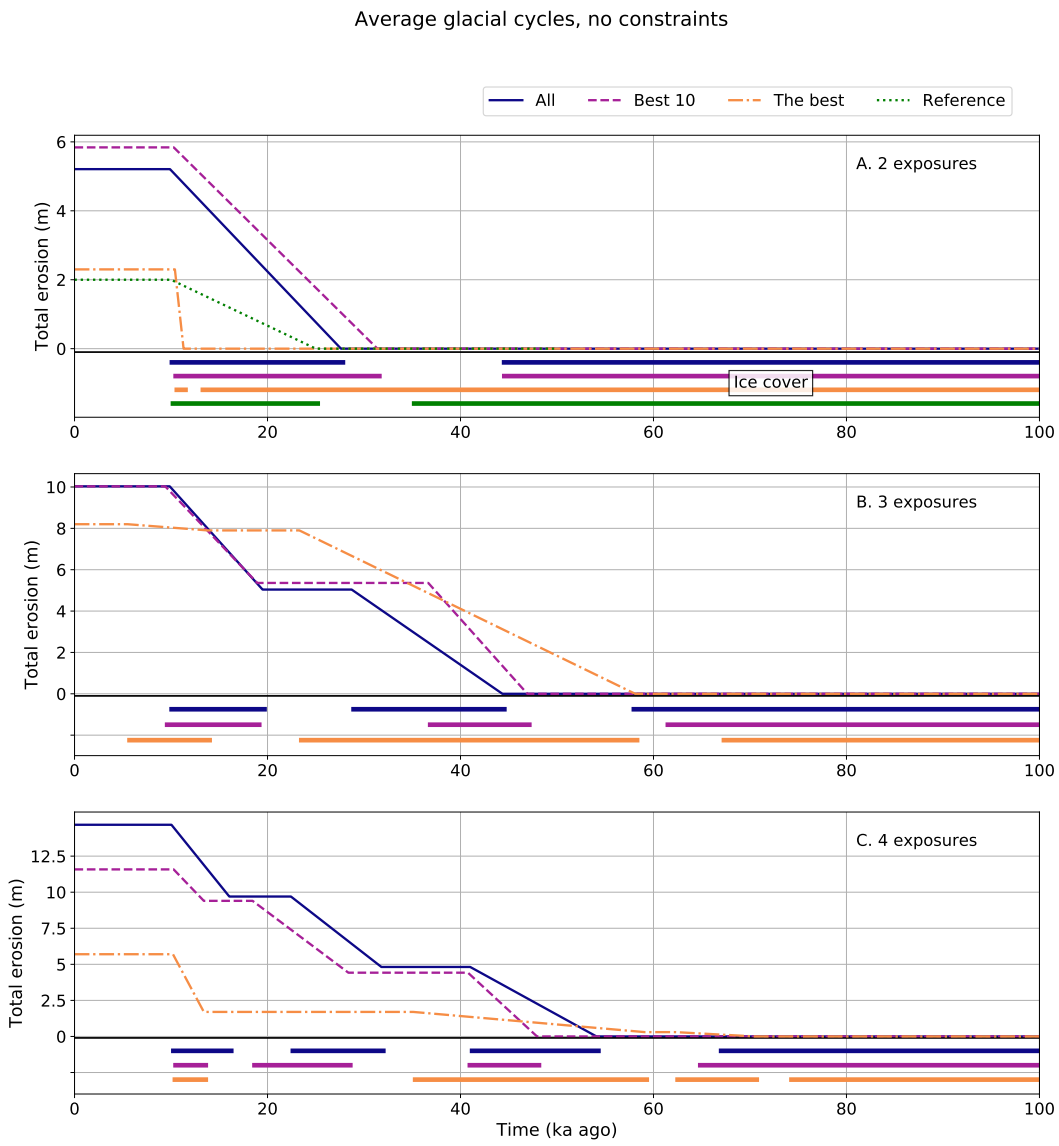

Figure 28. The glacial cycles of all the model types when there were no constraints for solutions. See the explanations from Figure 14. A. Two exposure models. All of the different types have the last deglaciation around 10 ka, which is close to the reference model. Most of the models have larger erosion than the reference model, but the best solution is rather close to it. Otherwise, the best model has a very different solution than the reference model. B. Three exposures. The last deglaciation is relatively precise in the average of all and the best ten solutions, but the amount of erosion is much larger. The best solution is quite far from the reference model. C. Four exposures. All of the cycles have a rather good fit to the last deglaciation of the reference model. The total erosion is much smaller in the best solution experiences than in other curves, but the value is still much larger than in the reference model. The other timings are not fitting to the reference.

4.5 Sample depth profile

One advantage of the inverse model is to study the sampling. Is it beneficial to take samples as depth profile or is the surface samples good enough. I studied this by running the inverse model using the realistic glaciation history as the reference model. The same inverse solutions were tested for each sample from different depths. The idea was to see that (1) which kind of models were accepted in each depth and (2) what was the most useful way to do the sampling. The set-up was similar to section 4.4.2 so that the last deglaciation was tied to 10 ka, but erosion could vary from 0 to 4 m per one glaciation period. This approach was chosen because the results were not as good than when the erosion was tied too and it is realistic to have the deglaciation time determined with some other way. I was trying to find out if using the profile, could allow us to have more information also from the erosion and the glaciation starting time by using just one isotope.

The results were interesting. It seemed that the depth profile can make the estimation of erosion and total exposure duration considerably better than taking a sample only from the surface (Figure 29). There were only a few accepted models near the expected values when the depth profile is used. If only surface sample is used, the erosion or the total exposure duration can not be estimated very well.

When average glacial cycles were compared, the erosion could be determined also from here when the depth profile is used (Figure 30). Otherwise, the models are quite different compared to the reference model. The duration of the glaciation or the previous deglaciation can not be dated.

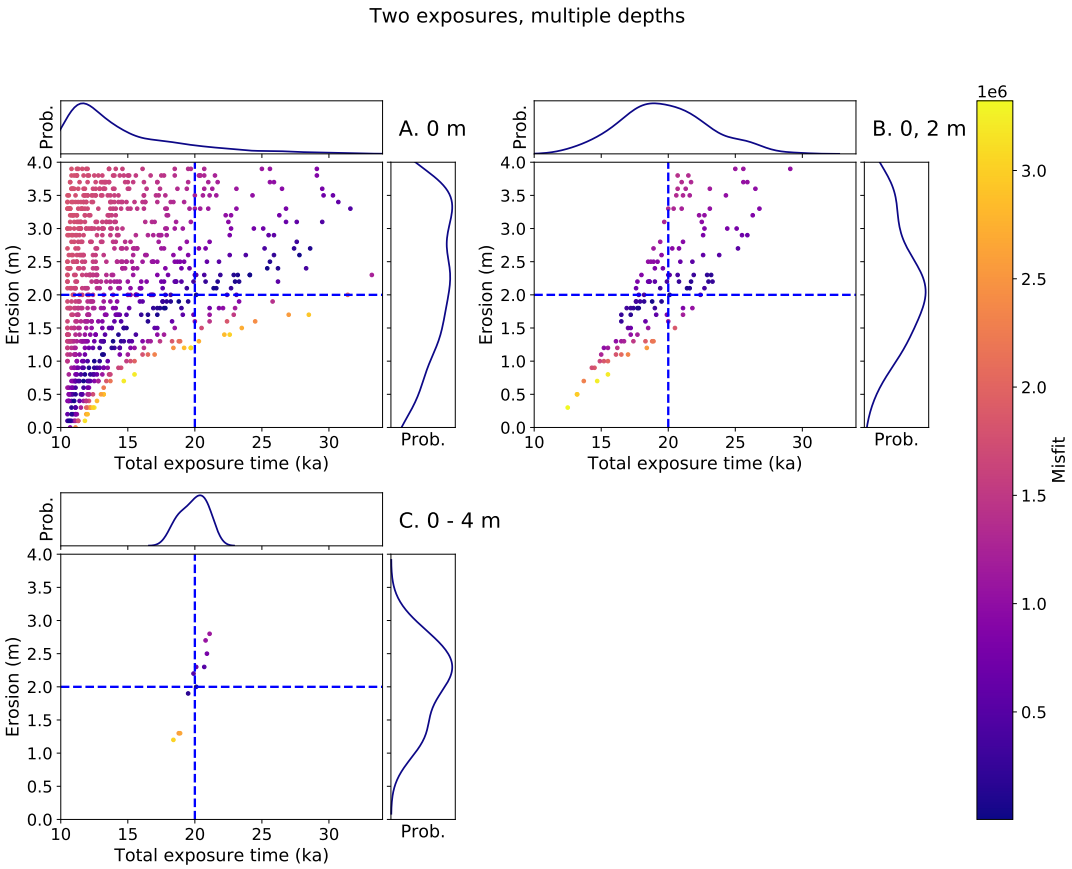

Figure 29. Erosion and total exposure duration determined with different depth profile options. The erosion was limited to a maximum 4.0 m and total duration to 50 ka. The last deglaciation was tied to 10.0 ka. Each dot presents one model and its color presents the misfit value so that darker corresponds to a smaller and better misfit value. The blue dashed line presents the parameter values used in the reference model. Density functions are shown adjacent to the axes for each parameter. A. Surface sample. This is identical to Figure 19. Erosion increases almost logarithmically with total exposure duration. There are several different combinations that produce a small misfit. B. Samples from the surface and 2.0 m depth. The shape is similar to Figure 21. Fewer models are accepted compared to using only a surface sample. C. Samples at every meter from the surface to 4.0 m depth. Only a few models are accepted. They are concentrated near the expected values of erosion and total exposure duration.

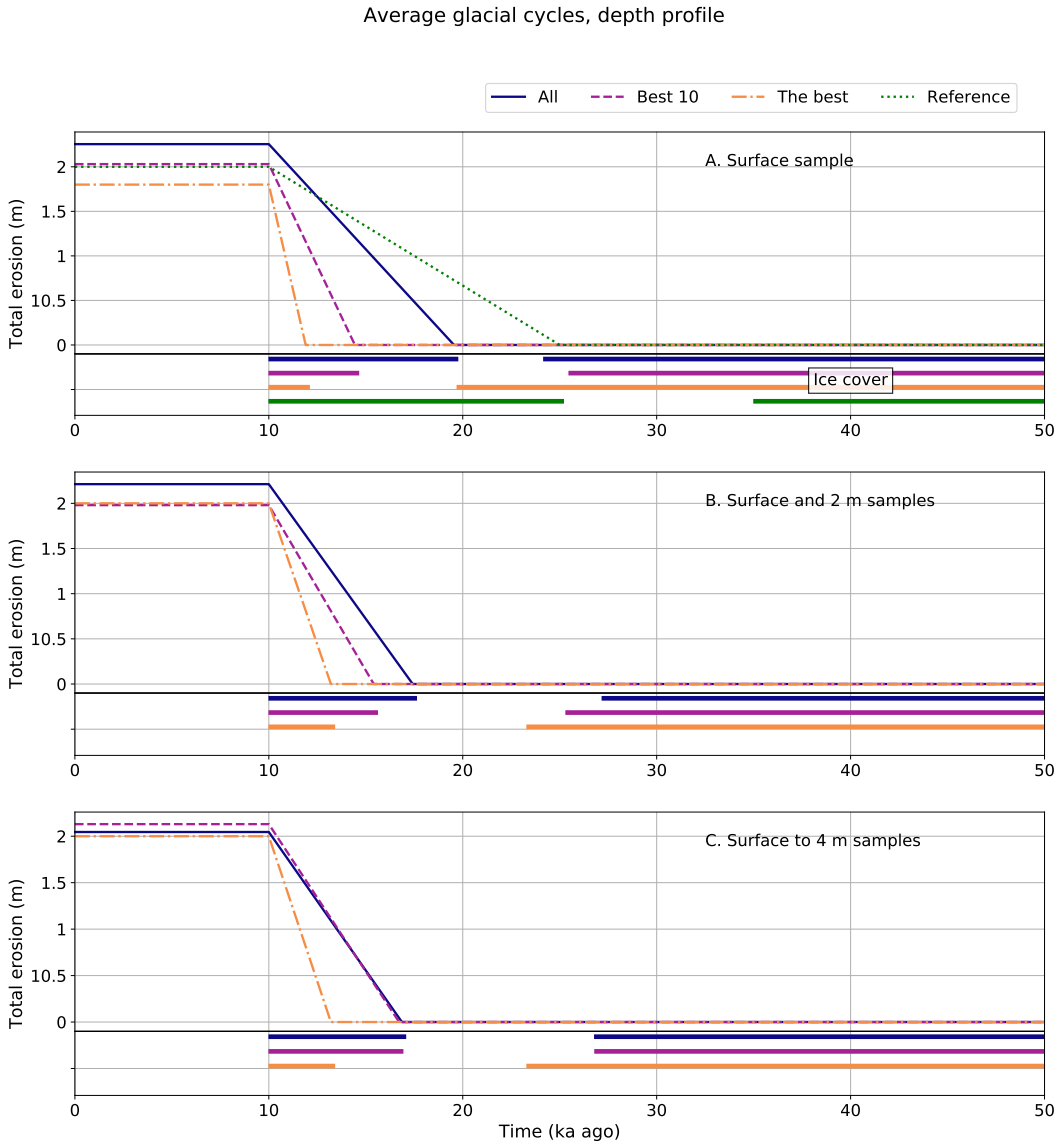

Figure 30. Average glacial cycles when the solutions have max 4.0 m erosion, the last deglaciation is tied to 10 ka and samples are taken from a depth profile. See the explanations from Figure 14. A. Surface sample. The amount of erosion is near the reference value, but the duration of the last glaciation or the previous deglaciation can not be dated. B. Samples from the surface and 2.0 m depth. The erosion is either the same than expected ("Best" and "Best 10") or it is neat that ("All"). The glaciation duration or the second last deglacation can not be dated. C. Samples taken at every meter from the surface to 4.0 m depth. Erosion is really close to the expected value in each case, but the glaciation starting time or the previous deglaciation can not be determined

5 Discussion

The accepted inverse solutions depend greatly on the constraints set for the solutions and the exposure history they are fitted for. If neither the exposure history nor the inverse solution had erosion, the expected age was the total exposure duration, because the inherited nuclides were not removed. In reality, the exposure history has, most likely, had erosion and then the results are harder to interpret. When the solutions did not have any constraints, the time of the last deglaciation was slightly larger than in the realistic exposure history. The strictest constraints were limiting the possible solutions, and then the duration of the last glaciation and the total exposure time could be detected reasonably well. If the timing of deglaciation and amount of erosion were both known, the duration of the glaciation could be found. If only one of them was known, the range of values for the other was wide, and the exact solution could not be found. Depth profiles made the accuracy of the inverse solutions better. One sample at the surface provided wide range of accepted solutions, while multiple samples from multiple depths reduced the amount of possible solutions and limited the possible parameter values.

5.1 Detection of realistic glaciation history

It is impossible to detect the realistic glaciation history, if there are not any constraints set for the solution. The timing of the last deglaciation can be observed sometimes rather well. It is around 10 ka no matter how complicated models are (Figure 28), but the history before that can not be detected clearly without major constraints (Figure 16). Without limitations, the best fitting deglaciation time can be observed to be higher than the reference deglaciation, and therefore there must have been some inherited nuclides. Despite that, the actual timing can not be determined since there are so many possible solutions that are accepted. Without any constraints, even the two exposure model did not reveal almost anything. The last deglaciation was around 10.5 ka with over 2.0 m erosion. With smaller erosion, the time began to decrease, but there still was not a clear trace to find the original model.

The past glaciations could possibly be observed if the limitations set for the solutions are strict enough. When the last deglaciation and the amount of erosion were set to be the same than in the reference model, the glaciations could be detected. Although it does raise a question, if these values used as constraints could be known in case of a real sample. Could it be possible that with a combination of the last deglaciation at 7 ka and erosion of 1.0 m the produced result would be the same than with deglaciation at 10 ka and erosion of 2.0 m. If that would be true, then the limitations are guiding the result strongly and the result may be presented as the only solution while it may be biased. If limitations are used, they must be based on reliable geological and paleoclimatological data. The latest deglaciation can be determined with varve dating, for example. The other variables, like amount of erosion or timings of earlier glaciations, are more challenging since usually there are not direct evidence of them.

It is interesting to notice that the best misfit values may not produce the most correct or the most realistic result. Many times the average of all accepted solutions formed a better glacial cycle than the best fitting models. I would have assumed that the poor fitting models would drag the average solution to be more unfitting, but the poor solutions may have cancelled each other. It would be nice to test if the average solutions really produce the best fit. Maybe this could be done in a controlled situation, where the glacial history of a rock is known really well or the artificial glacial history is produced in the rock. I am not completely sure how this artificial history could be produced, but in theory, the rock could be exposed to the known strong source of radiation. This would produce the nuclides in the rock. Then some of the surface would be removed and the rock would be exposed to the radiation again. This way the history would be known while it would not take tens of thousands of years and the inverse model could be tested.

The quality of the constraints set for the solutions is important, because they control the accepted solutions. If the constraints are geologically or paleoclimatically incorrect, then also the accepted solutions are incorrect. The constraints should be based on some other data like lake sediments, optically stimulated luminescence or varve dating to be sure that the limitations are reasonable. The most useful constraint is the last deglaciation time, because it can be known from the other studies. More challenging constraints are earlier deglaciations, total exposure duration and the amount of erosion. They are not known too well and setting limitations regarding of them may exclude the solution which would actually be closest to the real history.

It seems that using depth profile provides a way to get better results. If there are enough samples and they are taken deep enough, the values of some variables can

be limited. For example, when there were samples from every meter from surface to 4 m, the erosion in the solutions was varying from 1 to 3 m, while with only surface sample the range was from 0 to 4 m. The possible range was halved, which is seems to be a significant result. Similarly, the total exposure duration was limited between 18 and 21 ka, while otherwise it varies from 10 to 35 ka. The important thing that must be noticed is the number of accepted solutions is small in Section 4.5. There are only 11 accepted solutions when the depth profile is used, which makes the results a bit uncertain. It can not be said for sure if this is just a coincidence that the erosion is being limited so much or if this is a significant result by itself.

All in all, the realistic glaciation history can be detected if there are proper limitations for the models. Depth profile also seems to be a useful tool, but it still needs more inverse models to be confirmed.

5.2 Effect of erosion

Erosion has a huge impact to the possible inverse solutions. Most likely there has been erosion during the glaciations, and if it is not considered in the models, the results can be misleading. If the erosion is ignored and nor the fitted models have erosion, the best fitting solutions may imply that the total exposure time has been relatively short even though in reality that time is the last deglaciation (Figure 23).

It seemed that the exact amount of erosion was hard to detect. Sometimes, when the reference model had erosion of 2.0 m, the best fitting models had erosion up to 6 m. This can mean, that most of the inherited nuclides are already removed when the amount of erosion is 2.0 m. The nuclide concentration left can be produced with numerous different glaciation histories which allow much higher amount of erosion.

Erosion affects also to the glaciation cycles, since if the erosion is under or overestimated, the produced cycle may differ from the correct one. Too high erosion removes more inherited nuclides and shortens the time from the last deglaciation.

I would assume that the amount of erosion varies locally even though the glacial history is the same in the area. That could be a way to find out erosion during the deglaciation. If location A is on top of the hill and have experienced some erosion, while the location B is 100 m away from A at the foot of a hill and have not experienced erosion. The assumption would be that the B has not experienced as much erosion as the A even the deglaciation has occurred for both of them roughly at the same time.

5.3 Sampling

The sampling depth effects to the accepted models. The deeper the sample is from, the smaller is the range of accepted models. At a depth of 3 m, the range of accepted models is smaller than the half of the range of a surface sample. Thus the result is probably more accurate with deeper samples, but the concentration of the measured nuclides is small which may cause problems in the AMS. Therefore, the required amount of rock must be larger than with a surface sample. Also, if erosion is present, the surface could have been removed by 2 m. Then the amount of nuclides is even smaller if the sample is taken from 3 m depth. Without erosion, that sample would have been at 5 m depth. Of course after the removal the sample, now at 3 m depth, experiences similar conditions than the original sample at that depth, but the new sample do not contain as much of inherited nuclides than the original sample and thus the total number of nuclides is smaller. This may be a problem in the real measurements if the number of nuclides is rather small. That can be avoided by a large sample size. In the best case scenario, it might be possible to detect even 1000 atoms from a sample (Rood et al., 2010). If we assume the simplified glaciation history, the number of ^{10}Be atoms in kg of quartz at 3 m depth is 1 500 000 and if the sample size is 10 g, the number of ^{10}Be in the sample is 15 000 (Figure 6). It is low but still detectable. However the possible erosion, vegetation, shielding and snow reduce the number of formed ^{10}Be atoms and the sample from 3 m depth may not be the best choice unless the sample size is increased.

Notice that even if the misfit value is smaller with deeper samples, it does not mean that it is absolutely better to take sample below the surface. The misfit value depends greatly on depth because the way it was determined (Equation 3.11). The value is not normalized with the concentration but with the number of points compared to each other. It means that the misfit is still depending on the concentration and it may not be wise to compare misfit values of different depth samples to each other without normalizing the value with concentration. The misfit value can be used in comparison if the samples are at the same depth.

Using a depth profile while sampling might be a wise choice if the detection limit of the measurements is sensitive enough. The depth profile reduced the number of accepted models, and they were concentrated near the expected values (Figure 29). The number of inverse solutions in there was small, as mentioned before, so the cluster may have been coincidental, but all in all, the result is promising. It clearly showed that if the samples were taken from multiple depths, the range of accepted models is much smaller than if there would be just one sample from the surface. The advantage of the depth profile would also be that it might reveal the range for

total exposure duration and amount of erosion when the last deglaciation is known. The depth profile would not still reveal the total exposure history of the sample, but it would certainly provide more information of the erosion during the glaciation and it would give some range also for the timing of the previous glaciation.

Maybe the most significant benefit of the depth profile is that it could provide an estimation of erosion by using just one isotope. Usually, the amount of erosion is detected using paired nuclides, but the depth profile would allow the detection just with one isotope. This is an advantage if the measurements can not be done with multiple isotopes or there is no experience of using paired nuclides.

If the real measurements would be done with a depth profile, the road cuts could be used a nice option for that. Typically, at least in Finland, the road cuts are relatively young, about 100 years old. If the used isotope would be ^{10}Be, the amount of nuclides produced in the cut surface would be about 400 atoms. The significance of this number would depend on how deep samples would be used. Near the surface 400 atoms are not significant, but at 4 m is will cause a large uncertainty. If the road cuttings and the depth profile would be used, the cut should be as fresh as possible. It would also be wise to calculate how many atoms the deeper samples would theoretically have to avoid misleading results.

5.4 Limitations and sources of error

The forward and the inverse models do have several limitations, which effects to the results if they are used together with real samples. At this point, the models do not take into account any kind of shielding. It is assumed that the sampling surface would be infinitely exposed without any topography differences. Also, the possible coverage caused by vegetation was not considered. In Finland, one important factor during winters is a snow cover, which affects to the measured concentrations and was not taken into account. The final shielding type which was not included was the shielding effect of the sea right after the glacier retreated. Most likely, the surface was not exposed straight to the cosmic rays, but instead, it was covered with water.

The models have a possibility to include constant erosion rates during interglacials, but that was not used in any of the models. It was assumed that the erosion in Finland would be negligible. It would still have some influence on the concentrations, even if the rate was small.

One rather important thing in the models is the values of constant parameters. They are determined with experiments, but because the sampling sites and locations

are different, they may not be correct in Finnish settings. It is possible that, for example, the production rates would have different values in here than what they have in Norway where the determination was done. On the other hand, the latitudes of Norway are in the same range than in Finland, so there should not be too much difference because of that. Also, there might be some uncertainties in the path parameters that have quite large part in the calculations.

The models themselves have a few weaknesses. The first one is that the sampling was done from a synthetic forward model, and then the curve was compared to the inverse solutions. In real life, there will not be a forward solution that can be used, so the comparison can not be done that way, and the determination of the misfit must be changed. The new acceptance method should only consider the acceptance box and then compare the inverse solution curve to that one sample point. I believe that this problem could be solved and then the real samples could be accepted as input values in the inverse model.

The other weakness in the models is that the maximum timing may have been limited too much. In most of the models, it was limited to 50 ka, which may be too small value. It was done to get more accepted solutions, but at the same time it may have caused some solutions to be left out. In three and four exposure cases, the longer maximum value could have revealed some interesting solutions.

5.5 Future work

Future studies related to the models I created could adjust the models to a more realistic direction by adding details. The models should take into account all kinds of shielding such as snow coverage, vegetation, sloping surfaces and the early sea coverage. It would also be useful to rework the code to accept the sample depth and concentration when calculating the inverse solution. The path parameters and other constants should be chosen from areas as close as possible to the possible sampling site to be sure that they are as correct as possible.

Future work could also include the real testing of the code with samples. It would be necessary to study if the code works properly. The code could be studied together with a sample, which glaciation history is known. That could reveal if the accepted inverse solutions are even near the correct history. There should be more than one sample and preferably, at least one of the samples should not be from the surface.

If the code would be working correctly, it could be used to study local glaciation histories and erosion rates. Most likely, the deglaciation in a small area has occurred

at the same time, but the amount of erosion may not be the same. There might be a case, where the erosion has been strong on top of the hill, but much smaller on the side of the hill. In reality, the exposure time would be the same for both of the samples, but because of the different amount of erosion, the measured ages would be different. The erosion has removed more inherited nuclides on top of the hill than on the side of the hill, which would cause the difference. Presumably, the ages on top would be younger than on the side. This difference in age and in the number of nuclides could be used to estimate the erosion what that area experienced.

The sampling with a depth profile would also be an interesting thing to study. If the profile would limit the amount of erosion and the deglaciation time is known, the study could provide new information of the amount of erosion during glaciations in Finland by using just one isotope. If the study would also have two target isotopes, the reliability of the results could be confirmed. Usually, the paired nuclides are used to determine the erosion rates, so when the deglaciation and the erosion would be known, the past glaciations could be studied with even more certainty.

6 Conclusions

This study was aimed to find out if terrestrial cosmogenic nuclides could be used to study past glacial histories based on the nuclide concentrations. The concentrations were modelled with a forward model that took into account the exposure history of the rock and the erosion during the glaciation. Then the inverse model was used to find out possible glaciation histories that fit in the artificial samples, which were based on the forward model. The past histories were detected if the constraints for the inverse model were strict enough. If there was no constraints, the glaciations could not be detected. Depth profile used in sampling could limit the possible range of accepted models and help to provide more accurate results by using just one isotope.

Acknowledgement

I would like to thank my supervisors Ilmo Kukkonen and David Whipp for their guidance and discussions related to this work. They steered me in the right the direction in many points but let me still do this on my own way. I would also like to thank Seija Kultti for providing a geological perspective. I thank also my family and friends for supporting me and never doubting me through these years at University.

Bibliography

Aster, R. C. and Thurber, C. H. (2013). *Parameter Estimation and Inverse Problems*. Academic Press, Waltham, MA, 2nd ed edition.

Balbas, A. M., Barth, A. M., Clark, P. U., Clark, J., Caffee, M., O'Connor, J., Baker, V. R., Konrad, K., and Bjornstad, B. (2017). ^{10} Be dating of late Pleistocene megafloods and Cordilleran ice sheet retreat in the northwestern United States. *Geology*, 45(7):583–586.

Balco, G. (2011). Contributions and unrealized potential contributions of cosmogenic-nuclide exposure dating to glacier chronology, 1990–2010. *Quaternary Science Reviews*, 30(1-2):3–27.

Balco, G., Stone, J. O., Lifton, N. A., and Dunai, T. J. (2008). A complete and easily accessible means of calculating surface exposure ages or erosion rates from 10Be and 26Al measurements. *Quaternary geochronology*, 3(3):174–195.

Beer, J., Muscheler, R., Wagner, G., Laj, C., Kissel, C., Kubik, P. W., and Synal, H.-A. (2002). Cosmogenic nuclides during Isotope Stages 2 and 3. *Quaternary Science Reviews*, 21(10):1129–1139.

Benn, D. I. and Evans, D. J. A. (2014). *Glaciers & Glaciation*. Routledge.

Berger, A. (2001). The Role of CO $_2$, Sea Level, and Vegetation During the Milankovitch-forced Glacial-Interglacial Cycles. In Bengtsson, L. O. and Hammer, C. U., editors, *Geosphere-Biosphere Interactions and Climate*, pages 119–146. Cambridge University Press, first edition.

Bierman, P. R., Marsella, K. A., Patterson, C., Davis, P., and Caffee, M. (1999). Mid-Pleistocene cosmogenic minimum-age limits for pre-Wisconsinan glacial surfaces in southwestern Minnesota and southern Baffin Island: A multiple nuclide approach. *Geomorphology*, 27(1-2):25–39.

Björck, S. (1995). A review of the history of the Baltic Sea, 13.0-8.0 ka BP. *Quaternary International*, 27:19–40.

Braun, J., van der Beek, P., and Batt, G. (2006). *Quantitative Thermochronology: Numerical Methods for the Interpretation of Thermochronological Data*. Cambridge University Press, Cambridge.

Briner, J. P., Goehring, B. M., Mangerud, J., and Svendsen, J. I. (2016). The deep accumulation of ^{10} Be at Utsira, southwestern Norway: Implications for cosmogenic nuclide exposure dating in peripheral ice sheet landscapes: ^{10} Be in Peripheral Ice Sheet Landscapes. *Geophysical Research Letters*, 43(17):9121–9129.

Burke, K. D., Williams, J. W., Chandler, M. A., Haywood, A. M., Lunt, D. J., and Otto-Bliesner, B. L. (2018). Pliocene and Eocene provide best analogs for near-future climates. *Proceedings of the National Academy of Sciences*, 115(52):13288–13293.

Ceperley, E. G., Marcott, S. A., Reusche, M. M., Barth, A. M., Mix, A. C., Brook, E. J., and Caffee, M. (2020). Widespread early Holocene deglaciation, Washington Land, northwest Greenland. *Quaternary Science Reviews*, 231:106181.

Ciampalini, A., Persano, C., Fabel, D., and Firpo, M. (2015). Dating Pleistocene deltaic deposits using in-situ 26Al and 10Be cosmogenic nuclides. *Quaternary Geochronology*, 28:71–79.

Clark, P. U., Dyke, A. S., Shakun, J. D., Carlson, A. E., Clark, J., Wohlfarth, B., Mitrovica, J. X., Hostetler, S. W., and McCabe, A. M. (2009). The Last Glacial Maximum. *Science*, 325(5941):710–714.

Corbett, L. B., Bierman, P. R., Graly, J. A., Neumann, T. A., and Rood, D. H. (2013). Constraining landscape history and glacial erosivity using paired cosmogenic nuclides in Upernavik, northwest Greenland. *Geological Society of America Bulletin*, 125(9-10):1539–1553.

Corbett, L. B., Bierman, P. R., Rood, D. H., Caffee, M. W., Lifton, N. A., and Woodruff, T. E. (2017). Cosmogenic ^{26} Al/ ^{10} Be surface production ratio in Greenland: Cosmogenic ^{26} Al/ ^{10} Be Production Ratio. *Geophysical Research Letters*, 44(3):1350–1359.

Cuzzone, J. K., Clark, P. U., Carlson, A. E., Ullman, D. J., Rinterknecht, V. R., Milne, G. A., Lunkka, J.-P., Wohlfarth, B., Marcott, S. A., and Caffee, M. (2016). Final deglaciation of the Scandinavian Ice Sheet and implications for the Holocene global sea-level budget. *Earth and Planetary Science Letters*, 448:34–41.

Davis, R. and Schaeffer, O. A. (1955). Chlorine-36 in nature. *Annals of the New York Academy of Sciences*, 62(1):107–121.

Desilets, D., Zreda, M., and Prabu, T. (2006). Extended scaling factors for in situ cosmogenic nuclides: New measurements at low latitude. *Earth and Planetary Science Letters*, 246(3-4):265–276.

Dühnforth, M., Anderson, R. S., Ward, D., and Stock, G. M. (2010). Bedrock fracture control of glacial erosion processes and rates. *Geology*, 38(5):423–426.

Dühnforth, M., Densmore, A. L., Ivy-Ochs, S., Allen, P. A., and Kubik, P. W. (2007). Timing and patterns of debris flow deposition on Shepherd and Symmes creek fans, Owens Valley, California, deduced from cosmogenic ^{10} Be. *Journal of Geophysical Research*, 112(F3):F03S15.

Dunai, T. (2001). Influence of secular variation of the geomagnetic field on production rates of in situ produced cosmogenic nuclides. *Earth and Planetary Science Letters*, 193(1-2):197–212.

Dunai, T. J. (2010). *Cosmogenic Nuclides: Principles, Concepts and Applications in the Earth Surface Sciences*. Cambridge University Press.

Ehlers, J. and Gibbard, P. L. (1996). *Quaternary and Glacial Geology*. J. Wiley & Sons, Chichester ; New York.

Ehlers, J. and Gibbard, P. L. (2007). The extent and chronology of Cenozoic Global Glaciation. *Quaternary International*, 164-165:6–20.

Elmore, D. and Phillips, F. M. (1987). Accelerator Mass Spectrometry for Measurement of Long-Lived Radioisotopes. *Science*, 236(4801):543–550.

Frakes, L. A., Francis, J. E., and Syktus, J. I. (1992). *Climate Modes of the Phanerozoic*. Cambridge University Press, first edition.

Goehring, B. M., Brook, E. J., Linge, H., Raisbeck, G. M., and Yiou, F. (2008). Beryllium-10 exposure ages of erratic boulders in southern Norway and implications for the history of the Fennoscandian Ice Sheet. *Quaternary Science Reviews*, 27(3-4):320–336.

Gosse, J. C. and Phillips, F. M. (2001). Terrestrial in situ cosmogenic nuclides: Theory and application. *Quaternary Science Reviews*, 20(14):1475–1560.

Granger, D. E., Gibbon, R. J., Kuman, K., Clarke, R. J., Bruxelles, L., and Caffee, M. W. (2015). New cosmogenic burial ages for Sterkfontein Member 2 Australopithecus and Member 5 Oldowan. *Nature*, 522(7554):85–88.

Grosse, A. (1934). An unknown radioactivity. *Journal of the American Chemical Society*, 56(9):1922–1924.

Häuselmann, P. and Granger, D. E. (2016). Dating of Caves by Cosmogenic Nuclides: Method, Possibilities, and the Siebenhengste Example. *Acta Carsologica*, 34(1).

Heimsath, A. M., Chappell, J., Dietrich, W. E., Nishiizumi, K., and Finkel, R. C. (2001). Late Quaternary erosion in southeastern Australia: A field example using cosmogenic nuclides. *Quaternary International*, 83-85:169–185.

Hilger, P., Gosse, J. C., and Hermanns, R. L. (2019). How significant is inheritance when dating rockslide boulders with terrestrial cosmogenic nuclide dating?—a case study of an historic event. *Landslides*, 16(4):729–738.

Ivy-Ochs, S. and Briner, J. P. (2014). Dating Disappearing Ice with Cosmogenic Nuclides. *Elements*, 10(5):351–356.

Ivy Ochs, S. D. (1996). *The Dating of Rock Surfaces Using in Situ Produced Be-10, Al-26 and Cl-36, with Examples from Antarctica and the Swiss Alps*. PhD thesis, ETH Zurich.

Johansson, P., Lunkka, J. P., and Sarala, P. (2011). The Glaciation of Finland. In *Developments in Quaternary Sciences*, volume 15, pages 105–116. Elsevier.

Klein, J., Giegengack, R., Middleton, R., Sharma, P., Underwood, J. R., and Weeks, R. A. (1986). Revealing Histories of Exposure Using *In Situ* Produced ^{26} Al and ^{10} Be in Libyan Desert Glass. *Radiocarbon*, 28(2A):547–555.

Klein, J., Middleton, R., and Tang, H. (1982). Modifications of an FN tandem for quantitative 10Be measurement. *Nuclear Instruments and Methods in Physics Research*, 193(3):601–616.

Knudsen, M. F. and Egholm, D. L. (2018). Constraining Quaternary ice covers and erosion rates using cosmogenic 26Al/10Be nuclide concentrations. *Quaternary Science Reviews*, 181:65–75.

Kohl, C. and Nishiizumi, K. (1992). Chemical isolation of quartz for measurement of in-situ-produced cosmogenic nuclides. *Geochimica et Cosmochimica Acta*, 56(9):3583–3587.

Korschinek, G., Bergmaier, A., Faestermann, T., Gerstmann, U., Knie, K., Rugel, G., Wallner, A., Dillmann, I., Dollinger, G., von Gostomski, C. L., Kossert, K., Maiti, M., Poutivtsev, M., and Remmert, A. (2010). A new value for the half-life of 10Be by Heavy-Ion Elastic Recoil Detection and liquid scintillation counting. *Nuclear Instruments and Methods in Physics Research Section B: Beam Interactions with Materials and Atoms*, 268(2):187–191.

Lal, D. (1991). Cosmic ray labeling of erosion surfaces: In situ nuclide production rates and erosion models. *Earth and Planetary Science Letters*, 104(2-4):424–439.

Lal, D. and Peters, B. (1967). Cosmic Ray Produced Radioactivity on the Earth. In Flügge, S. and Sitte, K., editors, *Kosmische Strahlung II / Cosmic Rays II*, volume 9 / 46 / 2, pages 551–612. Springer Berlin Heidelberg, Berlin, Heidelberg.

Lehmann, B., Herman, F., Valla, P. G., King, G. E., Biswas, R. H., Ivy-Ochs, S., Steinemann, O., and Christl, M. (2020). Postglacial erosion of bedrock surfaces and deglaciation timing: New insights from the Mont Blanc massif (western Alps). *Geology*, 48(2):139–144.

Li, Y., Harbor, J., Stroeven, A. P., Fabel, D., Kleman, J., Fink, D., Caffee, M., and Elmore, D. (2005). Ice sheet erosion patterns in valley systems in northern Sweden investigated using cosmogenic nuclides. *Earth Surface Processes and Landforms*, 30(8):1039–1049.

Lifton, N., Sato, T., and Dunai, T. J. (2014). Scaling in situ cosmogenic nuclide production rates using analytical approximations to atmospheric cosmic-ray fluxes. *Earth and Planetary Science Letters*, 386:149–160.

Lifton, N. A., Bieber, J. W., Clem, J. M., Duldig, M. L., Evenson, P., Humble, J. E., and Pyle, R. (2005). Addressing solar modulation and long-term uncertainties in scaling secondary cosmic rays for in situ cosmogenic nuclide applications. *Earth and Planetary Science Letters*, 239(1-2):140–161.

Mackay, S. L. and Marchant, D. R. (2016). Dating buried glacier ice using cosmogenic 3He in surface clasts: Theory and application to Mullins Glacier, Antarctica. *Quaternary Science Reviews*, 140:75–100.

Mäkinen, K. (2005). Dating the Weichselian deposits of southwestern Finnish Lapland. *Special Paper of the Geological Survey of Finland*, (40):67–78.

Margreth, A., Gosse, J. C., and Dyke, A. S. (2016). Quantification of subaerial and episodic subglacial erosion rates on high latitude upland plateaus: Cumberland Peninsula, Baffin Island, Arctic Canada. *Quaternary Science Reviews*, 133:108–129.

Marrero, S. M., Phillips, F. M., Borchers, B., Lifton, N., Aumer, R., and Balco, G. (2016). Cosmogenic nuclide systematics and the CRONUScalc program. *Quaternary Geochronology*, 31:160–187.

Masarik, J. and Beer, J. (1999). Simulation of particle fluxes and cosmogenic nuclide production in the Earth's atmosphere. *Journal of Geophysical Research: Atmospheres*, 104(D10):12099–12111.

Masarik, J. and Reedy, R. C. (1995). Terrestrial cosmogenic-nuclide production systematics calculated from numerical simulations. *Earth and Planetary Science Letters*, 136(3-4):381–395.

Miller, G., Briner, J., Lifton, N., and Finkel, R. (2006). Limited ice-sheet erosion and complex exposure histories derived from in situ cosmogenic 10Be, 26Al, and 14C on Baffin Island, Arctic Canada. *Quaternary Geochronology*, 1(1):74–85.

Nishiizumi, K. (2004). Preparation of 26Al AMS standards. *Nuclear Instruments and Methods in Physics Research Section B: Beam Interactions with Materials and Atoms*, 223-224:388–392.

Nishiizumi, K., Winterer, E., Kohl, C., Klein, J., Middleton, R., Lal, D., and Arnold, J. (1989). Cosmic ray production rates of 10Be and 26Al in quartz from glacially polished rocks. *Journal of Geophysical Research: Solid Earth*, 94(B12):17907–17915.

Pillans, B. and Gibbard, P. (2012). The Quaternary Period. In *The Geologic Time Scale*, pages 979–1010. Elsevier.

Placzek, C., Matmon, A., Granger, D., Quade, J., and Niedermann, S. (2010). Evidence for active landscape evolution in the hyperarid Atacama from multiple terrestrial cosmogenic nuclides. *Earth and Planetary Science Letters*, 295(1-2):12–20.

Poutanen, M. and Steffen, H. (2015). Land uplift at kvarken archipelago / high coast UNESCO world heritage area. *Geophysica*, 50:49–64.

Putkonen, J. and Swanson, T. (2003). Accuracy of cosmogenic ages for moraines. *Quaternary Research*, 59(2):255–261.

Rinterknecht, V. R., Clark, P. U., Raisbeck, G. M., Yiou, F., Brook, E. J., Tschudi, S., and Lunkka, J. P. (2004). Cosmogenic 10Be dating of the Salpausselkä I Moraine in southwestern Finland. *Quaternary Science Reviews*, 23(23-24):2283–2289.

Rood, D. H., Hall, S., Guilderson, T. P., Finkel, R. C., and Brown, T. A. (2010). Challenges and opportunities in high-precision Be-10 measurements at CAMS. *Nuclear Instruments and Methods in Physics Research Section B: Beam Interactions with Materials and Atoms*, 268(7-8):730–732.

Saarnisto, M. and Saarinen, T. (2001). Deglaciation chronology of the Scandinavian Ice Sheet from the Lake Onega Basin to the Salpausselkä End Moraines. *Global and Planetary Change*, 31(1-4):387–405.

Shackleton, N. and Hall, M. (1997). 24. The late Miocene stable isotope record, Site 926. In *Proceedings of the Ocean Drilling Program, Sci. Results*, volume 154, pages 367–373.

Skov, D. S. n., Andersen, J., Olsen, J., Jacobsen, B., Knudsen, M., Jansen, J., Larsen, N., and Egholm, D. (2020). Constraints from cosmogenic nuclides on the glaciation and erosion history of Dove Bugt, northeast Greenland. *GSA Bulletin*.

Soldati, M., Barrows, T. T., Prampolini, M., and Fifield, K. L. (2018). Cosmogenic exposure dating constraints for coastal landslide evolution on the Island of Malta (Mediterranean Sea). *Journal of Coastal Conservation*, 22(5):831–844.

Stone, J. O. (2000). Air pressure and cosmogenic isotope production. *Journal of Geophysical Research: Solid Earth*, 105(B10):23753–23759.

Strobl, M., Hetzel, R., Niedermann, S., Ding, L., and Zhang, L. (2012). Landscape evolution of a bedrock peneplain on the southern Tibetan Plateau revealed by in situ-produced cosmogenic 10Be and 21Ne. *Geomorphology*, 153-154:192–204.

Stroeven, A. P., Hättestrand, C., Kleman, J., Heyman, J., Fabel, D., Fredin, O., Goodfellow, B. W., Harbor, J. M., Jansen, J. D., Olsen, L., et al. (2016). Deglaciation of fennoscandia. *Quaternary Science Reviews*, 147:91–121.

Stroeven, A. P., Heyman, J., Fabel, D., Björck, S., Caffee, M. W., Fredin, O., and Harbor, J. M. (2015). A new Scandinavian reference 10Be production rate. *Quaternary Geochronology*, 29:104–115.

Strunk, A., Knudsen, M. F., Egholm, D. L., Jansen, J. D., Levy, L. B., Jacobsen, B. H., and Larsen, N. K. (2017). One million years of glaciation and denudation history in west Greenland. *Nature Communications*, 8:14199.

Taylor, J. R. (1997). *An Introduction to Error Analysis: The Study of Uncertainties in Physical Measurements*. University Science Books, Sausalito, Calif, 2nd ed edition.

Tikkanen, M. and Oksanen, J. (2002). Late Weichselian and Holocene shore displacement history of the Baltic Sea in Finland. *Fennia-International Journal of Geography*, 180(1-2):9–20.

Tschudi, S., IVY-OCHS, S., Schlüchter, C., Kubik, P., and Rainio, H. (2000). 10 Be dating of younger dryas salpausselkä I formation in Finland. *Boreas*, 29(4):287–293.

University of Washington. CRONUS-Earth online calculator. Accessed on 28.5.2019. http://hess.ess.washington.edu/.

Vermeesch, P. (2007). CosmoCalc: An Excel add-in for cosmogenic nuclide calculations: COSMOCALC. *Geochemistry, Geophysics, Geosystems*, 8(8):n/a–n/a.

Wirsig, C., Ivy-Ochs, S., Akçar, N., Lupker, M., Hippe, K., Wacker, L., Vockenhuber, C., and Schlüchter, C. (2016). Combined cosmogenic 10Be, in situ 14C and 36Cl concentrations constrain Holocene history and erosion depth of Grueben glacier (CH). *Swiss Journal of Geosciences*, 109(3):379–388.

Wong, Kaufui Vincent, k. (2016). *Climate Change*. Environmental Engineering Collection. Momentum Press, New York, New York (222 East 46th Street, New York, NY 10017).

Zachos, J., Pagani, M., Sloan, L., Thomas, E., and Billups, K. (2001). Trends, Rhythms, and Aberrations in Global Climate 65 Ma to Present. *Science*, 292(5517):686–693.

Appendices

Appendix A: Parameter values used in results

Table A1: Parameter values of each section.

Model name	Section	Min no. of exposures	Max no. of exposures	Erosion	Tied	Sample depths (m)	Max exposure time (ka)	Max erosion (m)	Reference model
Simple exposure	4.1	1	1	-	-	0	35	-	A[a]
Sample depth	4.2	1	1	-	-	0,1,2,3	35	-	A[a]
Real without erosion	4.3	1	4	random	-	0	50	4	B[b]
Tied degla., constant erosion	4.4.1	1	4	2	10	0,2	50	2	C[c]
Tied degla., random erosion	4.4.2	1	4	random	10	0,2	50	4	C[c]
Constant erosion	4.4.3	1	4	2	-	0	50	2	C[c]
Without erosion	4.4.4	1	4	random	-	0	50	4	C[c]
No constraints	4.4.5	1	4	random	-	0	100	10	C[c]
Depth profile	4.5	1	4	random	10	0,1,2,3,4	50	4	C[c]

[a] Exposure 10 ka ago, no previous exposures
[b] Realistic history (0-10-25-35) without erosion
[c] Realistic history (0-10-25-35) with 2.0 m erosion at 10 ka

Appendix B: Additional three and four exposure models

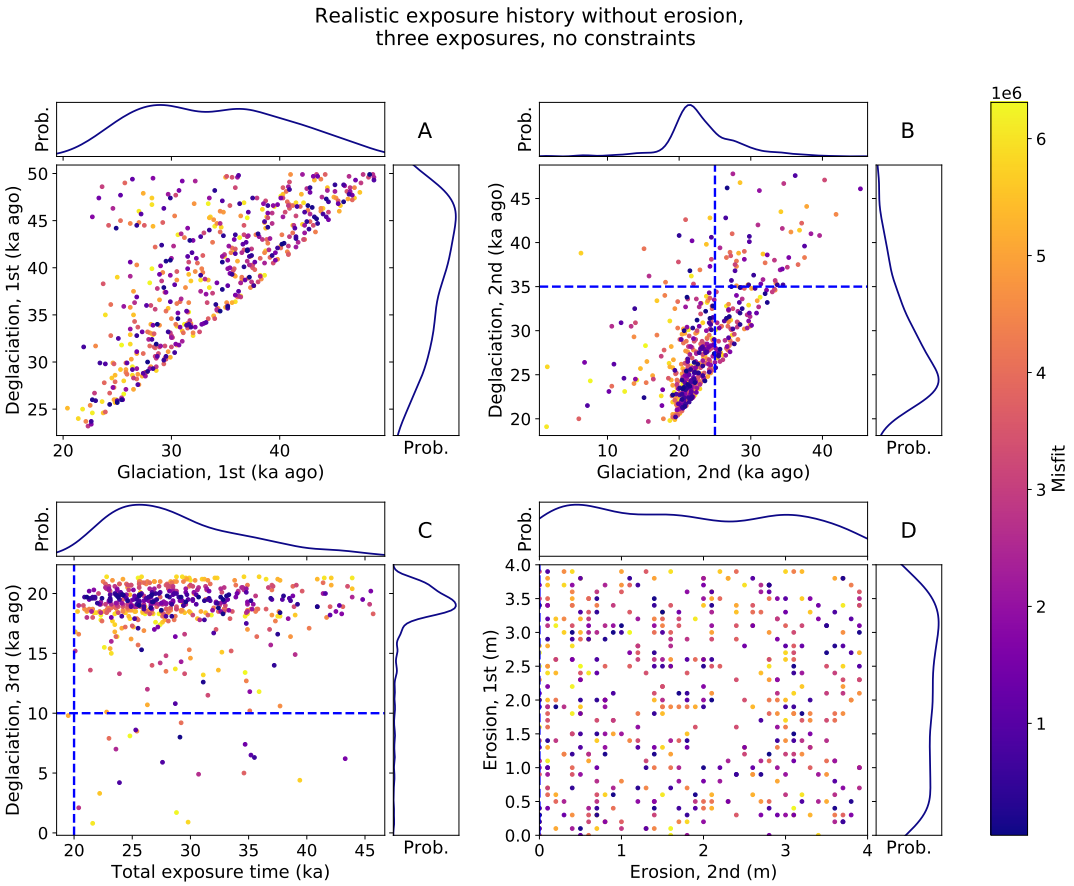

Figure B1. Realistic history without erosion compared to the three exposure models (Section 4.3). The limitation for the maximum duration of the model was 50 ka and the maximum erosion was 4.0 m in one glaciation. The models can have erosion, even if the reference model did not have. Each dot presents one model and its color corresponds to its misfit value so that darker color means smaller and better misfit. The blue dashed line presents the value used in the reference model. Density functions are shown adjacent to the axes for each parameter. A. The first glaciation and deglaciation do not reach a clear section of small misfit values. B. The second glaciation and deglaciation are more concentrated below 35 ka. The deglaciation do not fit to the deglaciation in the reference model C. The last deglaciation has smallest misfit values around 20 ka. The total exposure duration has values from 20 ka to 45 ka. D. Erosion values during glaciations do not cumulate to any value.

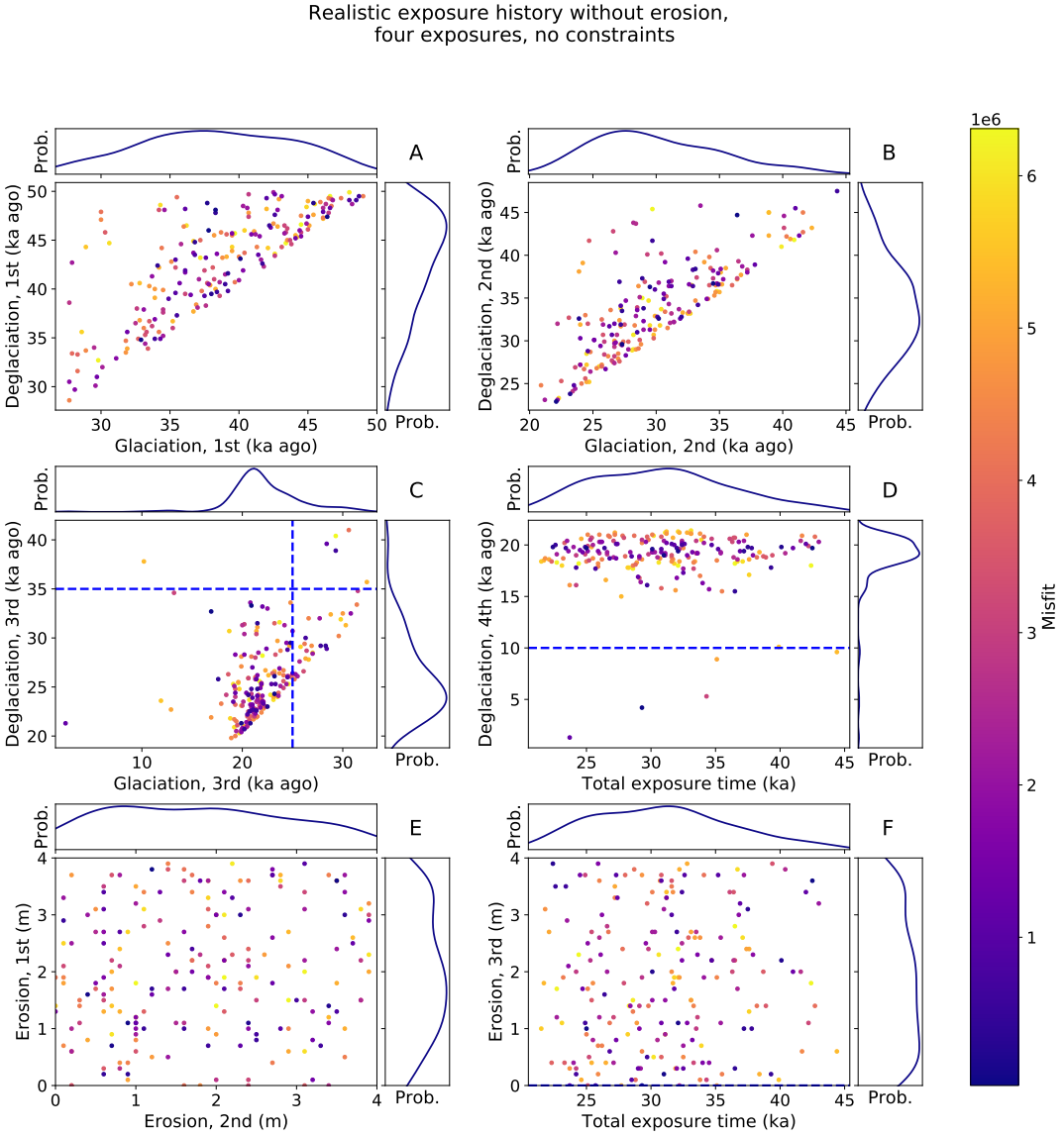

Figure B2. Realistic history without erosion compared to the four exposure models (Section 4.3). The limitation for the maximum duration of the model was 50 ka and the maximum erosion was 4.0 m in one glaciation. The models can have erosion, even if the reference model did not have. Each dot presents one model and its color corresponds to its misfit value so that darker color means smaller and better misfit. The blue dashed line presents the value used in the reference model. Density functions are shown adjacent to the axes for each parameter. A. The first glaciation and deglaciation do not reach a clear section of small misfit values. B. The second glaciation and deglaciation are not cumulated to any value. C. The third glaciation and deglaciation are more concentrated below 35 ka, but the is not clear trend for the minimum misfit. D. The last deglaciation is cumulated near 20 ka, while the total exposure duration does not have any kind of trend. E. Erosion values during the first and second glaciation are varying almost uniformly between 0 and 4 m. F. Erosion during the last glaciation varies also quite much and is not concentrated to any value.

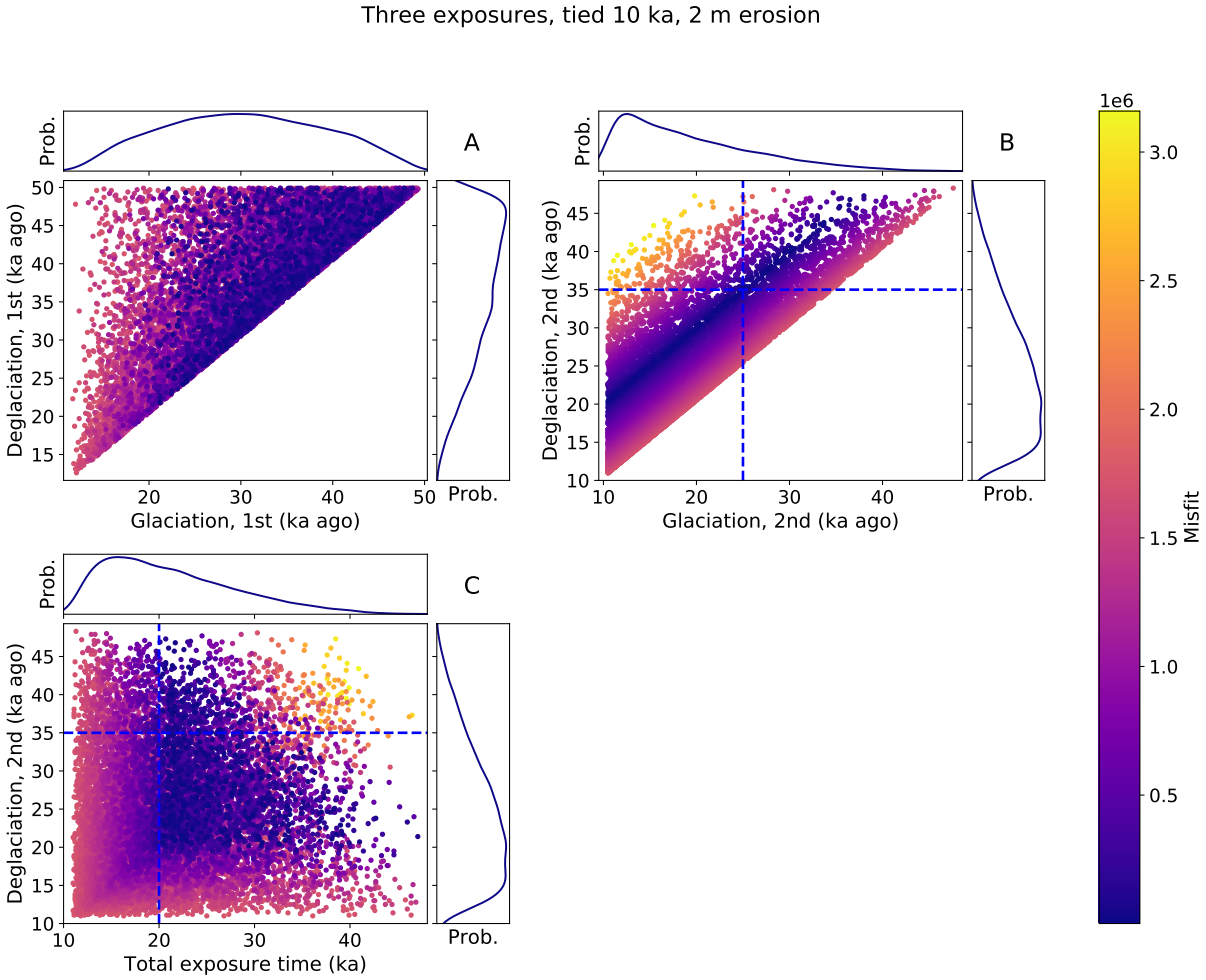

Figure B3. Three exposure models with tied last deglaciation and constant erosion (Section 4.4.1). The maximum exposure time was limited to 50 ka. Each dot presents one model and its color presents its misfit value so that darker corresponds to a smaller and better misfit value. The blue dashed line presents the parameter values used in the reference model. Density functions are shown adjacent to the axes for each parameter. A. The first glaciation and deglaciation do not have a clear dependency of each other. B. The second glaciation and deglaciation are proportional to each other. C. The second deglaciation and the toal exposure time have some kind of dependency of each other. The best fit is reached when the total exposure time is at least 20 ka and the deglaciation 20 ka.

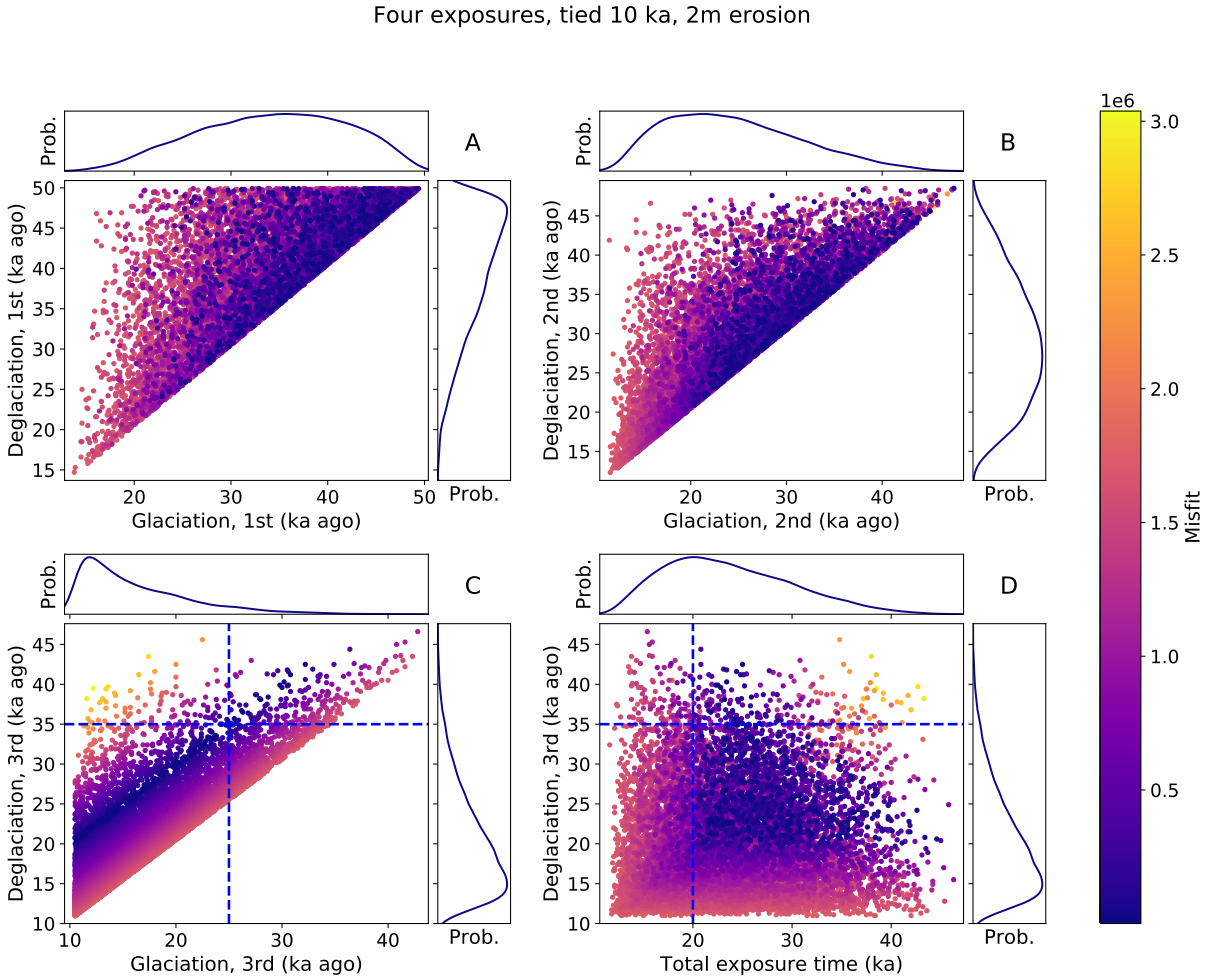

Figure B4. Four exposure models with tied last deglaciation and constant erosion (Section 4.4.1). The maximum exposure time was limited to 50 ka. Each dot presents one model and its color presents its misfit value so that darker corresponds to a smaller and better misfit value. The blue dashed line presents the parameter values used in the reference model. Density functions are shown adjacent to the axes for each parameter. A and B. The firsts and seconds glaciations and deglaciations are not depending each other with a clear pattern. C. The third, and last, glaciation and deglaciation have a linearly increasing dependency. D. Similarly to the three exposure models, the best fit of the last deglaciation and the total exposure time is gained when both of them are over 20 ka.

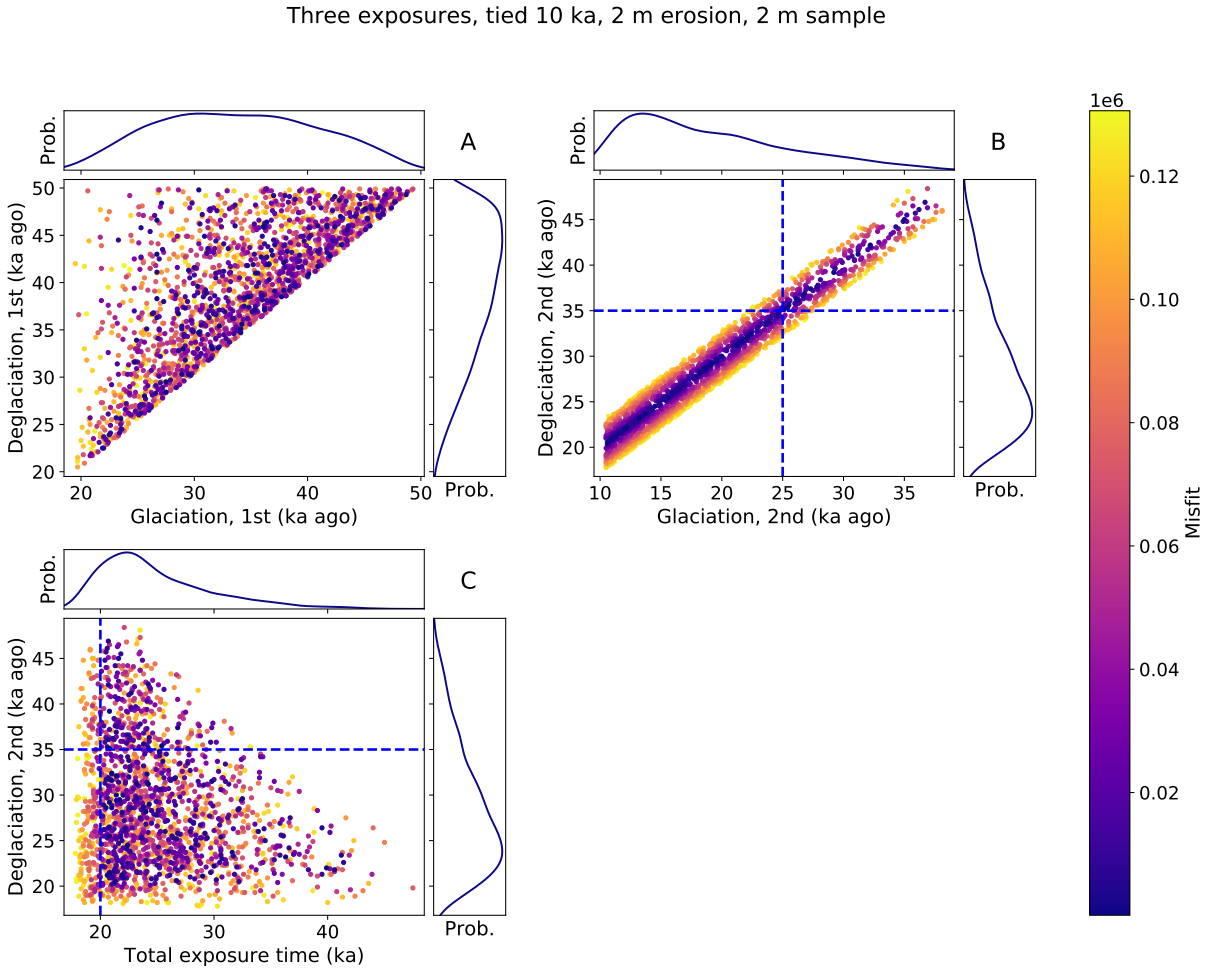

Figure B5. Three exposure models with tied last deglaciation, constant erosion and sampling depth of 2.0 m (Section 4.4.1). The maximum exposure time was limited to 50 ka. Each dot presents one model and its color presents its misfit value so that darker corresponds to a smaller and better misfit value. The blue dashed line presents the parameter values used in the reference model. Density functions are shown adjacent to the axes for each parameter. A and B. The firsts and seconds glaciations and deglaciations are not depending each other with a clear pattern. C. The third, and last, glaciation and deglaciation have a linearly increasing dependency. D. The best fit of the last deglaciation and the total exposure time is gained when both of them are over 20 ka.

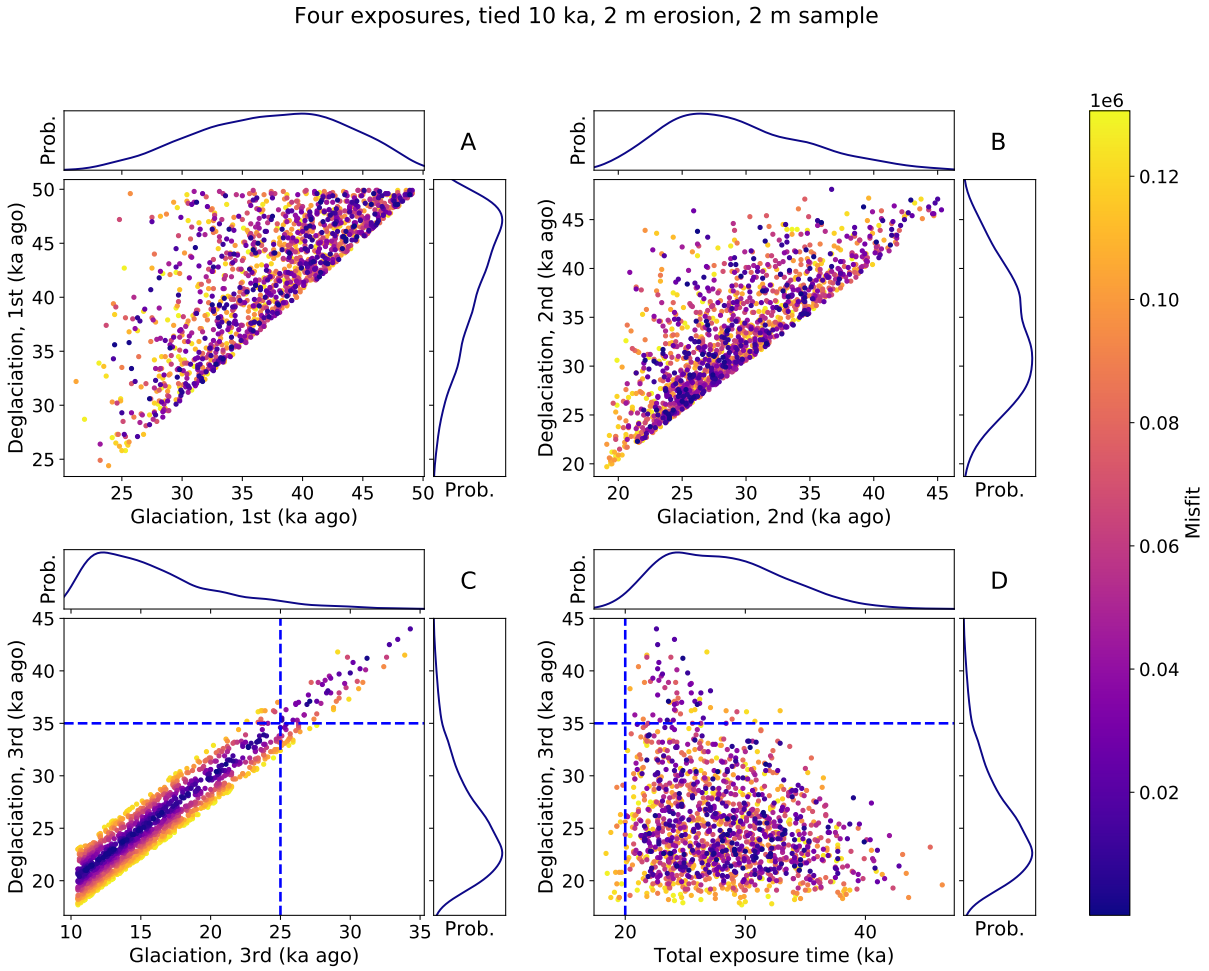

Figure B6. Four exposure models tied last deglaciation, constant erosion and sampling depth of 2.0 m (Section 4.4.1). The maximum exposure time was limited to 50 ka. Each dot presents one model and its color presents its misfit value so that darker corresponds to a smaller and better misfit value. The blue dashed line presents the parameter values used in the reference model. Density functions are shown adjacent to the axes for each parameter. A and B. The firsts and seconds glaciations and deglaciations are not depending each other with a clear pattern. C. The third, and last, glaciation and deglaciation have a linearly increasing dependency. D. Similarly to the three exposure models, the best fit of the last deglaciation and the total exposure time is gained when both of them are over 20 ka.

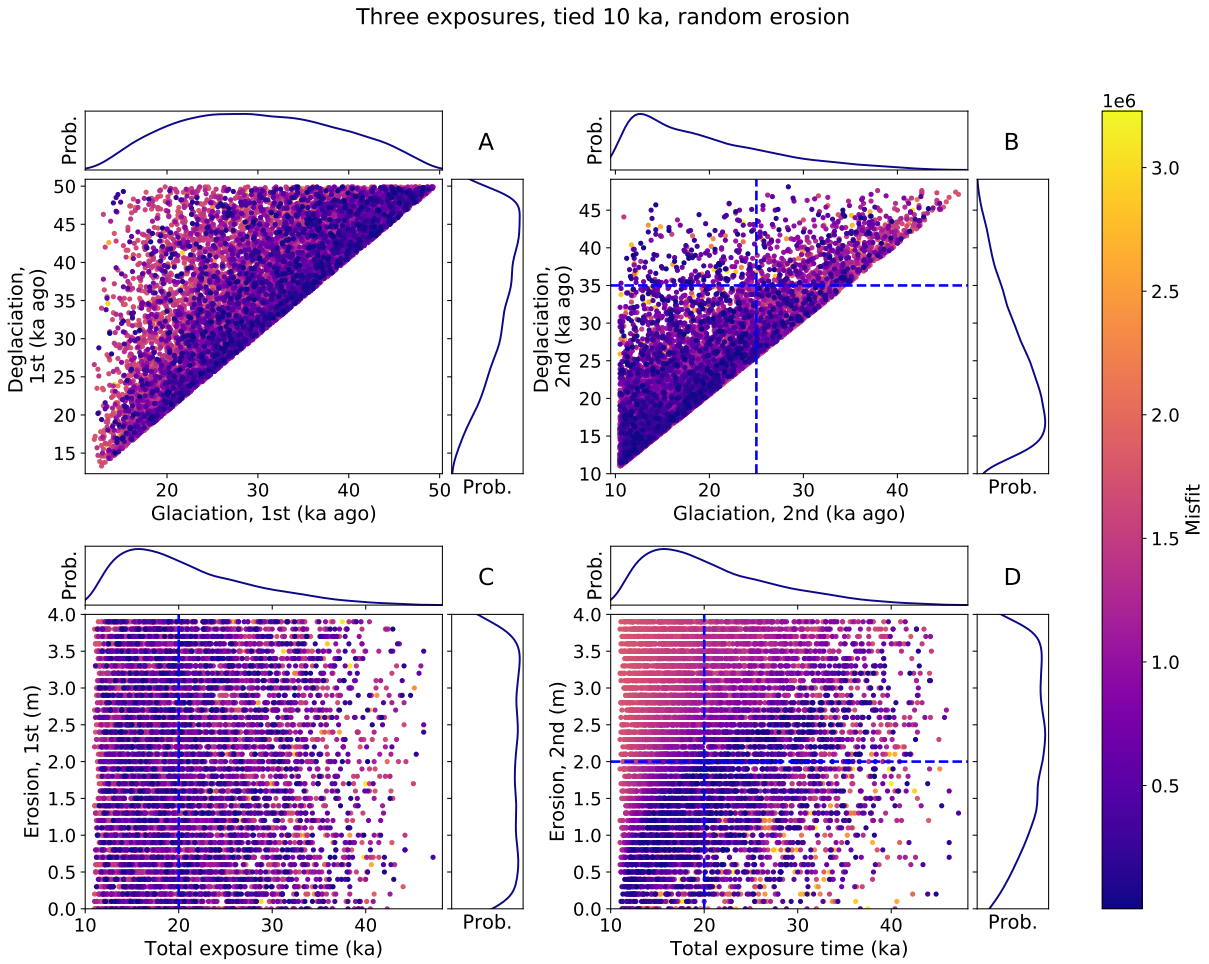

Figure B7. Three exposure models with tied timing of last deglaciation and randomly selected erosion fitted to realistic history with 2.0 m erosion (Section 4.4.2). The maximum exposure time was limited to 50 ka. Each point presents one model and its color refers to the misfit value. Darker color means a smaller and better misfit value. A. The first deglaciation and glaciation have several combinations when the smallest misfit is reached. They are widely distributed, mainly between 20 and 50 ka. B. The second deglaciation and glaciation are concentrated more below 30 ka. They have also several combinations where the best misfit is reached. C. The first erosion, during the first glaciation, and the total exposure time are randomly orientated. Erosion have values from 0 to 4 m and total exposure time varies between 10 and 50 ka. D. The last erosion and total exposure time have some kind of pattern, that can be recognized from the two exposure case. It is not logarithmic as obviously than the two exposure case.

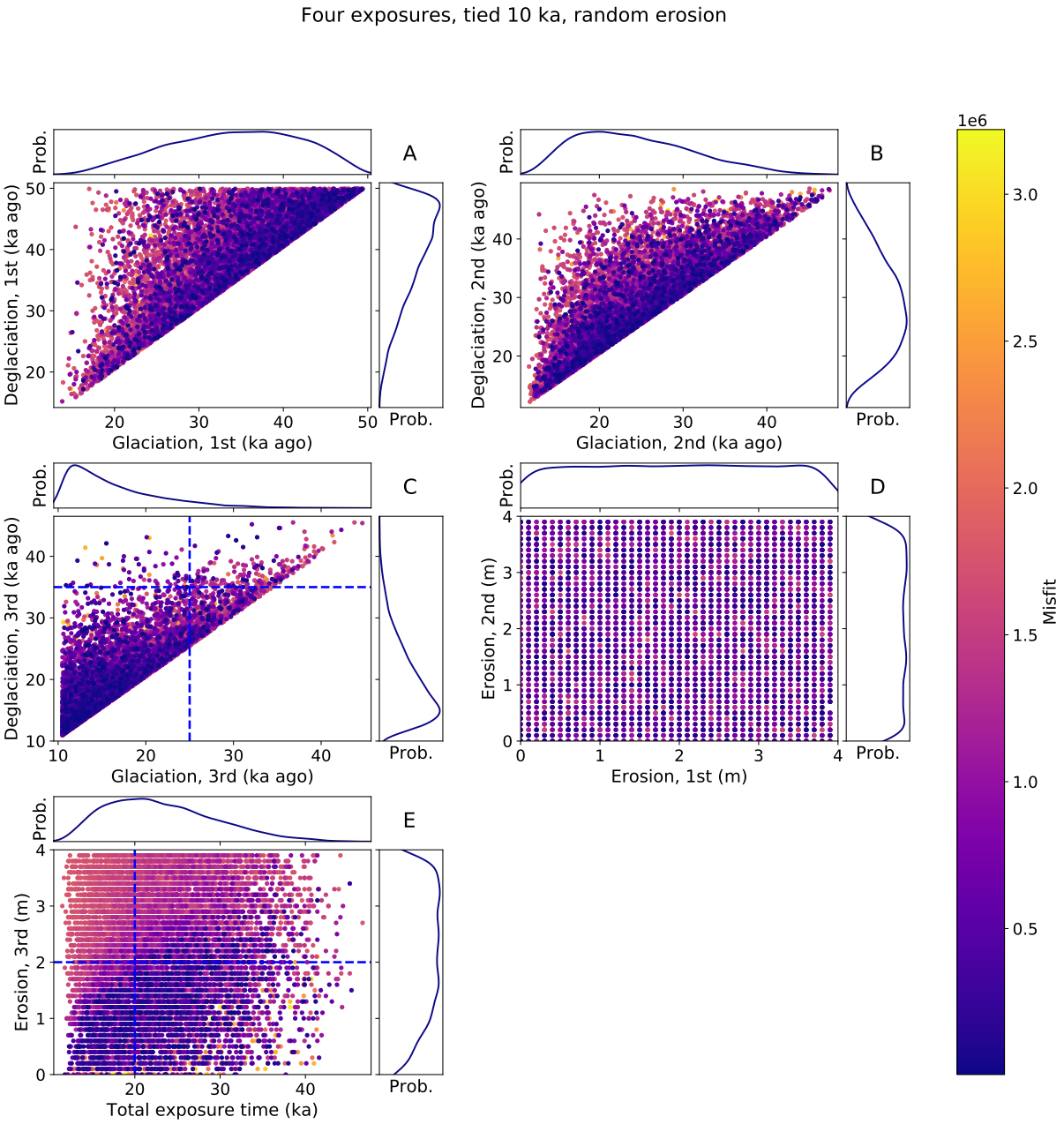

Figure B8. Four exposure models with tied timing of last deglaciation and randomly selected erosion fitted to realistic history with 2.0 m erosion (Section 4.4.2). The maximum exposure time was limited to 50 ka. Each point presents one model and its color refers to the misfit value. Darker color means a smaller and better misfit value. A-B. Glaciation as a function of the previous deglaciation. There is not any obvious combination for the smallest misfit and the values are distributed to a large area in both figures. C. The first erosion as a function of total exposure time. The values are scattered randomly between the boundary conditions, erosion 0 to 4 m and total exposure time 10 to 50 ka. D. The last erosion and the total exposure time might have also the same logarithmic connection than in the two and three exposure cases.

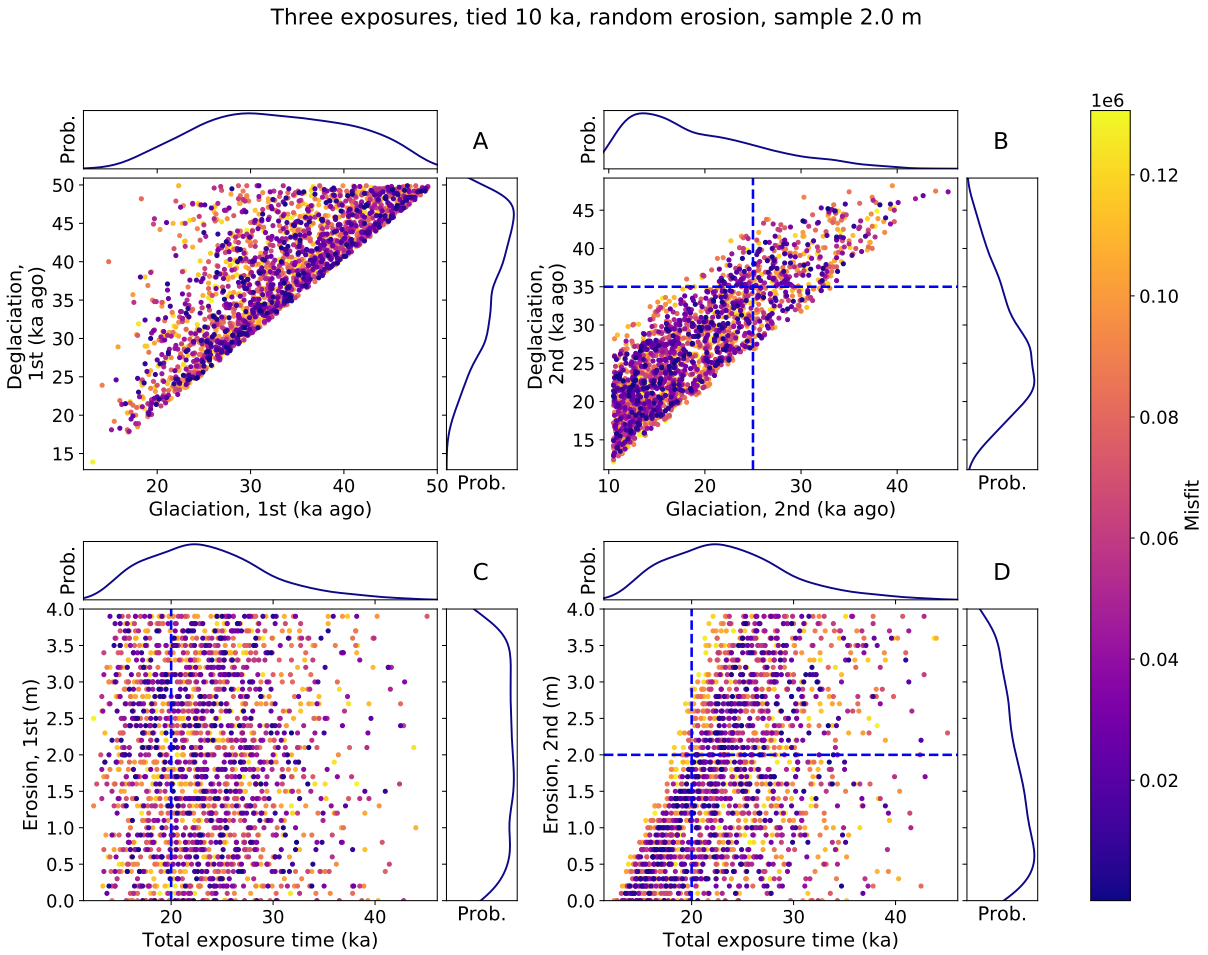

Figure B9. Three exposure models with tied timing of the last deglaciation and randomly selected erosion fitted to realistic history with 2.0 m erosion (Section 4.4.2). Sampling depth is 2.0 m. The maximum exposure time is limited to 50 ka. Each dot presents one model and its color presents the misfit value so that darker corresponds to a smaller and better misfit value. The blue dashed line presents the parameter values used in the reference model. Density functions are shown adjacent to the axes for each parameter. A and B. Deglaciation and glaciation are scattered and the minimum misfit is reached at several occasions. C. The first erosion and total exposure time are scattered to rather wide area. No clear indication of the small misfit zone. D. The last erosion and the total exposure time has a small misfit zone that increases linearly.

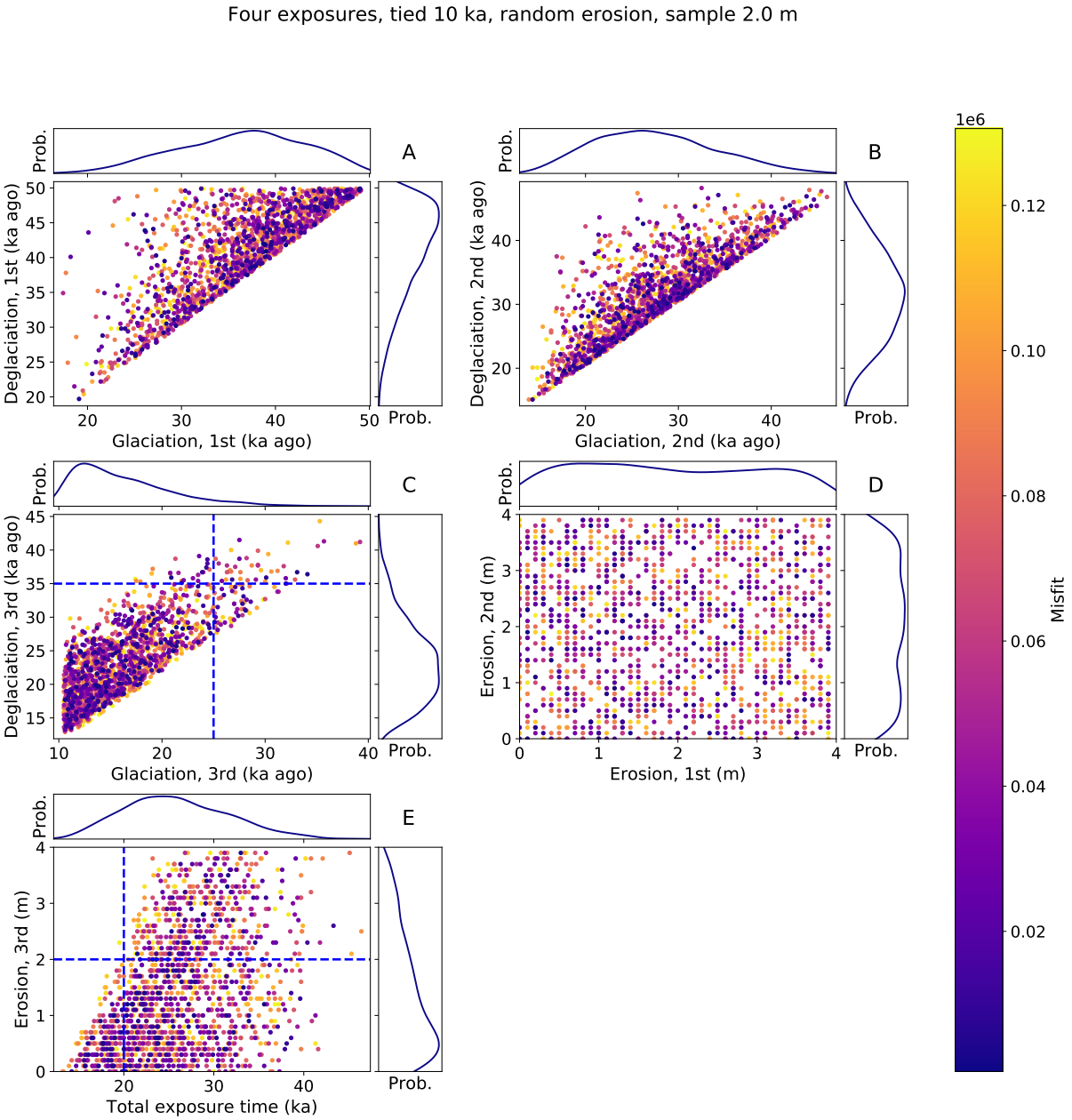

Figure B10. Four exposure models with tied timing of the last deglaciation and randomly selected erosion fitted to realistic history with 2.0 m erosion (Section 4.4.2). Sampling depth is 2.0 m. The maximum exposure time is limited to 50 ka. Each dot presents one model and its color presents the misfit value so that darker corresponds to a smaller and better misfit value. The blue dashed line presents the parameter values used in the reference model. Density functions are shown adjacent to the axes for each parameter. A , B and C. Deglaciation and glaciation are scattered and the minimum misfit is reached at several occasions. D. The first two erosions have widely spread values without a minimum misfit area. E. The last erosion and the total exposure time are somewhat concentrated, erosion below 2 m and total exposure time between 20 and 30 ka. Not as clear trend than in two and three exposure models.

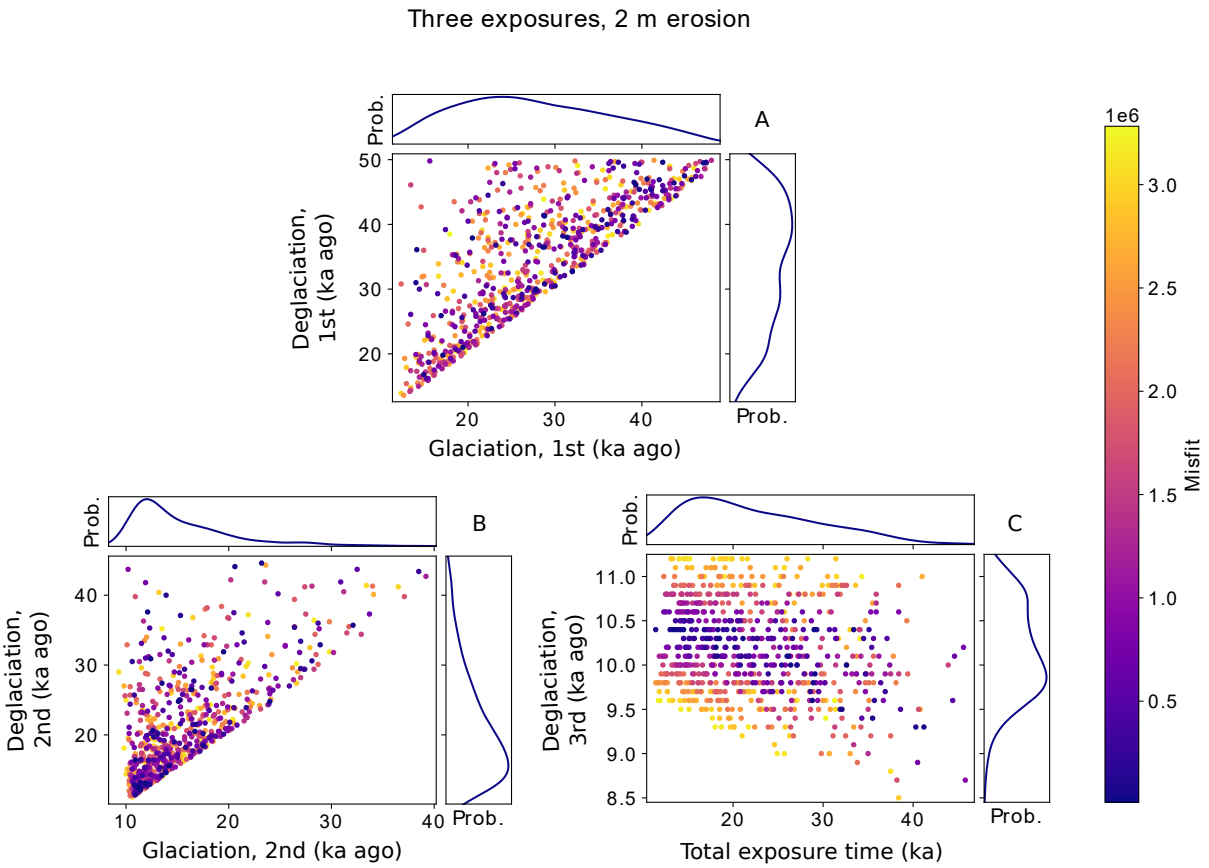

Figure B11. Three exposure models with constant 2.0 m erosion in the end of every glaciation fitted to realistic history with 2.0 m erosion (Section 4.4.3). The maximum exposure time was limited to 50 ka. Each point presents one model and its color refers to the misfit value. Darker color means a smaller and better misfit value. A. The first glaciation starting time and the first deglaciation time do not have a clear pattern of accepted combinations. The best fit is reached almost with any combination where the deglacation has larger value than glaciation. B. The second glaciation and deglaciation has a similar kind of pattern, except the values are concentrated to smaller times. C. Total exposure time and the last deglaciation has some kind of trend. When the total exposure time is increasing the last deglaciation is slightly decrasing. The best fit is reached with multiple combinations, but it seems that most of the values are in the range of 9.5 to 10.5 in deglaciation and 10 to 30 in total exposure time.

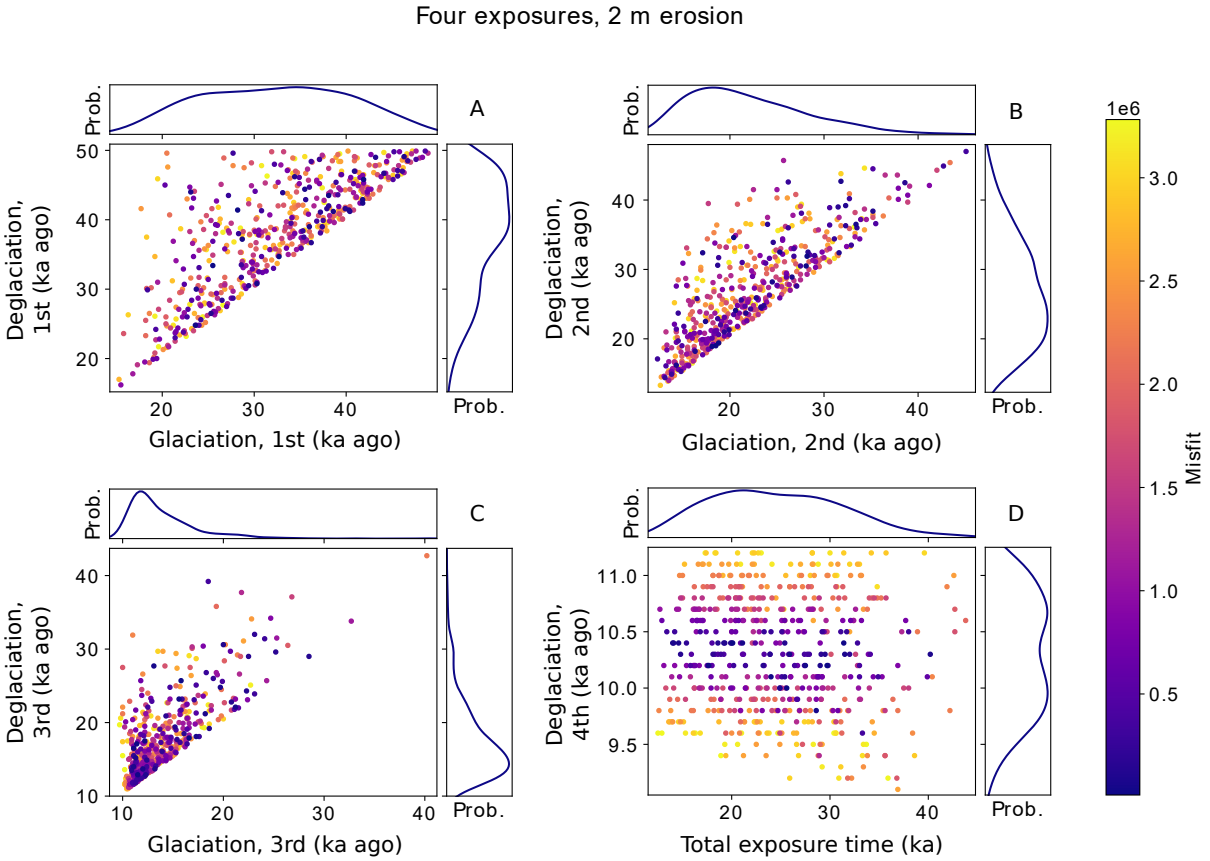

Figure B12. Four exposure models with constant 2.0 m erosion in the end of every glaciation fitted to realistic history with 2.0 m erosion (Section 4.4.3). The maximum exposure time was limited to 50 ka. Each point presents one model and its color refers to the misfit value. Darker color means a smaller and better misfit value. A. The first glaciation and deglaciation have values from wide range since both of them vary from 20 to 50 ka. B. The second glaciation and deglaciation has rather similar pattern than in the A except the values are concentrated to smaller numbers, below 30 ka. C. The third glaciation and deglaciation follow the same pattern than the previous two but the values are even more concentrated below 20 ka. D. The total exposure time and the last deglaciation has a trend where the best fit is found when the deglaciation remains between 10.0 and 10.6 ka while the total exposure time varies from 10 to 40 ka.

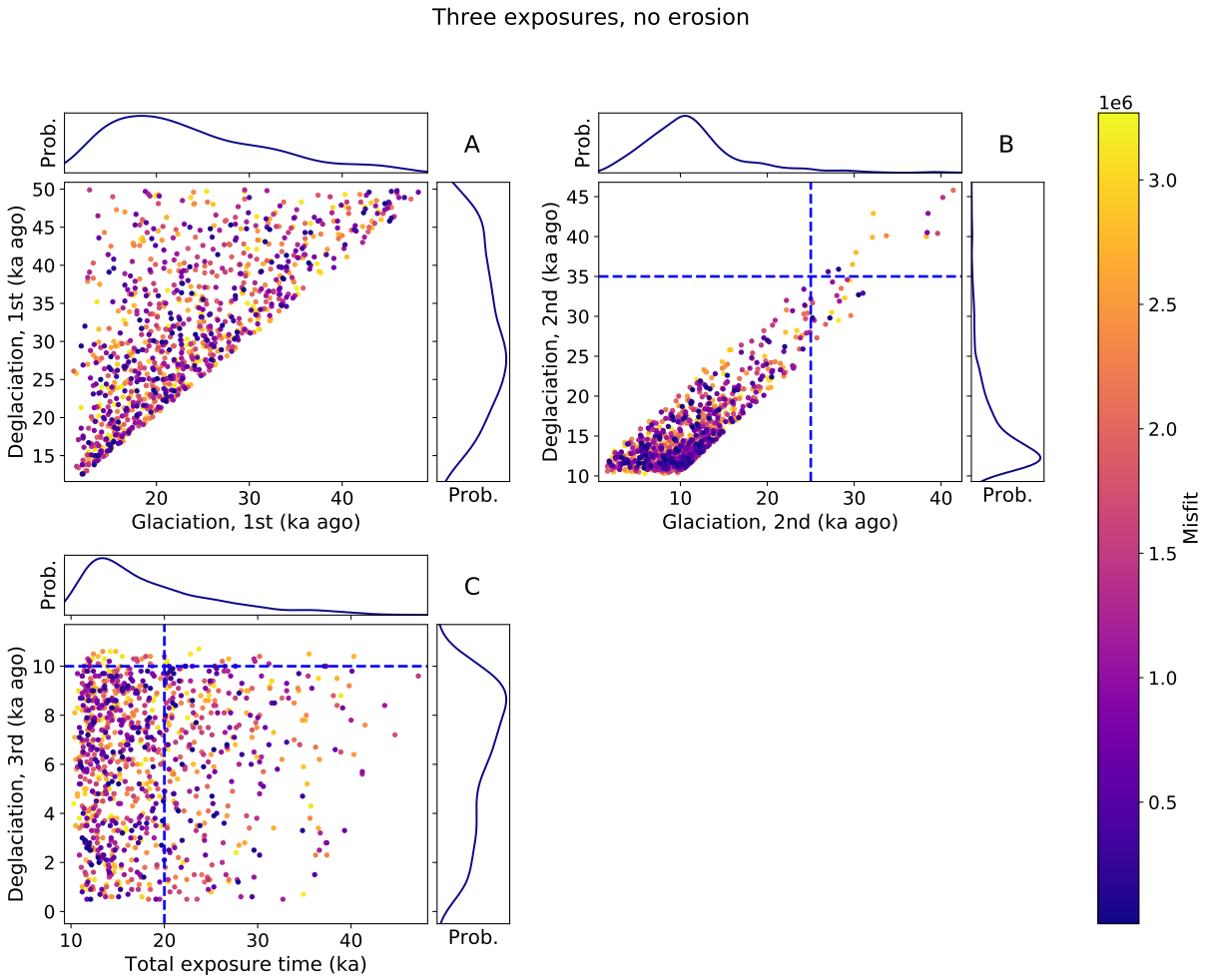

Figure B13. Three exposure models without erosion fitted to realistic history with 2.0 m erosion (Section 4.4.4). The maximum exposure time was limited to 50 ka. Each point presents one model and its color refers to the misfit value. Darker color means a smaller and better misfit value. A. The timing of the first glaciation and the first deglaciation are distributed between 10 and 50 ka. The glaciation is more clearly concentrated under 30 ka than the deglaciation. The best misfit values are gained with multiple very different combinations. B. The second glaciation and deglaciation has a linear kind of trend which reminds the two exposure case in Figure 25B. The lowest misfit values are mostly concentrated in the area where the deglaciation and glaciation are smaller than 20 ka. C. Total exposure time and the last deglaciation are widely scattered. The total exposure time is concentrated below 20 ka, but it still have good fits even over 40 ka. Last deglaciation varies between 0 and 11 ka.

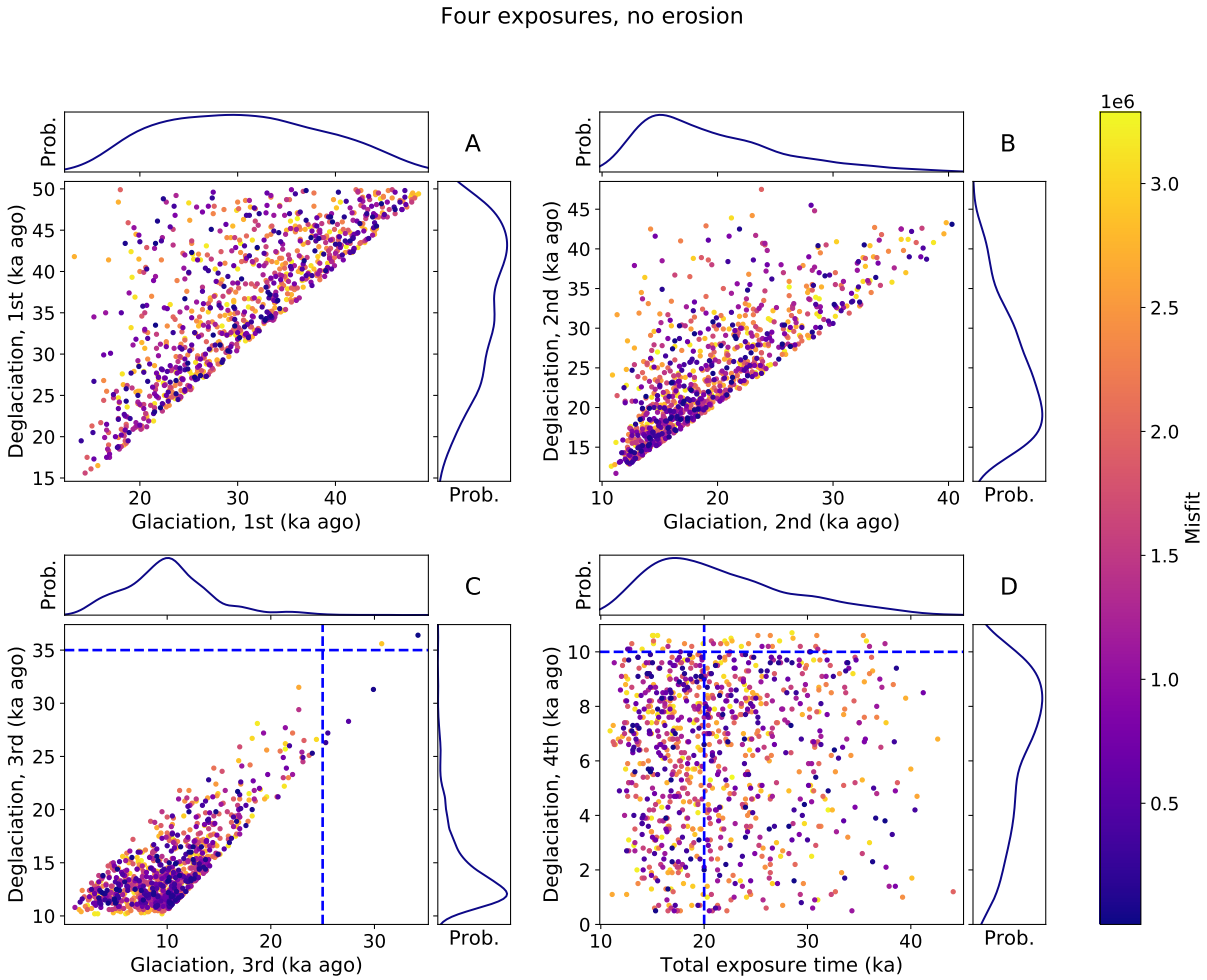

Figure B14. Four exposure models without erosion fitted to realistic history with 2.0 m erosion (Section 4.4.4). The maximum exposure time was limited to 50 ka. Each point presents one model and its color refers to the misfit value. Darker color means a smaller and better misfit value. A and B. The first two glaciations and deglaciations are widely scattered. C. The third glaciation and deglaciation are strongly concentrated below 20 ka, where is also most of the small misfit values. D. The total exposure time has a rather large range. It varies from 10 to 50 ka, but most of the best fitting values are below 30 ka. The last deglaciation varies from 0 to 11 ka.

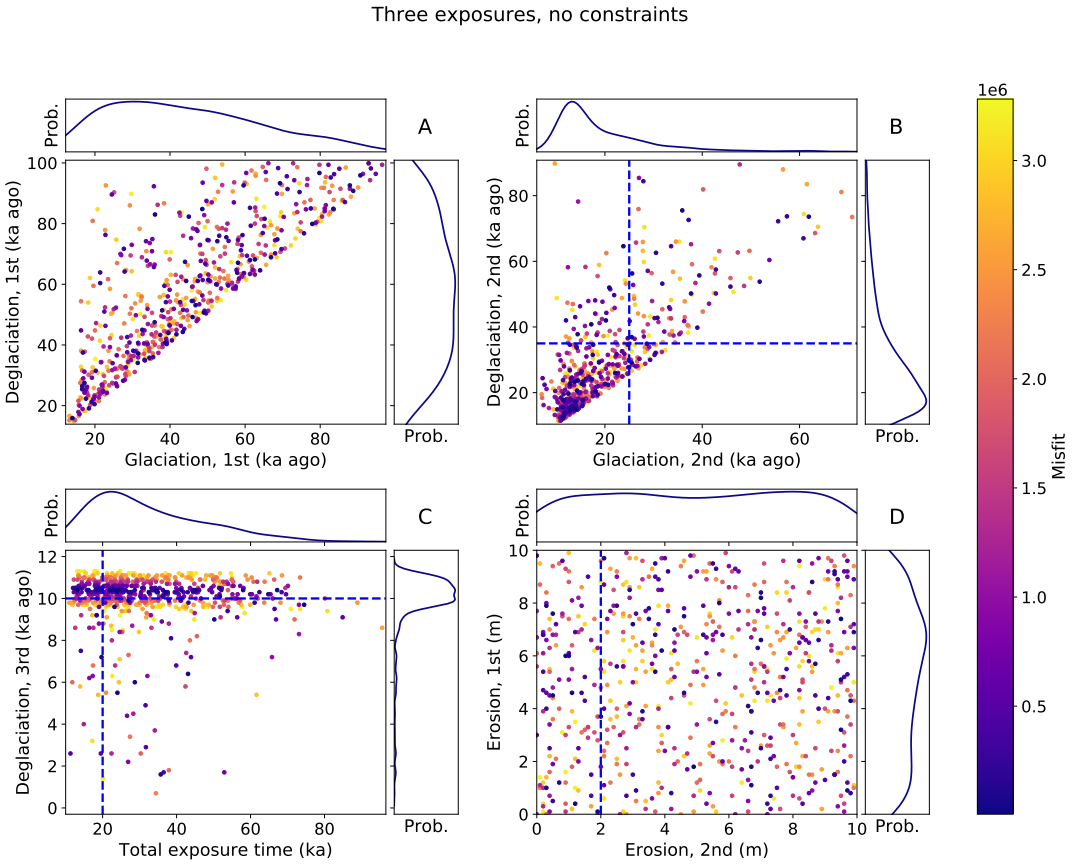

Figure B15. Three exposure models without constraints fitted to realistic history with 2.0 m erosion (Section 4.4.5). The only limitations were the maximum erosion of 10.0 m and the maximum duration of 100.0 ka. Each point presents one model and its color refers to the misfit value. Darker color means a smaller and better misfit value. A and B. The first two glaciations and deglaciations have multiple combinations where the misfit value is small. C. The last deglaciation has the best fit around 10.5 ka, while the total exposure time varies from 10 to 90 ka. D. Erosions during the deglaciations do not have a clear trend. Their values vary from 0 to 10 m.

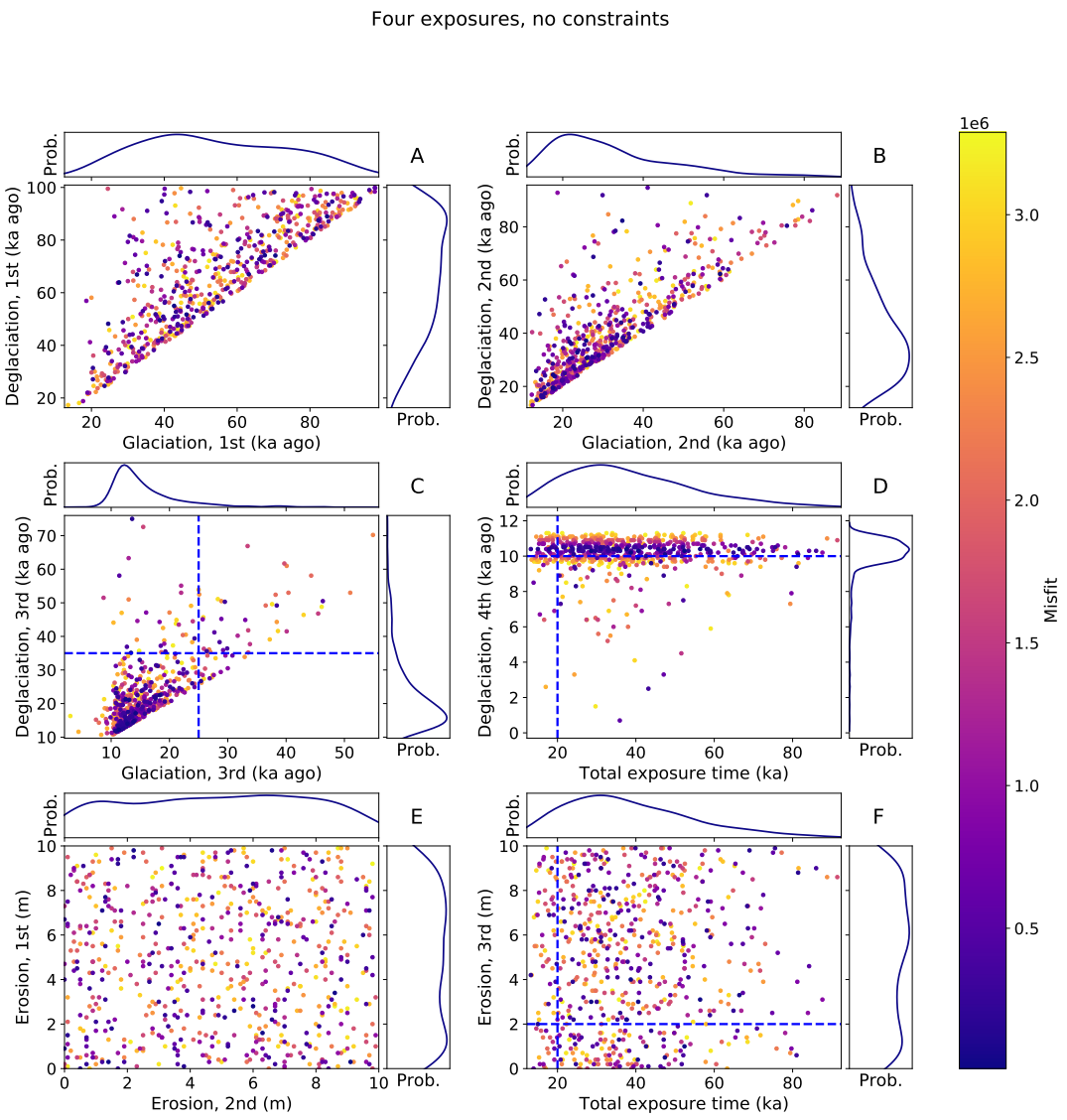

Figure B16. Four exposure models without constraints fitted to realistic history with 2.0 m erosion (Section 4.4.5). The only limitations were the maximum erosion of 10.0 m and the maximum duration of 100.0 ka. Each point presents one model and its color refers to the misfit value. Darker color means a smaller and better misfit value. A, B and C. The first three glaciations and deglaciations have multiple combinations where the misfit value is small. D. The last deglaciation has the best fit around 10.5 ka, while the total exposure time varies from 10 to 90 ka. E and F. Erosions during the deglaciations have a great variation in their values. There is no a distinct pattern that could be recognized.